Activity Report
2002-2003

Association
EURATOM / IPP.CR

INSTITUTE OF PLASMA PHYSICS
ACADEMY OF SCIENCES OF THE CZECH REPUBLIC

TABLE OF CONTENTS

PREFACE

This report presents the main results achieved during the years 2002-2003 of the existence of the Association EURATOM/IPP.CR which undertakes research and development within the European fusion energy research programme. The long term aim of this research is the realisation of fusion as a practically unlimited energy source with a minimum environmental impact. The Association participates in the joint European effort in this field by carrying out relevant plasma physics and technology R&D, including participation in JET and other European devices and design activities related to the proposed experimental reactor ITER.

The Association was founded on December 22, 1999 through a contract between the European Atomic Energy Community (EURATOM) represented by the European Commission and the Institute of Plasma Physics, Academy of Sciences of the Czech Republic (IPP). Several other institutions in Prague have been included in the Research Unit to contribute to the programme of physics and technology research:

- Faculty of Mathematics and Physics, Charles University in Prague (FMP)
- Institute of Physical Chemistry, Academy of Sciences of the Czech Republic (IPCH)
- Faculty of Nuclear Science and Physical Engineering, Czech Technical University (FNSPE)
- Nuclear Physics Institute, Academy of Sciences of the Czech Republic (NPI)
- Nuclear Research Institute, Rez, Plc (NRI)

At the end of 2003, the Institute of Applied Mechanics Brno (IAM) has jointed the Research Unit to participate in the simulation of welding of the vacuum vessel of ITER.

The overall manpower involved in the Association's fusion research at the end of 2003 was 69, of which 59 were professionals (those with a University degree). The total effort expended is about 39 personyear/year of which roughly 75% is devoted to physics tasks and the remaining 25% to underlying technology and technology tasks. The overall annual budget is about 1.7 M€ out of which the Commission contribution is about 0.57 M€.

The activities in physics have continued along the line of the approved Work programs 2002-2003 both in experiment and theory. Fusion-relevant plasma physics is experimentally studied on the small tokamak CASTOR. The research is focused on the study of phenomena at the plasma edge, such as biasing, impurity radiation, and the measurement of the structure of edge turbulence by arrays of electric probes. In addition, new advanced probes are being developed as edge plasma diagnostics. A part of the Association's activities was devoted to studies of wave-plasma interaction, in particular in the range of lower hybrid frequencies. Some selected atomic processes relevant to fusion plasmas, such as recombination and the interaction of ions with surfaces, were studied in test-bed experiments at FMP and IPCH.

The existing collaborations with other Associations were further strengthened. The Czech scientists took an active part in experiments on TORE-SUPRA, TCV and MAST. On the other hands, several experimental campaigns on the CASTOR tokamak were performed with a significant contribution of our colleagues from Associations CEA, the Belgium state, ENEA (RFX) and ÖAW. The further progress was achieved in the Association's participation in the collective exploitation of the JET facilities under EFDA.

In the technology area, the R&D was substantially enhanced and focused on the fields Vessel/In Vessel, Tritium Breeding and Materials and Physics Integration. In total 15 Technology Tasks were approved in the reported period, mostly exploiting the cyclotron at the NPI, the fission reactor at the NRI and computational capabilities at the IAM.

Keep-in Touch activities with ICF were continued by exploitation of the Prague Asterix Laser System (PALS).

Some effort was devoted to organization of international meetings in the Czech Republic and abroad. Special attention was paid to practical training of students. The First Summer Training Course on Tokamak Operation (SUMTRAIC 2003) was organized together with the Association EURATOM/HAS for 10 Hungarian students.

The Association has been active in the information about its activities and the dissemination of the why and how of fusion energy research and future energy supply including fusion energy as an environmentally clean and safe base load electricity source.

Jan Stöckel
Head of Research Unit
Association EURATOM/IPP.CR

I RESEARCH UNIT

1 Association EURATOM/IPP.CR

Composition of the Research Unit

IPP **Institute of Plasma Physics, Academy of Sciences of CR**
Address: Za Slovankou 3,
182 21 Praha 8, Czech Republic
Phone: +420 286 890 450
Fax: +420 286 586 389
Contact Person: Jan Stöckel
E-mail: stockel@ipp.cas.cz

IPCH **Institute of Physical Chemistry, Academy of Sciences of CR**
Address: Dolejškova 3,
182 23 Praha 8, Czech Republic
Phone: +420 266 053 514
Fax: +420 286 582 307
Contact person: Zdeněk Herman
E-mail: zdenek.herman@jh-inst.cas.cz

NPI **Institute of Nuclear Physics, Academy of Sciences of CR**
Address:
250 68 Řež, Czech Republic
Phone: +420 266 172 105
Fax: +420 220 941 130
Contact person: Pavel Bém
E-mail: bem@ujf.cas.cz

IAM **Institute of Applied Mechanics Brno, Ltd.**
Address: Veveří 85,
611 00 Brno, CR
Phone: +420 541 321 291
Fax: +420 541 211 189
Contact person: Lubomír Junek
E-mail: junekl.uam@telecom.cz

FMP **Faculty of Mathematics and Physics, Charles University**
Address: V Holešovičkách 2,
182 00 Praha 8, Czech Republic
Phone: +420 221 912 305
Fax: +420 221 912 332
Contact person: Milan Tichý
E-mail: tichy@mbox.troja.mff.cuni.cz

FNSPE **Faculty of Nuclear Science and Physical Engineering, Czech Technical University**
Address: Břehová 7,
115 19 Praha 1, Czech Republic
Phone: +420 224 358 296
Fax: +420 222 320 862
Contact person: Vojtěch Svoboda
E-mail: svoboda@br.fjfi.cvut.cz

NRI **Nuclear Research Institute Plc., Rez**
Address:
250 68 Řež, Czech Republic
Phone: +420 266 172 453
Fax: +420 266 172 045
Contact person: Milan Zmítko
E-mail: zmi@ujv.cz

Steering Committee

EURATOM

    Umberto Finzi
    Hardo Bruhns
    Johannes P.M. Spoor

IPP.CR

    Ivan Wilhelm (Charles University)
    Petr Křenek (Ministry of Education, Youth and Sports)
    Pavel Chráska (Institute of Plasma Physics)

Head of Research Unit

    Jan Stöckel

Secretary of the SC

    Pavol Pavlo

2 Manpower and Budget

Manpower Analysis of the Association EURATOM/IPP.CR 2002-2003

2002	Institution	Professional Person	Professional PY	Non-Prof Person	Non-Prof PY	Total Person	Total PY	%
Physics	IPP	25	19.2	6	4.5	31	23.7	
	IPCH	5	2.6	0	0	5	2.6	
	FNSPE	1	0.5	0	0	1	0.5	
	FMP	6	2.8	0	0	6	2.8	
	Total	**37**	**25.1**	**6**	**4.5**	**43**	**29.6**	**75.1**
Technology	NPI	10	4.4	2	1.5	12	5.9	
	NRI	5	1.9	3	2	8	3.9	
	Total	**15**	**6.3**	**5**	**3.5**	**20**	**9.8**	**24.9**
TOTAL		**52**	**31.4**	**11**	**8**	**63**	**39.4**	

2003	Institution	Professional Person	Professional PY	Non-Prof Person	Non-Prof PY	Total Person	Total PY	%
Physics	IPP	25	21	6	5	31	26	
	IPCH	5	2.6	0	0	6	2.6	
	FNSPE	1	0.5	0	0	1	0.5	
	FMP	8	3.4	0	0	8	3.4	
	Total	**39**	**27.5**	**6**	**5**	**45**	**32.5**	**75.0**
Technology	FNSPE	1	0.5	0	0	1	0.5	
	NPI	8	4.1	2	1.5	10	5.6	
	NRI	9	3.1	2	0.65	11	3.75	
	IAM	2	1	0	0	2	1.0	
	Total	**20**	**8.7**	**4**	**2.15**	**24**	**10.85**	**25.0**
TOTAL		**59**	**36.2**	**10**	**7.15**	**69**	**43.35**	

Expenditures 2002 – 2003 (in EURO)

2002

	Expenditures (basic support)	A fraction eligible for preferential support
Physics	564 673	
Underlying Technologies	130 261	
JET Notifications	15 373	
Collaborative Actions		0
Sub-total	**710 307**	
Technology tasks Art 5.1a	404 332	
Priority Actions in Technology		0
Technology tasks Art 5.1b	0	
EFDA Article 6.3 Contracts	0	
EFDA Article 9 - secondment to Culham	0	
EFDA Article 9 - secondment to Garching	0	
Sub-total	**404 332**	
TOTAL	**1 114 639**	

Mobility Actions 2002	**50 851**

2003

	Expenditures (basic support)	A fraction eligible for preferential support
Physics	611 403	
Underlying Technologies	128 560	
JET Notifications	4 658	
Collaborative Actions		500 000
Sub-total	**744 621**	
Technology tasks Art 5.1a	889 619	
Priority Actions in Technology		402 720
Technology tasks Art 5.1b	0	
EFDA Article 6.3 Contracts	4 779	
EFDA Article 9 - secondment to Culham	8 094	
EFDA Article 9 - secondment to Garching	0	
Sub-total	**902 492**	
TOTAL	**1 647 113**	

Mobility Actions 2003	**54 241**

3 International Collaboration

Collaborative Projects 2002 - 2003

International collaboration can be grouped into eight projects. For each project, the collaborating institutions are listed and main tasks are described.

Fluctuation measurements and edge plasma biasing

CEA Cadarache; Etat Belge - Ghent University; ENEA - Conzorcio RFX, Padova; IST, Lisbon; Ciemat Madrid; VR

Measurements of the edge plasma fluctuations using the Langmuir probe arrays in ohmic and polarized regimes.

Development of advanced probes

CEA Cadarache; Etat Belge- Ghent University; ENEA - Conzorcio RFX, Padova; OAW (Innsbruck Uni); Ciemat

Development of advanced probe such as the tunnel probe for electron and ion temperature measurements, emissive probe, etc. for the edge plasma diagnostics

Edge plasma measurements on large-scale devices

CEA Cadarache; Confederation Suisse; UKAEA; Ciemat; IST

Measurements of the edge plasma parameters (electron temperature, density, ion temperature and ion flows) in large - scale devices (Tore Supra, JET) and interpretation of experimental data.

Edge plasma modelling

OAW (Innsbruck Uni); VR

Modeling of the particle transport (bulk ions + impurities) at the plasma edge and comparison with experiment.

USX and VUV diagnostics on TCV and CASTOR

Confederation Suisse

Optimization of the USX and VUV diagnostics for spectroscopy measurements and study of the transport of impurities on TCV and CASTOR tokamaks.

EBW on MAST and CASTOR

UKAEA

Modelling of the Electron Bernstein Waves conversion and comparison of results with measurements of microwave radiation by means of radiometers.

Generation of fast particles in front of LH grills

CEA Cadarache; TEKES; OAW (Innsbruck Uni); UKAEA

Modeling of generation of fast particles in front of Lower Hybrid grills and comparison of the result with experiment.

Atomic data

OAW (Innsbruck Uni)

Study of interaction of hydrocarbon ions with fusion-relevant surface.

Representatives of the Association EURATOM/IPP.CR

in European Committees
2002-2003

Consultative Committee for the EURATOM Specific Programme
on Nuclear Energy Research - Fusion

Pavel Chráska   Institute of Plasma Physics, Academy of Sciences of the Czech Republic
Milan Tichý   Faculty of Mathematics and Physics, Charles University, Prague

Scientific and Technology Advisory Committee

Jan Stöckel   Institute of Plasma Physics, Academy of Sciences of the Czech Republic
Milan Zmítko   Nuclear Research Institute, Plc, Rež

EFDA Steering Committee

Jan Dobeš   Institute of Nuclear Physics, Academy of Sciences of the Czech Republic

International Board of Advisors
of the Association EURATOM-IPP.CR

The Board was established with the aim to form the scientific program and assess scientific achievements of the Association:

Dr. Michael Endler	Max-Planck-Institut für Plasmaphysik, Greisfwald, Germany
Dr. Carlos Hidalgo	CIEMAT, Madrid, Spain
Dr. Jochen Linke	Forschungszentrum Jülich GmbH, Jülich, Germany
Dr. Yves Peysson	CEA, Cadarache, France
Prof. Michael Tendler	Royal Institute of Technology, Alfven Laboratory, Stockholm, Sveden
Dr. Martin Valovič	UKAEA, Culham laboratory, United Kingdom
Prof. Guido Van Oost	Ghent University, Gent, Belgium
Dr. Henri Weisen	EPFL, Lausanne, Switzerland
Prof. Hannspeter Winter	Technische Universitaet, Wien, Austria

The first meeting was held in the year 1999, already before signing the Contract of Association. The two-day meetings are organized annually (usually in April) in the Institute of Plasma Physics, Prague.

Conferences and Meetings organized by the Association
(2002-2003)

1. *5th Workshop "Role of Electric Fields in Plasma Confinement and Exhaust"*
The Satellite meeting of the 29th EPS Conference on Plasma Physics and Controlled Fusion, Montreaux, June 23-24, 2002, 40 participants from 12 countries, Proceedings published in the Czechoslovak Journal of Physics, 52, 2002, No. 10

2. *6th Workshop "Electric Fields, Structures and Relaxation in Edge Plasmas"*
The Satellite Meeting of the 30th EPS Conference on Controlled Fusion and Plasma Physics, St. Petersburg, June 13-14, 2003, 32 participants from 12 countries. Proceedings published in the Czechoslovak Journal of Physics, 53, 2003, No. 10.

3. *20th Symposium on Plasma Physics and Technology*
June 10-13, 2002, Praha, 184 participants from 23 countries (co-organized together with the Faculty of Electrical Engineering, Czech Technical University, Prague). Proceedings published as the Supplement D of the Czechoslovak Journal of Physics, 52, 2002,.

4. *1st Summer Training Course in Tokamak Operation (SUMTRAIC 2003)*
co-organized together with the Association EURATOM/HAS at the CASTOR tokamak for 10 Hungarian students, June 2-6, 2003.

Survey of Technology Tasks solved by the Association (2002-2003)

| EFDA reference	Del.	Task description	Principal investigator
Field: Tritium Breeding and Materials, Area: Materials Development			
TW3-TTMA-001	D1	Morphological characterization of unradiated SiC/SiC composite: fibres, interface, matrix	V.Balek, NRI
TW2-TTMS-003	D7	Water corrosion effects inside Eurofer tube under PWR conditions	M.Zmítko, NRI
	D12	Water corrosion test under PWR conditions on Eurofer tube/tube and tube/plate weldments	
	D15	Testing of Eurofer under flowing PbLi	
TW2-TTMS-001b	D3	Static and dynamic toughness testing at the transition temperature; neutron irrad. of plates and weldments up to 2,5 dpa at 200-250°C and PIE	P.Novosad, NRI
TW2-TTMS-003b	D4	In-pile PbLi corrosion testing of TBM weldments up to 2 dpa	M.Zmítko, NRI
TW3-TTMS-003	D1	Crack growth kinetic and fracture toughness on Eurofer 97 in presence of hydrogen (up to 10 wppm) at RT 250°C	K.Splíchal, NRI
TW3-TTMN-002	D5ab	Experiments for the validation of cross-sections up to 55 MeV in an IFMIF-like neutron spectrum: a) activation experiment on EUROFER b) transport benchmark on iron	P.Bém, NPI
TW0-TTMI-003	D8	Activation foils and subminiature fission chambers (experimental tests)	P.Bém, NPI
	D13	D-Li reaction source term: Experimental verification of neutron yield based on a thin Li-target	
	D14	Neutron data above 20 MeV: Neutron transport benchmark tests	
TW2 -TTMI-003	D13d	Thin target yield from Li(d,xn) reaction at 17 MeV, angular distribution	P.Bém, NPI
	D14d	Neutron transport benchmark, collimated neutron flux	
TW3-TTMI-003	D6	Experimental verification of the D-Li source term	P.Bém, NPI
TW4-TTMN-002	D6	Experiments for the validation of cross-sections up to 55 MeV in an IFMIF-like neutron spectrum: activation experiment on W	P.Bém, NPI
Field: Tritium Breeding and Materials, Area: Breeding Blanket			
TW2-TTBC-004	D4	Pb-17Li auxillary and purification systems a) Design of auxilliary PbLi loop for HCLL TBM b) Purification system of PbLi (e.g. Bi) and evaluation of impact on Po production	M.Zmítko, NRI
Field: Physics integration, Area: TPDC Diagnostics - Ceramics			
TW3-TPDC-IRRCER	D9	Irradiation effects on candidate Hall probes	I.Ďuran, IPP
Field: Vessel/In Vessel, Area: TVB - Blanket			
TW3-TVB-INPILE	D3	Perform in-pile testing of Be protected PFW mock-ups under heat flux	M.Zmítko, NRI
TW3-TVM-CFCQ1		Measurement of Si content of SNECMA CFC	V.Hnatowicz, NPI
TW3-TVV-EVADIS		Evaluation of welding distortions of VV poloidal segment	L.Junek, IAM

4 Main facilities

The CASTOR Tokamak

The CASTOR tokamak is a small device built in the year 1958 in the Kurchatov Institute in Moscow, which is operational in the IPP Prague since 1977. The vacuum vessel and plasma control systems were substantially reconstructed in the year 1985. The basic characteristics of the device are:
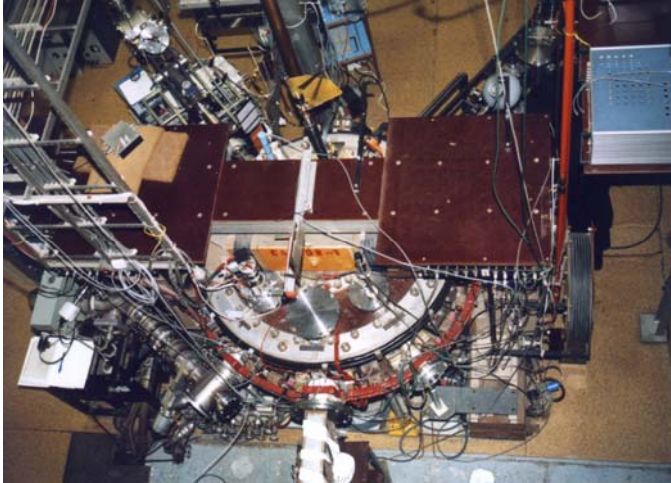
Major radius	40 cm
Minor radius	8,5 cm
Toroidal magnetic field	0,5-1,5 T
Plasma current	5-20 kA
Pulse length	<50 ms
Working gas	Hydrogen

The vacuum vessel (minor radius 100 mm) is made of stainless steel. The plasma cross section is defined by the poloidal limiter made of Molybdenum. The tokamak is equipped by feedback system to control the plasma position within the vessel.

Furthermore, the additional microwave power (f=1.25GHz, P=40kW) can be injected into the ohmic plasma via a multijunction grill for the non-inductive current drive. A graphite electrode is routinely used to polarize the edge plasma.

Vacuum and Conditioning:

The vessel is pumped by one turbomolecular pump (360 l/s), which is switched on in the morning (no pumping during night). Then, it is inductively baked to 250° for 2 hours. The glow discharge in hydrogen (400 V, 0.5 A for 15 min) is used for conditioning of the first wall during the baking. Reasonable plasma discharges can be achieved within 1-2 days after opening the vessel to the atmospheric pressure. The CASTOR tokamak is routinely operating device. Up to 70 reproducible discharges can be achieved during one experimental day.

The typical plasma parameters:

Central electron temperature	100-300eV
Central ion temperature	50-100 eV
Line average density	$0.5-3.10^{19}$ m^{-3}
Energy confinement time	<1 ms

Diagnostics:

- Magnetic diagnostics
- Microwave interferometer at 70GHz

- Photomultipliers with interference filters for measurement of hydrogen and light impurities lines
- VUV spectrometer Seya-Namioka with a high spatial resolution
- XUV spectrometer with multi-layer mirror as disperse element
- Bolometer array for measurements of radiation losses
- Langmuir probe arrays for edge plasma monitoring both in radial and poloidal directions
- Advanced probes for measurements of ion and electron temperatures, plasma potential, and flows in the edge plasma
- Array of coils for measurement of magnetic fluctuations
- Radiometer of electromagnetic radiation at 17-27 GHz and 27-40 GHz
- Microwave reflectometer at 29, 33, and 35 GHz
- Charge exchange analyzer for measurement of ion temperature

Data acquisition systems:

Measured signals are digitized by several A/D converters. Basic data (24 channels) are digitized with the sampling frequency 40 kHz. For fluctuation data, the digitizers with a higher sampling frequency (80 channels, 1 MHz) are used.

Data are stored in a database and processed *a posteriory* either by IDL or Matlab based software.

An example of temporal evolution of the discharge
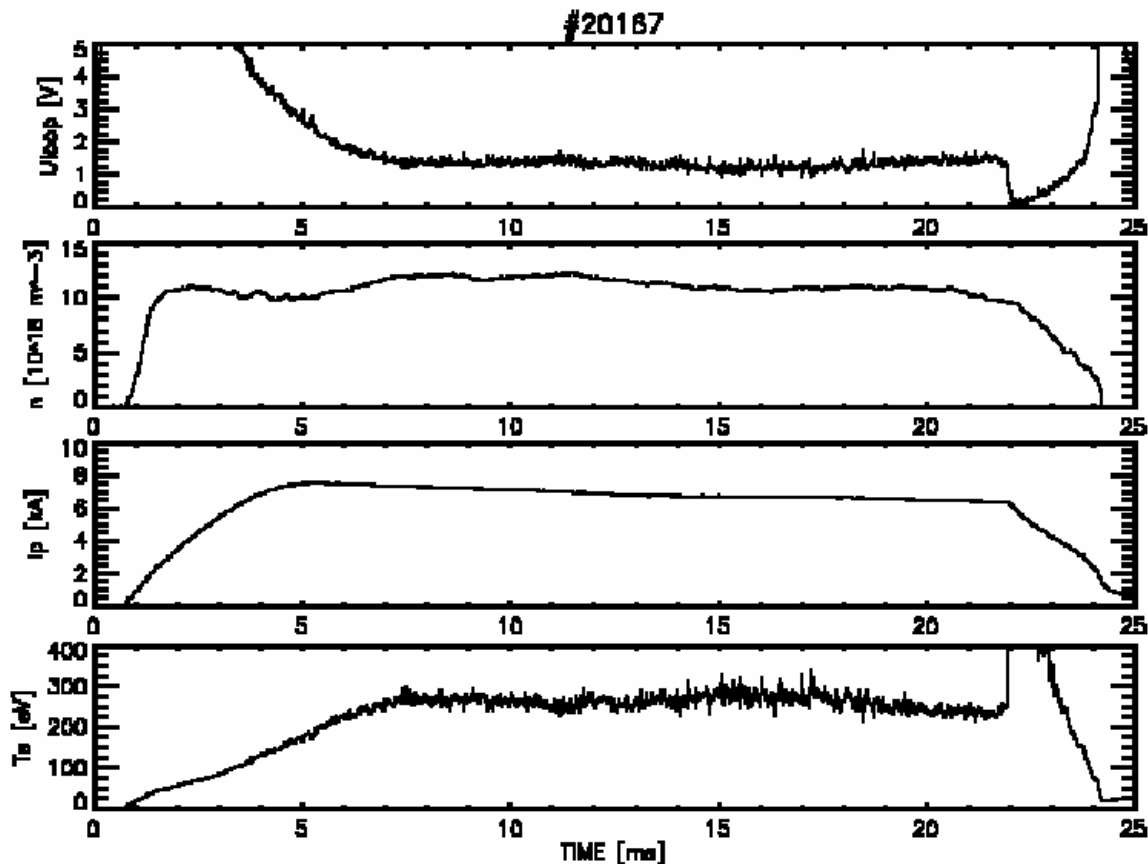
Fission reactor LVR-15

The LVR-15 is a light water moderated and cooled tank nuclear reactor with forced cooling. The maximum power of the reactor is 10 MW. The reactor core is situated in the reactor vessel (outer diameter 2300 mm, total height of the vessel 6235 mm), which is made of stainless steel, the internal part of the rector are made of an aluminium alloy. The reactor has a forced circulation of the coolant. The generated heat is transported via three cooling circuits to the river.

The irradiation capacity

Main irradiation channels	Thermal neutron flux density ($cm^{-2}.s^{-1}$)
Irradiation channels 60 mm in fuel	1.10^{14}
Irradiation channels 60 mm, core periphery	7.10^{13}
Irradiation channels 60/40 mm in reflector	$3-5.10^{13}$
Horizontal channels 100/60 mm	1.10^{8}
Graphite thermal column	1.10^{11}
High pressure water loop	5.10^{13}
Doped silicon facility	1.10^{13}

The irradiation facilities are complemented with well-equipped hot chambers, which allow the irradiated specimens handling.

Experimental facilities:
Light water loops
RVS-3: The loop is designed for material and radioactivity transport investigation under PWR/VVER conditions. It enables to perform irradiation experiments in wide range of operational parameters limited by the following maximum parameters:

Pressure	16,5 MPa
Temperature	345°C
Water flow rate	10 000 kg/hour
Neutron flux	10^{18} n/m^{2}s^{-1}
Electrical capacity heat	100 kW

BWR-1: The loop is designed for investigation of structural materials behaviour and radioactivity transport under BWR conditions

Pressure	10MPa
Temperature	300°C
Water flow rate	2 000 kg/hour
Neutron flux	10^{18} n/m^{2}s^{-1}

BWR-1: The loop is designed for material research simulating conditions of BWR reactors

Pressure	12MPa
Temperature	300°C
Water flow rate	1 000 kg/hour
Force applied to the specimen	152 kN
Duration of the speciment loading cycle	30 hours
Working fluid	ultra-pure water

The NPI cyclotron-based Fast Neutron Facility (NPI FNF)

The project of International Fusion Material Irradiation Facility (IFMIF) aims to provide neutron irradiation tests of fusion materials at fusion-reactor relevant fluency. For testing the neutronic calculations of the IFMIF test cell, the NPI cyclotron-based Fast Neutron Facility (FNF) provides neutron beams with the IFMIF-like spectrum – the only operated within EU countries.

Accelerator

The variable-energy cyclotron U-120M (K=40) of the Nuclear Physics Institute Rez is a versatile machine operating in both positive and negative regimes and accelerating light particles with the mass-to-charge ratio A/Z = 1-2.8. Accelerated beams and energy ranges are shown in the Table 1.

Tab. 1. *Beam parameters of the cyclotron U-120M*

Accelerated ions	H(+)	D(+)	^{3}He(++)	^{4}He(++)	H(-)	D(-)
Energy range (MeV)	10 - 24	10 - 17	17 - 53	20 - 40	10 - 37	10 - 18
Internal beam current (µA)	100	80	40	40	40 -15	25 -10
External beam current (µA)	3	3	3	3	40 -15	25 -10

Beam-line system with ion-optic equipments and target stations consists of three lines in the experimental hall (positive-ion mode, extraction by the deflection system) and one line in the cyclotron hall (negative-ion mode, extraction by the stripping-foil method) - see the Fig. 1. Two of them are dedicated to fast-neutronic experiments within the IFMIF project:
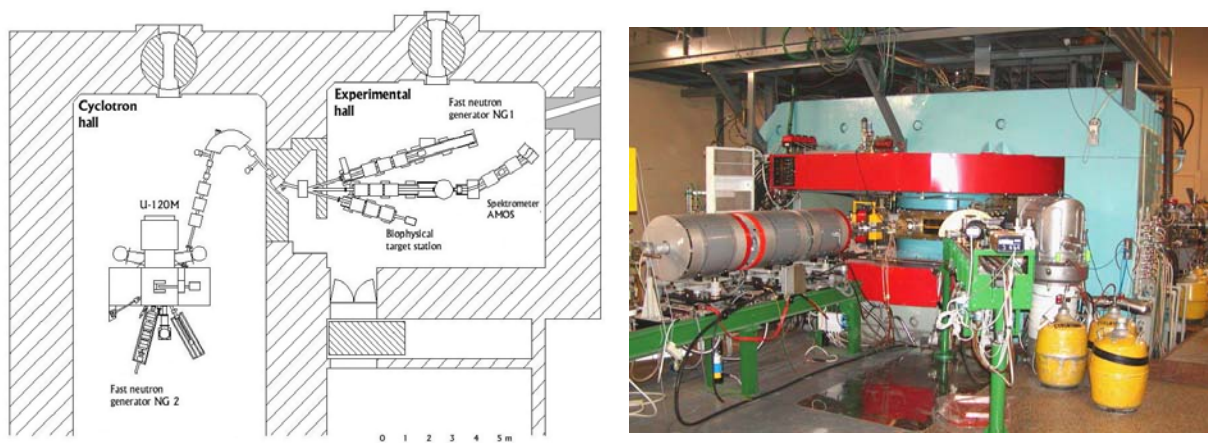

Fig. 1. *Scheme of the NPI cyclotron-based Fast Neutron Facility (left side). The neutron-target stations NG1 and NG2 are installed on the beam-lines of cyclotron operating in the positive- and negative-ion mode (left side), respectively.*

Neutron-spectrometry facility NG1

The cross-section data of neutron emitting reactions induced by charged-particle beams on investigated nuclides are experimentally investigated at the NG1 target station. The angular distributions of emitted fast neutrons (in the energy range from 0.7 to 35 MeV) are measured by the scintillator pulse-height unfolding technique based on the n-gamma discrimination hardware and many-parameter data-acquisition on PC. Different target

technique (including solid, liquid and gas samples) can be utilized on the NG1 target station. To conduct the benchmark tests of neutron-transport calculations provided for fusion relevant materials the neutron source reactions $D_2O(^3He,xn)$ and $D_2O(p,xn)$ were investigated and for the first time employed as the best simulation of the IFMIF spectrum.

Fig. 2. *The experimental arrangement of the neutron transport- (left side) and cross-section measurements (right-side) employing the NG1 target station.*

High-power neutron beam facility NG2

To reach a high-fluence neutron field for the activation-cross-section benchmark tests relevant to IFMIF neutronic calculations, the novel fast-neutron source was developed taking advantage in high beam current of a negative-ion mode of cyclotron operation. With this aim, the proton-induced reaction on heavy-water flow target was investigated for the first time and utilized for the NG2 target station. Besides, the standard Be-targets for protons and deuterons of the NG2 beam line are routinely operated as well. The white-spectrum neutron fields with energy range up to 35 MeV and the flux density up to 3×10^{11} n/cm^2/s are available for the irradiation purposes.
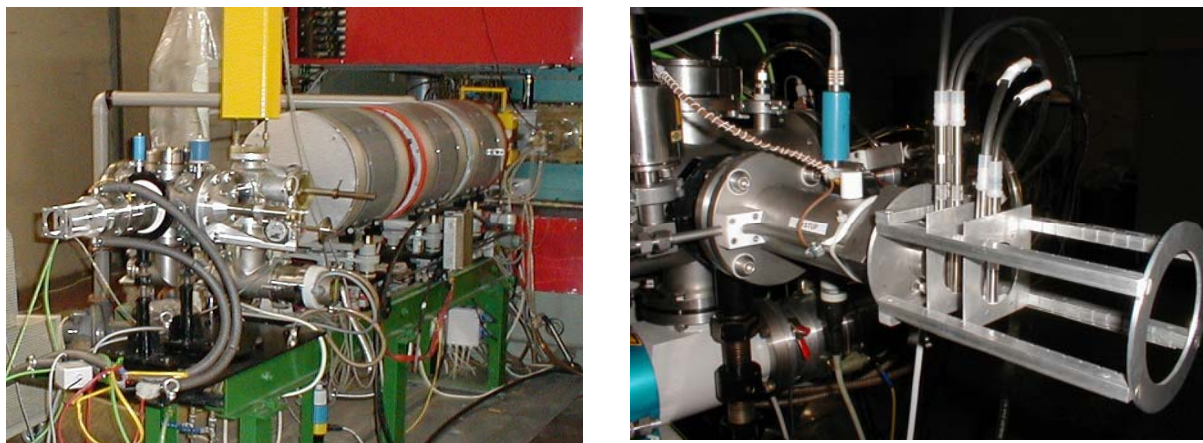

Fig. 3. *The beam line (left side) and the heavy-water-flow target (right side) of the high-power neutron target station NG2.*

II PHYSICS

Physics - summary of the main achievements

The structure and the main topics of the research undertaken in the Association EURATOM/IPP.CR within the reporting period are summarized in the following list.

1) **Edge Plasma and Magnetic Confinement Physics**
   - Generation of convective cells in the SOL plasma on the CASTOR tokamak by biasing material objects localized in this region (electrode, limiter).
   - Active control of the SOL fluctuations by a properly biased poloidal ring of electrodes (the electrostatic limiter) on the CASTOR tokamak.
   - Transport of light impurities through the edge plasma with sheared electric fields.
   - Development and investigation of applicability of lattice Boltzmann methods for MHD flows in plasmas.

2) **Diagnostic Development**
   - Design and tests of advanced probes for measurement of T_e and T_i fluctuations.
   - Enlargement of the viewing angle of existing SXR and UXR monochromators and improvement of their spatial resolution.
   - Verification of the possibility to use diagnostics based on Hall sensors for measurements of magnetic field on ITER in terms of their sufficient radiation and thermal stability as well as their performance in tokamak environment.
   - Design and construction of the hybrid probe head for the TJ-II stellarator to investigate link between electrostatic and magnetic turbulence.

3) **Wave Interactions in Plasmas**
   - Measurements of EC emission on the CASTOR tokamak to study conversions of electron Bernstein waves to X-mode at the upper hybrid resonance. Finalizing the numerical code for interpretation of EC emission on the MAST tokamak. Development of the numerical code for sweeping of antenna beam direction during a discharge to optimise ECRH&CD on MAST.
   - Generation of fast electrons in front of the LH grill, exploration of random field effects on particle acceleration. Current drive simulation in JET and ITER. Formation of plasma vortex in front of the LH grills - modelling and interpretation of experiments.
   - Biasing of protecting limiters to manipulate the density profile in front of the LH grills.

4) **Atomic Physics and Data for Edge Plasma and Plasma Wall Interaction**
   - Systematic scattering studies on collisions of projectile hydrocarbon ions with carbon surfaces.

- Measurements of the recombination of H_3^+ and D_3^+ using direct detection of ions by means of cavity ringdown spectroscopy. Alternatively, measurements of both the recombination rates in a Flowing Afterglow Langmuir Probe (FALP) apparatus at higher D_2 (H_2) densities.

1. Edge Plasma and Magnetic Confinement Physics

Main result

- The convective cells are generated in the SOL plasma on the CASTOR tokamak by biasing material objects localized in this region (electrode, limiter). An electrode is inserted into the SOL region with a long parallel connection length and biased with respect to the poloidal limiter. Formation of a biased flux tube emanating from the electrode and following helicity of magnetic field lines in the SOL is proved. The resulting electric field is two-dimensional and drives the SOL plasma due to the E×B drift. The density profile is locally modified (by a factor of 2-3) both in the radial and poloidal direction. These observations are consistent with results of recent experiment with biasing of divertor plates on the MAST tokamak. [1]

Further achievements

- The poloidal structure of the SOL turbulence is investigated on CASTOR by means of the new ring of 124 Langmuir probes surrounding the full poloidal cross-section. The spatial resolution is sufficient to study details of poloidal distribution of density and potential fluctuations as well as the fluctuation induced flux. The analysis of experimental data reveals a wave-like feature with the poloidal mode number which equals to the local safety factor q and propagates poloidally due to the $E_r \times B_t$ drift. This observation is preliminary interpreted as an existence of a *single* dipole structure in the SOL, which snakes q-time around the torus from the electron to ion side of the poloidal limiter. This dominant feature is superimposed to the broadband turbulence. Under some conditions, the turbulent structures with a significantly lower poloidal mode (m=0 or 1) appear intermittently (50 - 300 μs). Their nature is not yet understood and further experiments are envisaged [2],[3],[4],[5],[6].

- Systematic measurements of the ratio of CVI/CV spectral lines were performed on the TCV tokamak in different discharge conditions (ohmic, L-mode, H-mode with different triangularity and elongation). Remarkable increase of this ratio was observed after the transition from L- to H-mode. According to simulations by the STRAHL code, the increase of the line ratio is due to a drop of the diffusion coefficient inside the edge transport barrier.

- Edge density, temperature and Mach number were systematically measured on Tore Supra in discharges with the supersonic pulsed gas injection fuelling. It was found that the maxima of the relative change of the SOL density and the absolute change of the Mach number are proportional to the amount of injected gas. Moreover, the sign of the Mach number depends whether the gas is injected either from the high or low field side of the torus [7],[8]. Coupling of parallel flows and fluctuation induced transport was investigated on JET [9],[10],[11],[12],[13]. The perpendicular and parallel flows were measured at limiter biasing on the ISTTOK tokamak by using the optimised Gundestrup probe developed in IPP Prague [14].

- The poloidal ring of 32 electrodes has been used for preliminary experiments on active control of the edge turbulence on CASTOR. Two biasing schemes of the electrodes were tested: In the first case, the AC voltage (40 V, 20-40 kHz was applied simultaneously on all the electrodes. An increase of fluctuation level in the SOL was observed. Secondly, a

travelling wave of potential (with the poloidal mode m=4) was applied to the poloidal ring of electrodes. Synchronization of the edge fluctuations with this mode was observed [15],[16],[17],[18]. Further progress in this technique requires a new electronic system for biasing in particular digital delay units. Design and construction of these units is underway.

- Relaxation of plasma potential and poloidal flows after electrode biasing in CASTOR [19] was studied. The observed damping times, 10-30 μs, are smaller than the expected damping time based on magnetic pumping mechanism (~100 μs) and atomic physics via charge exchange (500 μs) and slightly larger than the correlation time of plasma turbulence. This suggests an existence of anomalous (turbulent) mechanism in damping rates of electric fields and poloidal flows in the boundary of tokamak plasmas [20].

- The mechanism of the diffusion of light impurities (C^+) in Hasegawa-Mima model of the turbulent potential was studied numerically, taking into account the finite Larmor radius effects. The dynamics of impurity ions is characterized by means of a variance and diffusion coefficient. It was found that the carbon C^+ ions diffuse considerably faster than electrons, which is different from a commonly used drift approximation (i.e. neglecting the finite Larmor radius of the ions). This difference between the cross-field ion and electron diffusion might cause a charge separation and, consequently a possible generation of radial electric fields in turbulent plasmas [21]. This effect was also identified, when a real turbulent potential measured experimentally by the 2D array of 64 Langmuir probes at CASTOR tokamak was used for simulation. The diffusion coefficient of C^+ ions is approximately two times higher than the electron one in this case.

- The ways of application of the Lattice Boltzmann (LB) methods to resistive MHD problems were further exploited. A model based on octagonal streaming lattice using a scalar distribution function to recover the density, velocity field and momentum flux tensor and a vector distribution function to recover the magnetic field and magnetic flux tensor has been derived. This scalar-vector distribution function approach decouples the viscosity from the resistivity and also allows greater freedom in choosing expansion coefficients for the distribution functions, resulting in a better numerical stability. A number of standard test case simulations have been performed. Additionally, an algorithm for a non-uniform grid LB modelling has been developed. It allows refining the grid in the regions where large gradients in the fields develop thus decreasing the field gradients with respect to the grid density. This grid refinement proved to be a robust methodology [22],[23],[24],[25],[26],[27].

2. Diagnostic Development

Main result

- Development and extensive testing of several variants of a new Langmuir probe for fast measurement of plasma edge T_e, $T_{i\parallel}$, and $T_{i\perp}$, so-called tunnel probe, was done at CASTOR. The systematic difference has been found between T_e measured by the standard Langmuir probes and the tunnel probe which gives lower values of T_e by a factor of 2-3. Several reasons were suggested to explain the observed discrepancy, but no of them was found to be decisive. The self-consistent, two-dimensional kinetic code XOOPIC is used to understand physical processes inside the probes and to interpret correctly the experimental data. This work was performed in close collaboration with the Tore Supra team. The experiments with optimised version of the so-called tunnel probe are currently under preparation on Tore Supra tokamak [28],[29],[30]. Preliminary measurements of perpendicular ion temperature were performed with the modified tunnel

probe (Katsumata version) [31],[32]. These experiments were supplemented by measurements of plasma potential fluctuations done by emissive probes [33],[34],[35],[36],[37].

Further achievements

- Ion temperature was measured in the SOL of the JET tokamak using the bi-directional RFA probe head mounted on the fast reciprocating probe drive. A kinetic model that describes impact of plasma flow on the RFA measurements was used to obtain correct T_i. The T_i was found to be ~ 2 times of T_e near the separatrix in JET ohmic plasmas [38], [39],[40],[41].

- The optimized versions of the VUV and USX spectrometers (monochromators) were put into routine operation on the CASTOR tokamak. The precise spatial calibration of both monochromators was performed. The spatial profiles of the chord integrated line intensity have been measured in the wavelength range of 50 – 200 nm. The first experiments were dedicated to the spectroscopic characterisation of various configurations of the CASTOR regimes with edge plasma polarisation [42],[43],[44],[45],[46],[47].

- A microwave frequency sweeping radiometer for measurement of microwave radiation on the CASTOR tokamak has been constructed. It consists of two super-heterodyne receivers 17-27 GHz and 27-40 GHz. Each band has 16 frequency channels. The sweep time cycle is 160 μs. A single frequency can be measured with the temporal resolution 1 μs.

- Correlation reflectometer, which consists of two identical antenna systems spaced 90° toroidally apart has been constructed. Each system is composed of three horns. Both the systems can operate either in O- or X-mode at three fixed frequencies, 29, 33 35 GHz. First successful tests of the system were performed.

- Magnetic probes based on Hall effect offer several advantages over the standard magnetic coils among them smaller size, and the ability to measure the DC magnetic field. The magnetic probe head containing 9 Hall sensors was successfully tested on TEXTOR tokamak [48],[49]. The hybrid magnetic probe having 6 coils and 2 Hall sensors has been constructed and it is being prepared for use on the TJ-II stellarator. Effort to prepare a prototype magnetic probe head for ITER Steady State Magnetic Diagnostics has been undertaken in collaboration with Lviv Polytechnic National University, Ukraine and the ITER International Team.

- The reciprocating sample holder, containing 10 CFC samples, was used to study impact of Tore Supra SOL plasma irradiation on the properties of CFC. The software for evaluation of heat flows onto the individual samples was developed. The heat fluxes measured in the Tore Supra SOL are comparable to those that are expected to occur near the ITER divertor target plates between the ELMs.

3. Wave Interactions in Plasmas

Main result

- A 3D model of Electron Bernstein Waves propagation, absorption and X- and O-mode conversion has been developed and used to determine ECE emission from the MAST plasma. The instantaneous magnetic field and its spatial derivatives are reconstructed from a 2D splining of two potentials determined by an EFIT equilibrium reconstruction code. The plasma density and temperature profiles are obtained in the whole *RZ* cross-section of the plasma from mapping the high spatial resolution Thomson scattering

measurements on magnetic surfaces. The intersection of the antenna pattern with the separatrix determines both the spot position (at which the antenna is aimed) as well as the components of the wave vector of the outgoing waves. The auxiliary plane-stratified plasma slab is used to determine the mode conversion efficiency by a numerical full wave solution of the wave propagation. To determine the radiative temperature we must study the propagation of EBW in 3D. For this purpose we adopt standard ray tracing. The antenna beam is supposed to be Gaussian and is replaced by a set of rays. An angular divergence of the rays is determined from the geometry of experiment [50],[51] [52],[53].

Further achievements

- The plasma density variations in front of the grill mouth at growing LH power resulting from the local fast particle production in front of the LH grill were explored by our 3D numerical code describing the plasma vortex in front of active LH grills. The results agree with measurements of the reflection coefficient in Tore Supra. According to these numerical simulations, the power flux carried by the plasma outflow (including ions) toroidally from the grill grows approximately as the third power of the average energy of the locally accelerated electrons. This again roughly agrees with experiments. As found in Tore Supra, the heat flux on the bottom limiter can grow even more steeply. Further, hot spots due to parasitic absorption of the LH power in the near field of the LH grill have been observed at JET with a CCD camera and their brightness was analysed with IRMA software. The analysis of the observed hot spots and of the magnetic field connections demonstrates that the fast particles produced in a thin layer in front of the grill mouth can travel several times around the torus, similarly as in Tore Supra. According to the analysis, the brightness of the spots clearly decreases with increasing distance between the last closed flux surface and the poloidal limiter, which is beneficial from the point of view of the ITER design [54],[55],[56],[57],[58].

- The fast particles generated in front of the LH grill on the CASTOR tokamak were identified by means of Langmuir probes. The measurements show that the floating potential drops significantly in a narrow (~ mm) region in front of the antenna, which is a signature of particle acceleration. Moreover, the maximum drop is slightly shifted from the grill mouth into the plasma. This is in accordance with the JET measurement [59], showing the maximum of the hot spots brightness at the divertor apron, if the LH grill is slightly retracted behind the limiter. The double probes (with two floating tips spaced either toroidally or poloidally) are used to estimate the toroidal electric field and the poloidal rotation. The main results of these measurements are summarized in [60].

- In order to simulate the electron and ion response along magnetic field lines along the LH grill to a distant target, a quasi-neutral PIC (QPIC) code which dispenses with the Poisson equation has been developed. Quasi-neutrality is imposed via a charge separation (i.e. ambipolar) electric field calculated from the electron momentum fluid equation. The Langevin method leads to a spatially much smoother electron response than that from the spatially discontinuous grill electric field structure, which is explicit in the Newton representation. Correspondingly, the number of simulation cells needed for spatial resolution is greatly reduced. For simulations with about 10^5 to 10^6 electrons this results in substantial CPU time savings [61],[62].

- The non-linear mechanism of the stochastization of particle motion in a spatially localized monochromatic lower hybrid wave of high amplitude was studied. Such a model of the interaction enables a simple analytic formulation and numerical elaboration.

Using this simple model we have found strong acceleration of electrons with velocities far from the phase velocity of the wave, the change of the distribution function, and formation of a bump-on-tail distribution. This simple model might help in explanation of the spectral-gap problem, especially at the plasma edge, where the spatial envelope of the RF field is rectangular [63],[64],[65].

4. Atomic Physics and Data for Edge Plasma and Plasma Wall Interaction

Main result

- Interaction of hydrocarbon ions $C_2H_n^+$ (n=2,3,4,5) with heated (1000 K) and room temperature carbon surfaces was investigated in beam-surface scattering experiments. Dissociation pathways of surface-excited projectile ions were elucidated. The ion survival probability for closed-shell ions (about 10%) is more than 10-times higher than for the open-shell ions. The main chemical reaction with hydrocarbons adsorbed on the carbon surface leads to the stable $C_3H_3^+$ product ion [66],[67],[68],[69],[70],[71],[72],[73],[74].

Further achievements

- The effect of initial internal energy on the surface-induced dissociation of polyatomic projectile ions $C_2H_n^+$ was investigated. It was found that the $C_2H_n^+$ projectiles with initial internal energy fragmented more profoundly when excited in a surface collision. Thus it appears that their internal energy was preserved in the surface collision and available in subsequent dissociation processes.

- Recombination of H_3^+ and D_3^+ ions with electrons was studied in He-Ar-H_2 stationary and flowing plasma. The rate coefficient of the overall recombination of D_3^+ ions with electrons was determined. It is found that the dominant process is tree body recombination, while the dissociative recombination appears to be negligible [75],[76],[77],[78],[79],[80],[81],[82],[83],[84].

LIST OF PUBLICATIONS (PHYSICS)

1. Edge Plasma and Magnetic Confinement Physics

[1] P. Devynck, M. Farge, K. Schneider, J. Stöckel, M. Hron, I. Ďuran, J. Adámek, G. Van Oost: *Diffusive and Convective Parts of the Turbulent Flux in the SOL of Tokamaks*, 30th EPS conference on Plasma Physics and Controlled Fusion, St Petersburg, July 2003, ECA, **27A** (2003) P1.168.

[2] J. Stöckel, P. Devynck, G. Bonhomme, E. Martines, G. Van Oost, M. Hron, I. Voitsekhovitch, J. Adámek, F. Doveil, I. Ďuran, J. Gunn, P. Stejskal, V. Weinzettl: *Poloidal structure of the scrape off layer turbulence in the CASTOR tokamak*, 30th EPS conference on Plasma Physics and Controlled Fusion, St Petersburg, July 2003, ECA, **27A** (2003) P1.179.

[3] Hron M., Martines E., Devynck P., Benhomme G., Gravier E., Adámek J., Doveil F., Voitsekhovitch I., Stockel J., Azeoual A., Ďuran I., Van Oost G., Žáček F.: *Probe array diagnostics for spatially resolved fluctuation measurements*, 29th EPS conference on Plasma Physics and Controlled Fusion, Montreux, 17-21 June 2002, ECA, **26B** (2002) P5.043.

[4] P. Devynck, J. Stöckel, J. Adámek, I. Ďuran,, M. Hron, G. Van Oost: *Poloidal structure of the turbulence and turbulent flux during edge plasma biasing in the CASTOR tokamak*, 6th Satellite meeting on the Electric Field, Structures and Relaxation in the Edge Plasma, published in Czech. J. Phys **53** [10] (2003) 853-862.

[5] Martines E., Hron M., Stöckel J.: *Coherent structures in the edge turbulence of the Castor tokamak.* Plasma Phys. Contr. Fusion **44** (2002) 351-359.

[6] Martines E., Antoni V., Cavazzana R, Regnoli G., Serianni G., Spoalore M., Vianello N. Hron M., Stöckel J.: *Coherent structures in the plasma edge of the RFX and CASTOR experiments.* Czech. J. Phys. **52** (2002) D13-D24.

[7] I. Duran, J.P. Gunn, , R. Pánek, J. Adámek, J. Bucalossi, T. Loarer, J.-Y. Pascal, B. Pégourie, E. Tsitrone, J. Stöckel: *Scrape-Off Layer Response to Supersonic Gas Injection in Tore Supra,* 30th EPS conference on Plasma Physics and Controlled Fusion, St Petersburg, July 2003, ECA, **27A** (2003) P1.181.

[8] E. Tsitrone, J. Bucalossi, T. Loarer, B. Pegourie, C. Brosset, E. Delchambre, A. Adamek, I. Duran, A. Grosman, P. Ghendrih, C. Grisolia, J. Gunn, J. Hogan, R. Mitteau, R. Panek, V. Philips, R. Reichle**,** D. Reiter, P. Roubin, and Tore Supra team: *Steady state density control in Tore Supra long discharges,* 30th EPS conference on Plasma Physics and Controlled Fusion, St Petersburg, July 2003, ECA, **27A** (2003) O-2.5A.

[9] C Hidalgo, B Gonçalves, M A Pedrosa, J Castellano, K Erents, A L Fraguas, M Hron, J A Jiménez, G F Matthews, B van Milligen, C Silva: *Empirical similarity in the probability density function of turbulent transport in the edge plasma region in fusion plasmas*, Plasma Phys. Contr. Fusion, **44** (2002) 1557-1564.

[10] Gonalves B., Hidalgo C., Pedrosa M. A., Silva C., Balbín R., Erents K., Hron M., Loarte A., Matthews G.: *Edge localized modes and fluctuations in the JET SOL region.* Plasma Physics and Controlled Fusion **45** [9] (2003) 1627-1635.

[11] C. Hidalgo, B. Gonçalves, C. Silva, M. A. Pedrosa, K. Erents, M. Hron, and G. F. Matthews: *Experimental Investigation of Dynamical Coupling between Turbulent Transport and Parallel Flows in the JET Plasma-Boundary Region*, Phys. Rev. Lett., **91** (2003) 065001.

[12] C. Hidalgo, B. Gonçalves, C. Silva, M.A. Pedrosa, K. Erents, M. Hron, G. F. Matthews, R. Pitts: *Experimental investigation of dynamical coupling between turbulent transport and parallel flows in the JET plasma boundary region*, 30th EPS conference on Plasma Physics and Controlled Fusion, St Petersburg, July 2003, ECA, **27**A (2003) P3.200.

[13] B. Goncalves, C. Hidalgo, M.A. Pedrosa, C. Silva, K. Erents, G. Matthews, M. Hron, A. Loarte, R.A. Pitts: *Statistical properties of turbulence: a new approach to characterize transport in fusion plasmas*, Czech. J. Phys, **53** [10] (2003) 827-852.

[14] Silva C, Nezdelskiy I., Figuerredo H., Cabral JAC, Varandas C, Stockel J: *Limiter biasing experiments on the ISTTOK tokamak*, 6th Satellite meeting on the Electric field, structures and relaxation in the edge plasma, Czech. J. Phys, **53** [10] (2003) 937-944.

[15] Stockel J., Devynck P., Voitsekhovitch I., Adámek J., Azeoual A., Benhomme G., Doveil F., Ďuran I., Gravier E., Hron M., Martines E., Van Oost G.: *Turbulence and transport with constant and spatial-temporal biasing in the scrape-off layer of CASTOR tokamak*, O2.03, 29th EPS conference on Plasma Physics and Controlled Fusion, Montreux, 17-21 June 2002, ECA, **26B** (2002) O2.03.

[16] Stockel J., Devynck P, Voitsekhovitch I., Benhomme G., Martines E., Van Oost G., Adámek J., Azeoual A., Doveil F., Ďuran I., Hron M., Gravier E., Zacek F.: *Turbulence and transport with spatial temporal biasing in the scrape-off layer of CASTOR tokamak,* Proc. 19th IAEA Conference on Controlled Fusion, Lyon, October 2002.

[17] G Van Oost, J Adamek, V Antoni, P Balan, JA Boedo, P Devynck, I Duran, L Eliseev, J Gunn, M Hron, C. Ionita, S Jachmich, G Kirnev, E Martines, A Melnikov, R Schrittwieser, C Sylva, J Stockel, M Tendler, C Varandas, M Van Schoor, V Vershkov, R Weynants: *Turbulent Transport Reduction by ExB Velocity Shear during Edge Plasma Biasing: Recent Experimental Results*, Plasma Phys. Contr. Fusion, **45** (2003) 1-23.

[18] V. Weinzettl, I. Ďuran, J. Zajac, V. Piffl: *Edge plasma biasing experiments on the CASTOR tokamak: spectroscopic investigation and microwave measurements,* Czech. J. Phys, **53** [10] (2003) 925-935.

[19] Van Oost G., Adámek J., Antoni V., Balan P., Boedo J.A., Devynck P., Duran I., Eliseev L., Gunn, J., Hron M., Ionita C., Jachmich S., Kirnev G., Martines E., Melnikov A., Schrittwieser R., Silva C., Stöckel J., Tendler M., Varandas C., Van Schoor M., Vershkov V., Weynants R.: *Turbulent Transport Reduction by ExB Velocity Shear during Edge Plasma Biasing: Recent Experimental Results.* Plasma Phys. Contr. Fusion **45** [1] (2003) 1-23.

[20] M. Hron, C. Hidalgo, I. Ďuran, J. Gunn, J. Stöckel: *Relaxation of plasma potential and poloidal flows in the boundary of tokamak plasmas*, 30th EPS conference on Plasma Physics and Controlled Fusion, St Petersburg, July 2003, ECA, **27**A (2003) P1.172.

[21] Panek R, Krlin L, Tsakaya D., Kuhn S, Stockel J., Pavlo P., Svooboda V., Tendler M., Klima R., Petrzilka V., Zapotocky M., *Radial electric field generation due to edge plasma turbulence*, 30th EPS Conference on Contr. Fusion and Plasma Phys., St Petersburg, Russia, July 7- 11, 2003, ECA, **27**A (2003) P1.178.

[22] Pavlo P., Vahala G., Vahala L.: *Preliminary results in the use of energy-dependent octagonal lattices for thermal lattice Boltzmann Simulations*, J. Stat. Phys. **107**, No.1/2 (2002) 499-519.

[23] Macnab A., Vahala G., Vahala L., Pavlo P., Soe M.: Some progress in the development of Lattice Boltzmann *Methods for Dissipative MHD,* Czech. J. Phys. **52**, Suppl. D (2002) D59-D64.

[24] Macnab A., Vahala G., Vahala L., Pavlo P.: *Lattice Boltzmann Model for Dissipative MHD,* 29th EPS Conference on Contr. Fusion and Plasma Phys., Montreux, Switzerland, June 17- 21, 2002, ECA, **26**B (2002) P1.111.

[25] Macnab A., Vahala G., Vahala L., Pavlo P., Soe M.: *Lattice Boltzmann Approach to Resistive MHD*, Bull. Am. Phys. Soc. **47** (2002) 51.

[26] Macnab A., Vahala G., Vahala L., Pavlo P.: *A Non-Uniform Lattice Boltzmann Method for Fluid Flow Simulations* 30th EPS Conference on Contr. Fusion and Plasma Phys., St Petersburg, Russia, July 7- 11, 2003, ECA, **27**A (2003) P3.188.

[27] Vahala L., Vahala G., Pavlo P.: *Non-Uniform Spatial Grids in Lattice Boltzmann MHD Algorithms*, Bull. Am. Phys. Soc. **48** (2003) FP1.107.

2. Diagnostics development

[28] Gunn JP, Devynck P., Pascal J.-Y, Adamek J, Duran I., Hron M, Stockel J, Zacek F, Barina O, Hrach R, Vicher M, Van Oost G: *A DC probe diagnostics for fast electron temperature measurements in tokamak edge plasmas*. Czech J. Phys, **52** (2002) 1107-1114.

[29] Gunn J.P. Adamek J., Bařina O., Devynck P., Ďuran I., Hrach R., Hron M., Pascal J.-Y., Stockel J., Van Oost G., Vicher M., Žáček F.: *A DC diagnostics for fast electron temperature measurements in tokamak edge plasma*, 29th EPS conference on Plasma Physics and Controlled Fusion, Montreux, 17-21 June 2002, ECA, **26**B (2002) P5.093.

[30] Gunn J,P, Stöckel J., Adamek J., Balan P., Barina O., Devynck P., Duran I., Hrach R., Hron M., Ionita C., Schrittwieser R., Van Rompuy T., G. Van Oost, Vicher M., Zacek F.: *Advances in the measurements and control of tokamak edge turbulence,* in Proc 19th IAEA Fusion Energy Conferencs, Lyon, October 2002 poster EX/P1- 06.

[31] P. Balan, J. Adámek, O. Bařina, P. DeBeule, I. Ďuran, J.P. Gunn, M. Hron, C. Ionita, E. Martines, R. Panek, R. Schrittwieser, J. Stöckel, G. Van Den Berge, G. Van Oost, T. Van Rompuy: *Simultaneous Measurement of Electron and Ion Temperatures with a New Kind of Langmuir Probe*, 30th EPS conference on Plasma Physics and Controlled Fusion, St Petersburg, July 2003, ECA, **27**A (2003) P-1.84.

[32] P. Balan, R. Schrittwieser, J. Adámek, O. Bařina, P. DeBeule, I. Ďuran, J.P. Gunn, M. Hron, C. Ionita, E. Martines, R. Panek, , J. Stöckel, G. Van Den Berge, G. Van Oost, T. Van Rompuy: *Measurement of the Parallel and Perpendicular Ion Temperatures by means of an Ion sensitive Segmented Tunnel Probe*, Workshop on Electric probes in magnetized plasmas, Greisfwald, July 2003, published in Contribution to Plasma Physics **44**, No 7-8, (2004) 683-688.

[33] P. Balan, J. Adámek, I. Ďuran, M. Hron, C. Ioniță, E. Martines, R. Schrittwieser, J. Stöckel, M. Tichý, G. Van Oost, "Measurements of the Plasma Potential Fluctuations and the Fluctuations-Induced Flux in the CASTOR Tokamak", *Workshop on Turbulence and Anomalous Transport in Plasmas and Fluids* (Risø, Roskilde, Denmark, 2002), Oral Presentation.

[34] Adamek J., Duran I., Hron M., Stockel J., Balan P., Schrittwieser R, Ionota C., Martines E., Tichy M., Van

Oost G., *Fluctuation measurements with emissive probes in tokamaks,* Czech J. Phys, **52** (2002) 1115-1120.

[35] Balan P., Adamek J., Duran I., Hron M., Ionota C., Martines E., Schrittwieser R., Stockel J., Tichy M., Van Oost G.: *Measurements of the fluctuation induced flux with emissive probe in the CASTOR tokamak*, 29th EPS conference on Plasma Physics and Controlled Fusion, Montreux, 17-21 June 2002, ECA, **26**B (2002) P2.072.

[36] P. Balan, R. Schrittwieser, C. Ionita, J.A. Cabral, H.F.C. Figureiredo, H. Fernandes, C. Varandas, J. Adamek. M. Hron, J. Stockel, E. Martines, M. Tichy, G.Van Oost: *Emissive probe measurements of the plasma potential fluctuations in the edge plasma regions of tokamaks,* Review of Scientific Instruments, **74** (2003) 1583-1587.

[37] R. Schrittwieser, J. Adámek, P. Balan, M. Hron, C. Ioniţă, K. Jakubka, L. Kryska, E. Martines, J. Stöckel, M. Tichý, G. Van Oost: *Measurements with an emissive probes in the CASTOR tokamak*, Plasma Phys. Contr. Fusion **44** (2002) 567-578.

[38] R.A. Pitts, I. Duran, S.K. Erents, J. Horacek, G.F. Matthews, *Retarding field analyzer measurements in the JET plasma boundary*, 30th EPS Conference on Contr. Fusion and Plasma Phys., St Petersburg, Russia, July 7- 11, 2003, ECA, **27**A (2003) P-2.84.

[39] R.A. Pitts, R. Chavan, S.K. Erents, G. Kaveney, G.F. Matthews, G. Neill, J.E. Vince, I. Duran, *A retarding field energy analyzer for the JET plasma boundary*, Review of Scientific Instruments, **74** (2003) 4644-4657.

[40] R.A. Pitts, R. Chavan, S.K. Erents, G. Kaveney, G.F. Matthews, G. Neill, J.E. Vince, I. Duran: *A retarding field energy analyzer for the JET plasma boundary*, CRPP EPFL Internal report LRP 765/03, pp 1-35.

[41] R. A. Pitts, I. Ďuran, S. K. Erents, J. Horáček, G. F. Matthews: *Retarding field analyzer measurements in the JET plasma boundary,* CRPP EPFL Internal report LRP 766/03, pp 73-76.

[42] V.Piffl, V.Weinzettl, A.Burdakov, S.Polosatkin: *Diagnostic potential of the VUV&XUV imaging spectroscopy*, Transaction of Fusion Science and Technology, January 2003, **43**, [1T] (2003) 231 – 236.

[43] V.Piffl, V.Weinzettl, A.Burdakov, S.Polosatkin: *VUV Imaging Seya-Namioka spectrometer*, Czechoslovak Journal of Physics, **52** (2002) D70-D76.

[44] V.Piffl, V.Weinzettl, A.Burdakov, S.Polosatkin: "VUV Imaging Spectroscopy on CASTOR Tokamak", 29th EPS Conference on Plasma Phys. And Contr. Fusion Montreux, 17-21 June 2002, ECA, **26**B (2002) P4.123.

[45] V.Piffl, V.Weinzettl, A.V.Burdakov, S.V.Polosatkin: *Line Intensity Radial Profiles Evolution in VUV and XUV Spectral Range*, 30th EPS Conference on Controlled Fusion and Plasma Physics, St.Petersburg, ECA, **27**A (2003) P-1.061.

[46] A.V.Burdakov, V.Weinzettl, V.Piffl, S.V.Polosatkin, V.V.Postupaev: *VUV imaging diagnostics on GOL-3 device.* 10th Russian Conference on High-Temperature Plasma Diagnostics, 8-13 June 2003, Troick, Russia, contrib. N5, p. 77-78.

[47] A.V.Burdakov, V.Weinzettl, V.Piffl, S.V.Polosatkin: *Dynamics of light impurities on GOL-3 and CASTOR devices.* 30th Zvenigorod Conference on Plasma Physics, 24-28 February 2003, Zvenigorod, Russia, contrib. MS-2-16, p. 81.

[48] Duran I., Stockel J., Mank G., Finken K.H., Fuchs G., Van Oost G.: *Measurements of magnetic field fluctuations using an array of Hall detectors on the TEXTOR tokamak*, Review of Scientific Instruments, **73** (2002) 3482-3489.

[49] Duran I., Stockel J., Mank G., Finken K.H., Fuchs G., Van Oost G.: *First results of magnetic turbulence measurements using an array of Hall detectors in the TEXTOR tokamak,* Czech. J. Phys., **52**, Suppl. D, (2002), D38-D48.

3. Wave Interactions in Plasmas

[50] J. Preinhealter, V. Shevchenko, M.Valovic, P. Pavlo, L. Vahala, G. Vahala and the MAST team: Interpretation of ECE measurement on MAST.29th EPS Conf. on Contr. Fusion and Plasma Physics, Montreux, (2002), ECA, **26**B (2002) P5.095.

[51] J. Preinhealter, P. Pavlo, V. Shevchenko, M.Valovic and MAST team, L. Vahala, G. Vahala: *Electron Bernstein wave-X-O mode conversion and elefctron cyclotron emission in MAST.* 14th Topical conference on High-Temperature Plasma Diagnostic, Madison 2002, Rev. Sci. Instruments, **74** [3] Part 2 Sp. Iss. (2003) 1437-1440.

[52] J. Preinhealter, V. Shevchenko, M.Valovic, P. Pavlo, L. Vahala, G. Vahala: EBW-X-O and ECE in MAST.Presented at 44th Annual Meeting of the Division of Plasma Physics, Orlando, Florida , November 11-15, 2002. Bulletin of APS 47 (2002) KP1 107, p. 211.

[53] J. Preinhealter, V. Shevchenko, M.Valovic, P. Pavlo, L. Vahala, G. Vahala and the MAST team: ECE in MAST: theory and experiment. 15th Topical Conf. on Radio Frequency Power in Plasmas, Jackson Lake

Lodge, Wyoming, May, (2003), in print.

[54] V.Petržílka. et al. "A 3-D model of the plasma vortex in front of LH grills" "in *Proc of the 28th EPS conference on Cont. Fus. and Plasma Phys., Funchal, Portugal, ECA* Vol. **25**A, (2001) 289-292.

[55] V. Petržílka, A. Ehedahl, V. Fuchs, M. Goniche, J. Guán, L. Krlín, S. Kuhn, K. Rantamäki, D. Tskhakaya, F. Žáček: *LH Driven Plasma Density Variations and Flows in Front of LH Grills and Resulting Reflection Coefficient Changes and Thermal Loads,* 30th EPS Conference on Contr. Fusion and Plasma Physics, St. Petersburg, Russia, 7-11 July 2003, ECA, **27**A (2003) P1.195.

[56] Ekedahl, G. Granucci, J. Mailloux, V. Petrzilka, K. Rantamäki, Y. Baranov, K. Erents, M. Goniche, E. Joffrin, P.J. Lomas, M. Mantsinen, D. McDonald, J.-M. Noterdaeme, V. Pericoli, R. Sartori, C. Silva, M. Stamp, A.A. Tuccillo, F. Zacek and EFDA-JET Contributors, *Long distance coupling of LH waves under ITER relevant edge conditions in JET optimized shear plasmas,* 15th Topical Conf. on RF power in plasmas, May 19-21, 2003, Jackson Lake Lodge, WY, USA, Invited paper I8.

[57] G. Granucci, A. Ekedahl, J. Mailloux, K. Erents, M. Hron, E. Joffrin, P.J. Lomas, M. Mantsinen, J.-M. Noterdaeme, V. Pericoli-Ridolfini, V. Petrzilka, K. Rantamäki, R. Sartori, C. Silva, A.A. Tuccillo, D. McDonald and JET EFDA contributors: *Recent Results of LHCD Coupling Experiments with Near Gas Injection in JET*, 30th EPS conference on Plasma Physics and Controlled Fusion, St Petersburg, July 2003, ECA, **27**A (2003) P1.191.

[58] M.Goniche, V.Petržílka, A.Ekedahl, V.Fuchs, J.Laugier, Y.Peysson, and F.Žáček, *Efect of the launched LH spectrum on the fast electron dynamics in the plasma core and edge,* 15th Topical Conf. on RF power in plasmas, May 19-21, 2003, Jackson Lake Lodge, WY, USA, contributed paper C42.

[59] K.M. Rantamäki, V. Petržílka, A. Ekedahl, K. Erents, V. Fuchs, M. Goniche, G. Granucci, S.J. Karttunen, J. Mailloux, M.-L. Mayoral, F. Žáček and contributors to the EFDA – JET work programme: *Hot Spots Generated by Lower Hybrid Wawes on JET,* 30th EPS Conference on Contr. Fusion and Plasma Physics, St. Petersburg, Russia, 7-11 July 2003, ECA, **27**A (2003) P1.190.

[60] F. Žáček, V. Petržílka, P. Devynck, M. Goniche, S. Nanobashvili, *Toroidal electric field in front of the lower hybrid grill of the CASTOR tokamak,* 30th EPS Conference on Contr. Fusion and Plasma Physics, St. Petersburg, Russia, 7-11 July 2003, ECA, **27**A (2003) P-1.196.

[61] L. Eriksson, C. Fourment, V. Fuchs, X. Litaudon, C. D. Challis, F. Crisanti, B. Esposito, X. Garbet, C. Giroud, N. Hawkes, P. Maget, D. Mazon, G. Tresset.: *Discharges in the JET Tokamak Where the Safety Factor Profile is Identified as the Critical Factor for Triggering Internal Transport Barriers. P*hys. Rev. Lett. **88** (2002) 145001.

[62] V. Fuchs, V. Petržílka, J. P. Gunn, M. Goniche*: Removal of the lower hybrid (LH) frequency time scale in test electron simulations of LH-induced tokamak edge electron flow,* Czech J. Phys. **52** (2002) D45-D50.

[63] V. Fuchs. J. P. Gunn, M. Goniche, V. Petržílka: *Tokamak edge electron diffusion and distribution function in the lower hybrid electric field.* Nucl. Fusion **43** (2003) 341-351.

[64] V. Fuchs. J. P. Gunn, M. Goniche, V. Petržílka: *Removal of the lower hybrid (LH) frequency time scale in quasi-neutral PIC simulations of LH-induced tokamak edge plasma flow*, 29th EPS Conference on Plasma Physics and Controlled Fusion , Montreux, June 2002, ECA, **26**B (2002) P1.086.

[65] Krlín L., Pavlo P., Pánek R., Klíma R., Petržílka V.: *Non-linear effects in LHW plasma interaction.* Plasma Phys. Control. Fusion **44** (2002) 159.

4. Atomic Physics and Data for Edge Plasma and Plasma Wall Interaction

[66] A. Qayyum, T. Tepnual, C. Mair, S. Matt-Leubner, P. Scheier, Z. Herman, T.D. Mar, *The role of internal energy of polyatomic projectile ions in surface induced dissociations.* Chem. Phys. Lett. **376** (2003) 539-547.

[67] Z. Herman, Collisions of slow polyatomic ions with surfaces: *The scattering method and results*, J. Am. Soc. Mass Spectrom. **14** (2003) 1360-1372.

[68] A. Qayyum, Z. Herman, T. Tepnual, C. Mair, S. Matt-Leubner, P. Scheier, T.D. Mark, *Surface induced dissociation of polyatomic hydrocarbon projectile ions with different initial internal energy content.* J. Phys. Chem. (accepted).

[69] C. Mair, Z. Herman, J. Fedor, M. Lezius, T.D. Märk: Surface *induced dissociations and reactions of acetonitrile monomer, dimer and trimer ions*, J. Chem. Phys. **118** (2003) 1479.

[70] C. Mair, M. Lezius, Z. Herman, T.D. Märk: *Surface induced dissociations of protonated ethanol monomer, dimer, and trimer ions: Monomer binding energy and trimer break-down graph.* J. Chem. Phys. **118** (2003) 7090-96.

[71] C. Mair, J. Fedor, M. Lezius, P. Scheier, M. Probst, Z. Herman, T.D. Märk: *Surface-induced reactions and dissociations of small acetone, acetonitrile and ethanol clusterions: Competitive chemical reactions, dissociation mechanisms and determination of binding energy.* New Journal of Physics, **5** (2003) 9.1-9.18.

[72] K. Gluch, J. Fedor, S. Matt-Leubner, R. Parajuli, C. Mair, A. Stamatovic, O. Echt, C. Lifshitz, J. Harvey,

F. Hagelberg, Z. Herman, M. Probst, P. Scheier, T.D. Märk: *Energetics and dynamics of decaying cluster ions*. Eur. Phys. J. D **24** (2003) 131-136.

[73] J. Žabka, Z. Dolejšek, J. Roithová, V. Grill, T.D. Märk, Z. Herman, Int. J. Mass. Spectrom. 213 (2002) 145-156.

[74] J. Roithová, J. Žabka, Z. Dolejšek, Z. Herman, *J. Phys. Chem*. B, 106 (2002) 8293-8301.

[75] V. Poterya, J. Glosík, R. Plašil, M. Tichý, P. Kudrna, A.Pysanenko, *Recombination of D_3^+ ions with electrons in He - Ar - D_2 plasma*, Phys. Rev. Lett. **88** (2002) 044802-1.

[76] R. Plašil, J. Glosík, V. Poterya, P. Kudrna, J. Rusz, M. Tichý, A. Pysanenko, *Advanced integrated stationary afterglow method for experimental study of recombination of H_3^+ and D_3^+ ions with electrons,* International J. Mass. Spectrom., **218** (2002) 105-130.

[77] J. Glosík, O. Novotný, A. Pysanenko, P. Zakouřil, R. Plašil, P. Kudrna, V. Poterya, K. Dryahina, *The recombination of H_3^+ and H_5^+ ions with electrons in hydrogen plasma: Dependence on temperature and on pressure of H_2*, Plasma Sources Sci. Technol. **12** (2003) S117-S122.

[78] P. Macko, G. Bánó, P. Hlavenka, R. Plašil, V. Poterya, A. Pysanenko, J. Glosík, *Decay of H_3^+ dominated low-temperature plasma*, Acta Phys. Slov. 2003 in print.

[79] P. Macko, R. Plašil, P. Kudrna, P. Hlavenka, V. Poterya, A. Pysanenko, G. Bano, J. Glosík, *High-resolution cw-diode laser cavity ring-down spectroscopy in hydrogen plasma at room temperature*, Czechoslovak J. Phys., Vol. **52** (2002) D695-704.

[80] A. Pysanenko, O. Novotný, P. Zakouril, R. Plašil, V. Poterya, J. Glosík, *Recombination of H_3^+ and H_5^+ ions with electrons in He-Ar-H_2 flowing afterglow plasma*, Czechoslovak J. Phys., Vol. **52** (2002) D681-694.

[81] M. Tichý, V. Poterya, R. Plašil, A. Pysanenko, P. Kudrna, O. Novotny, P. Zakouril, J. Glosík, *Application of Langmuir probe for study of recombination of D_3^+ ions with electrons in He-Ar-D_2 stationary and flowing afterglow plasma*, Australia 2002, XXVI International Conference on Phenomena in Ionized Gases - ICPP 2002, Sydney (Australia), July, 2002, 4 pages, in print.

[82] J. Glosík, A. Pysanenko, O. Novotny, P. Zakouril, R. Plasil, V. Poterya, *The recombination of D_3^+ and D_5^+ - Dependence on partial pressure of D_2 and on temperature*. ISPC Sicilia 2003, June 2003.

[83] G. Bano J. Glosík, P. Macko, P. Hlavenka, R. Plasil, A. Pysanenko, V. Poterya, K. Dryahina, *Recombination of $H_3^+(v=0)$ ion. Cavity Ring-down Spectroscopy in pulsed microwave discharge*. ISPC Sicilia 2003, June 2003.

[84] J. Glosík, V. Poterya, A. Pysanenko, R. Plašil, M. Tichy, *Recombination of HCO^+ ions with electrons at thermal energy*, ICPIG, Greifswald, 15.-20.7. 2003.

1   Edge Plasma and Magnetic Confinement Physics

This part of the Report describes some of the achieved results in more detail.

At first, we describe measurements performed in the edge plasma of the CASTOR tokamak by means of arrays of Langmuir probes. The arrays allow measurement with a sufficient spatial and temporal resolution. A full poloidal array of 124 Langmuir tips was used for detail analysis of the edge turbulence. Because of a downward shift of the plasma column, only a bottom part of the ring (~one quarter) acts as the limiter. The remaining tips are effectively localized in the scrape-off layer with the connection length much longer than the toroidal circumference, L>> 2πR. The most interesting result is that only a *single* turbulent structure exists in the SOL in any time instant, being however superimposed to the broadband turbulence. This structure follows helical magnetic field lines, snakes around the torus several times, and propagates poloidally. We also attempt to develop a method for an active control of the edge turbulence. The poloidal array of 32 electrodes was designed for this purpose. If the AC or DC voltage is applied to the individual electrodes, a clear impact on the edge turbulence is observed. We propose to continue these experiments with a more sophisticated hardware. In particular, a new electronics (32 amplifiers and 32 delay units) are manufactured; these will render possible to apply the voltage in a more controllable way.

Measurements were performed also in discharges with a biased electrode immersed in the edge plasma. The aim of these experiments was to amplify electric fields and consequently influence the particle transport. It is found that if the electrode is inserted into the SOL region with a long parallel connection length, a biased flux tube emanating from the electrode is formed. The resulting electric field is two-dimensional, having the radial as well as the poloidal components. The convective motion of the SOL plasma in such field due to the ExB drift was clearly demonstrated. These observations are consistent with recent results from the MAST tokamak, where divertor plates were biased with the same aim. It has to be noted that the above-mentioned experiments were performed on the CASTOR tokamak in close collaboration with the Associations EURATOM – CEA, ENEA (RFX Padova) and Belgium State.

Furthermore, relaxation of plasma potential and poloidal flows after electrode biasing was studied in collaboration with CIEMAT. The observed damping times, 10-30 µs suggest an existence of anomalous (turbulent) mechanism in damping of electric fields and poloidal flows in the boundary of tokamak plasmas.

At Tore Supra, the edge density, temperature and Mach number were systematically measured in discharges with the supersonic gas injection. It was found that the maxima of the relative change of the SOL density and the absolute change of the Mach number are proportional to the amount of injected gas. Moreover, the sign of the Mach number depends on whether the gas is injected from the high or low field side of the torus.

Finally, the motion of light impurities (C^+) in a model turbulent potential is studied numerically. A strong diffusion of impurity ions in this potential is observed. This leads to charge separation and, consequently, to the ambipolar generation of electric fields. This might play a role in the formation of transport barriers at the plasma edge.

Formation of convective cells at the scrape off layer biasing in the CASTOR tokamak

J.Stöckel, M.Hron, P.Stejskal

In collaboration with:

P.Devynck, J.Gunn, Association Euratom/CEA, France,
E.Martines, Associazione Euratom/ENEA sulla Fusione, Padova, Italy,
G.Bonhomme, Université Henri Poincaré, Nancy, France,
G.Van Oost, Ghent University, Gent, Belgium

The experiments on formation of convective cells in the SOL have been carried out on the CASTOR tokamak, which is a small size torus with a major radius of 0.4 m and a minor radius of 0.1 m. In the present experiment, the poloidal limiter with the radius a = 58 mm is equipped with 124 Langmuir probes, uniformly distributed along its circumference. This is apparent from the photo shown in Fig. 1. The individual tips are 2.5 mm long and spaced poloidally by ~3 mm.
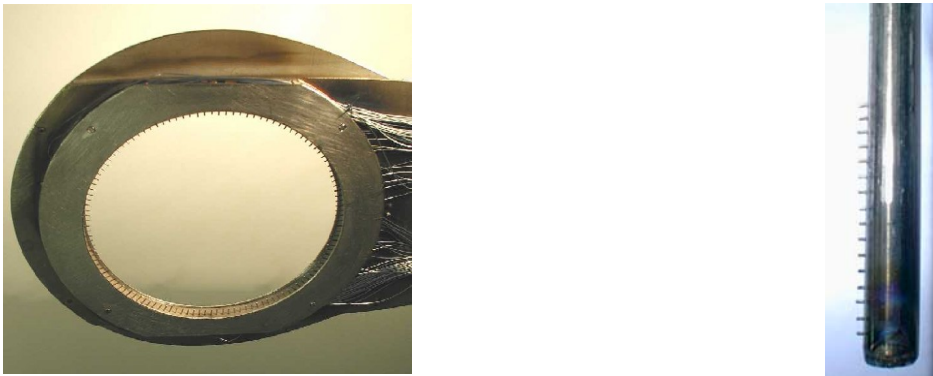
Fig. 1. *Probe arrays for spatially resolved measurements. Left picture - the poloidal limiter with 124 Langmuir probes; Right picture - the rake probe.*
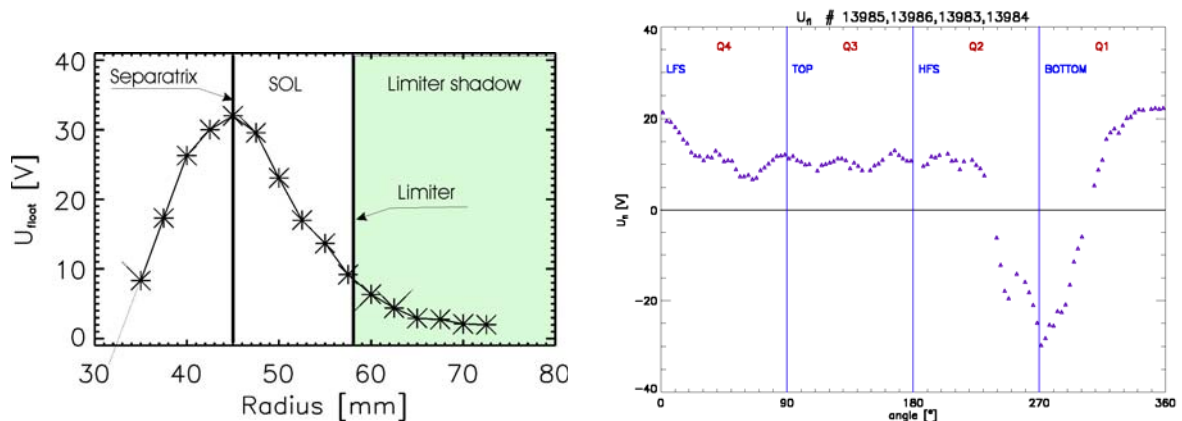
Fig. 2. *Typical distribution of the mean floating potential in ohmic discharge. Left- Radial profile measured at the top of the torus by the rake probe. Radius of the poloidal limiter is marked. Right- Poloidal distribution as measured by the poloidal ring in four reproducible shots.*

The rake probe, seen also in Fig. 1, is used to measure radial profiles of the edge plasma parameters (density, plasma potential) in a single shot. The probe head is composed

of 16 tips spaced radially by 2.5 mm and inserted into the edge plasma from the top of the torus 180° toroidally away from the poloidal limiter. The tips of both the probe arrays can measure either the floating potential or operate in the ion saturation current mode to measure the local plasma density. The signals are digitized with the 1 MHz sampling rate, 32 synchronized data. Simultaneous measurements with the radial and poloidal probe arrays allow to estimate positioning of the plasma column within the vacuum vessel of the CASTOR tokamak. First, let us discuss the distribution of the time - averaged floating potential U_{fl} in the radial direction measured by the rake probe during the ohmic discharge, see left panel of Fig. 2.

As seen from the figure, the floating potential exhibits a maximum, which is located in the proximity of the separatrix (the last closed magnetic surface) [6]. The position of the separatrix at the top of the torus is at $r_s \sim 45$ mm in this particular case, which is noticeably deeper than the leading edge of the poloidal limiter a= 58 mm. Assuming a circular shaped plasma cross section, the observed difference between the separatrix and limiter radii at the top of the torus is interpreted as a downward shift of the plasma column by about 6-7 mm.

The right panel of Fig. 2 shows the distribution of the floating potential along the poloidal ring. As seen, the distribution at the top of the torus is relatively uniform, which means that the probes are located roughly at the same magnetic surface. Moreover, those top probes measure the positive floating potential. This indicates their positioning within the scrape-off layer (compare the value of U_{fl} with that measured at r=58 mm in the left panel). On the other hand, the potential of the probes located at the bottom quarter of the poloidal circumference (in the range of poloidal angles 200° - 320°) is negative, which could imply that these tips are effectively deeper than the separatrix. The reason of this observation is not fully understood yet.

We interpret these observations as follows: the SOL plasma is divided into two regions, regarding to the parallel connection length L to a material surface, which is represented by the poloidal limiter:

- *Limiter shadow* (green area in Fig. 2) is the region between the chamber wall and the leading edge of the poloidal limiter (58 mm < r < 100 mm). The corresponding connection length is about one toroidal circumference, L~ 2π R.
- *Additional Scrape-off layer* (ASOL) with a much longer connection length is formed at the upper part of the plasma column because of the vertical shift of the plasma. The connection length L~ q2 π R is proportional to the local safety factor q (typically q = 6-9 in the CASTOR). The radial extent of the ASOL is largest at the top of the torus and depends on the value of plasma displacement. It is interesting to note that this additional SOL is of similar magnetic configuration to that of a tokamak equipped with divertor.
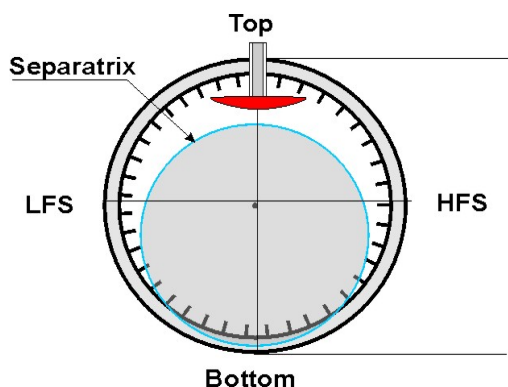

Fig. 3. *Schematic picture of the poloidal cross section of the CASTOR tokamak showing the respective position of the biasing electrode, plasma column and the poloidal limiter. The biasing electrode is located in the additional SOL.*

The magnetic configuration described above is employed for formation of convective cells in the SOL of the CASTOR tokamak. The biasing electrode is immersed into the additional scrape-off layer from the top of the torus, 80° toroidally away from the limiter. The resulting positioning of the plasma column with respect to the poloidal limiter is schematically depicted in Fig. 3.

The electrode is of a mushroom-like shape, made of graphite. Its poloidal extent is 50 mm and the total collecting area ~ 15 cm^2. The electrode is biased positively with respect to the vessel up 100-200 V.

A rather complex picture is observed during the biased period of the discharge. This is seen in Fig. 4, where the poloidal distribution of the mean floating potential in ohmic and biasing phase of a discharge is compared.
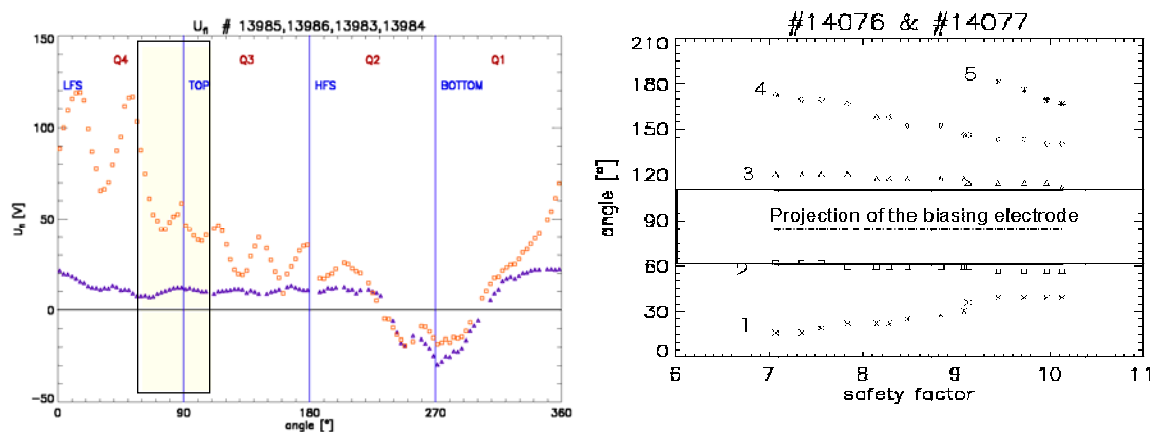
Fig. 4. *Left - Poloidal distribution of the mean floating potential U_{fl} along the ring in ohmic (blue symbols) and biasing (red symbols) phase, as measured in four reproducible discharges. The poloidal position of the biasing electrode is marked by the yellow bar. Right – Poloidal position of five peaks (1-5) versus the edge safety factor.*

It is seen that the whole upper part of the torus is biased relatively with respect to the ohmic level. Moreover, a strong poloidal modulation is observed in the range of poloidal angles 0-200°. The peaks are interpreted as a signature of a biased flux tube, which emanates from the electrode along the helical magnetic field line. This flux tube is evidently biased because the electrode current flows predominantly in parallel with respect to the magnetic field lines in the upstream and downstream direction and terminates on the electron and ion side of the bottom part of the poloidal limiter. It is interesting to note that the amplitude of peaks strongly depends on the direction of the electrode current. The peaks corresponding to the downstream direction (located at $\theta_1 \sim 15^o$ and $\theta_2 \sim 50^o$) are significantly higher than those corresponding to the upstream direction on the electrode current ($\theta_{n\geq 3} > 90^o$).

To check whether the biased flux tube really follows the local helicity of the magnetic field lines, a discharge with the ramped down plasma current was performed. The plasma current decreases during the biasing period of the discharge so that the local safety factor at the plasma edge increases from q~7 up to q~10. The resulting angular position of five potential peaks (denoted as 1-5) is shown in right panel of Fig. 4. As seen, the angular difference between the peak position decreases as expected. However, the angular position of the peaks denoted as 2 and 3 is q-independent. These two peaks are the first projections (in the upstream and downstream direction) of the biasing electrode to the poloidal ring. Indeed, they can not be closer than the angular width of the biasing electrode, which is ~50°.

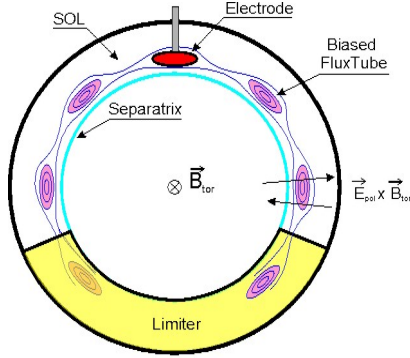The projection of the biased tube on a poloidal plane is schematically depicted in the Fig. 5.

Fig. 5. *Projection of the biased flux tube emanating from the electrode to a poloidal plane is shown schematically for $q_{edge} \sim 8$.*

It is evident that the resulting perpendicular electric field is two-dimensional, having not only a radial, but also a poloidal component. The amplitude and even the sign of the poloidal electric field E_{pol} changes with the poloidal angle. Consequently, one would expect a convective motion of the SOL plasma directed either inward or outward according the sign of the $E_{pol} \times B_t$ force. To check it, we operate the tips of the ring either in the floating potential or the ion saturation current mode in two subsequent reproducible discharges. A detail distribution of these two quantities along one quarter of the poloidal ring is shown in the left panel of Fig. 6.
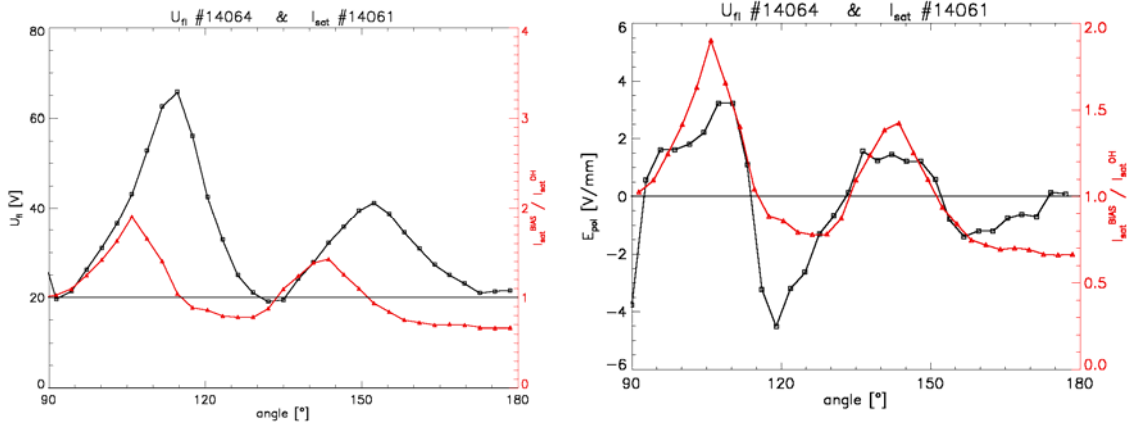
Fig. 6. *Left -Poloidal distribution of the floating potential and the ion saturation current along one quarter of the poloidal ring (High field side - top. The ion saturation current is normalized to its ohmic value.Right- Distribution of the poloidal electric field and the ion saturation current along one quarter of the poloidal ring (High field side - top. The ion saturation current is again normalized to its ohmic value.*

It is seen from the figure that the poloidal distribution of the ion saturation current (proportional to the plasma density) is modulated with biasing with the same periodicity as the potential distribution, but shifted poloidally. The ion saturation current (plasma density) increases at one side of the potential hills, while it is reduced below the ohmic level on the other side. This suggests a variation of the edge density with the poloidal electric field.

Therefore, the poloidal field is calculated as the difference of floating potentials of adjacent tips of the poloidal ring divided by their distance and compared again with the poloidal distribution of the plasma density. The result is shown in the right panel of Fig 6. It is evident that the relative change of the plasma density is practically proportional to the local value of

the poloidal electric field. Some observed differencies could appear due to an imperfect reproducibility of the analysed shots.

These measurements demonstrate a strong impact of the poloidal electric field on the edge plasma. This is further confirmed by measurements of the radial profile of the ion saturation currrent (by the rake probe) shown in Fig. 7.
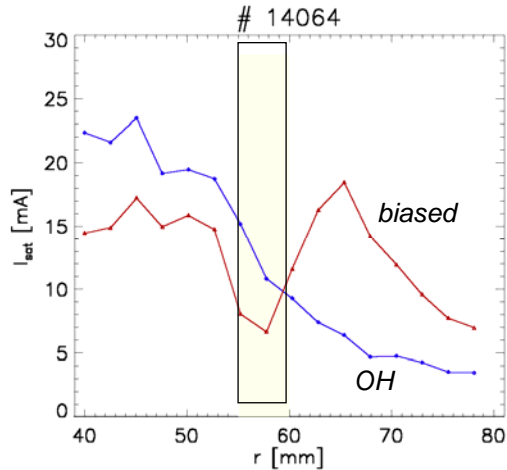

Fig. 7. *Comparison of the radial profile of the ion saturation current in the ohmic (blue symbols) and the SOL biasing (red symbols) phase of the discharge.*

The rake probe is located poloidally at $\theta \sim 90^o$ and it appears in the region of positive poloidal electric field during the biasing phase of the discharge. As it is seen from Fig. 7, the density profile at biasing is not further monotonic as in the ohmic phase. The plasma density is dramatically enhanced outside the electrode, while it decreases at radii in front of it.

Further plans:
- Analyse the edge fluctuations and compare the relative importance of the convective and fluctuation-induced transport.
- Investigate modification of the heat transport by measurements of the electron temperature distribution in the edge plasma.

Turbulence and Transport with Spatial-Temporal Biasing in the Scrape-off layer of the CASTOR Tokamak

J.Stöckel, M.Hron, J.Adámek

In collaboration with:

P.Devynck, Association Euratom/CEA, France,
I.Voitsekhovich, F.Doveil, Université de Provence, Marseille, France,
G.Bonhomme, Université Henri Poincaré, Nancy, France,
E.Martines, Associazione Euratom/ENEA sulla Fusione, Padova, Italy,
G.Van Oost, Ghent University, Gent, Belgium

Introduction

An active control of edge turbulence is an important tool for efficient tokamak operation. A reduction of edge fluctuations within the separatrix is required to form edge transport barriers, while their enhancement in the scrape-off layer (SOL) is beneficial for broadening the deposition profiles and consequently reduce the power density load on the limiter/divertor plates.

Recently, the CASTOR tokamak (R = 0.4 m, a = 0.085 m, B_t= 1 T, I_p= 5-10 kA) was equipped with a full poloidal array of 32 plane electrodes (see Fig.1) with the aim of actively controlling the edge turbulence, along the line of successful experiments performed on the linear machine MIRABELLE [1]. Two types of experiments were carried out with this equipment:

- *Passive measurements* - individual electrodes of the ring are used as Langmuir probes to investigate the full poloidal structure of edge electrostatic turbulence. The measurements are carried out both in standard Ohmic discharges and under edge biasing [2].
- *Active measurements* - a properly phased AC voltage, matching in frequency the edge fluctuations, is applied to the individual electrodes of the ring in order to try to synchronize the turbulence with it.

Here, we present some results achieved in both the arrangements, additional information is available in [3] and [4].

Experimental set-up

The plasma minor radius in CASTOR is usually defined by a poloidal ring limiter. However, for the present experiments the radius was reduced by the poloidal ring of electrodes down to 60 mm. This system consists of a poloidal array of 32 steel plates mounted on a support structure. Each plate, made of stainless steel, is 7 cm long in the toroidal direction and 1 cm
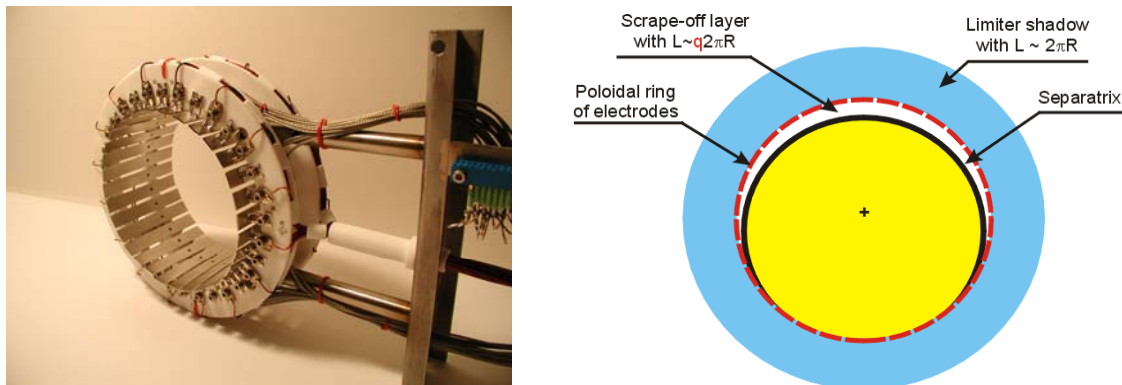

Fig. 1. *Picture of the poloidal ring and its schematic position with respect to the Last Closed Flux Surface (separatrix).*

wide in the poloidal one and equipped with a flush mounted probe. The respective position of the ring and the Last Closed Flux Surface (separatrix) is schematically shown in Fig.1.

In CASTOR, the plasma column is slightly shifted downward, which is apparent from the distribution of the floating potential along the poloidal ring, shown in Fig. 2. The positive floating potential measured by an electrode indicates its position in the SOL. On the other hand, the negative potential is a signature of its apparent position within the separatrix, which is the case of 10 electrodes localized at the bottom quarter of the ring. This has to be taken into account in the interpretation of data measured at this range of poloidal angles. The observed poloidal asymmetry has an important consequence: the connection length at the upper part of the SOL is significantly longer than the circumference of the torus and may reach the value q2πR, where q is the edge safety factor. The poloidal asymmetry is also confirmed independently by measurements of the radial electric field (made with a rake probe) and flow velocities (made with a Gundestrup probe [5]).

In addition to standard Ohmic regimes, the radial electric fields can be amplified in the proximity of the separatrix. For that purpose, a graphite electrode is inserted into the SOL from the top of the torus and biased positively with respect to the vacuum vessel to 100-300 V. Then, the poloidal ring of electrodes, if used as an array of floating Langmuir probes, provides unique information on the poloidal distribution of the potential at biasing. An example of such measurement is shown in Fig. 2. It is seen in the figure that only the upper part of the plasma column is biased to a potential comparable with the biasing voltage. The bottom plates remain unbiased which means that they are effectively deeper into the plasma than the electrode. It is also seen that even the upper part is not biased uniformly, since four distinct peaks are observed. Their poloidal separation corresponds to the angle of rotational transform for the given combination of B_t and I_p.
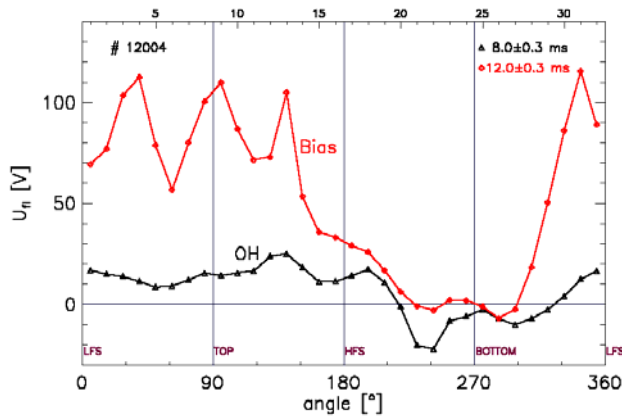

Fig. 2. *Poloidal distribution of the floating potential as measured by the poloidal ring of electrodes in Ohmic (black triangles) and biased (red points) phase of a discharge.*

Therefore, we interpret these peaks as a signature of the existence of a biased flux (or current) tube, which goes q-times around the torus and connects the biasing electrode with the bottom part of the grounded limiter. Consequently, *steady state poloidal electric fields* are formed. They modify locally the net radial particle flux via E_{pol} x B_{tor} drift. This particle flux is inward or outward, depending on the poloidal angle.

Edge turbulence at DC biasing

The edge turbulence has been investigated with the poloidal ring, by using the individual plates as large Langmuir probes. Consequently, the small size turbulent structures (with dimensions less than the poloidal extent of a plate) are spatially smoothened. Large structures become better "visible", even by plotting the raw signals [3]. Here, we present the result of the cross-correlation analysis of the floating potential fluctuations, using a plate at the top of

the torus as the reference one. The result, shown in Fig. 3 - left, clearly demonstrates the existence of a quasi-coherent turbulent structure, propagating poloidally with $v_\theta \sim 3$ km/s. This velocity is in agreement with the value and sign of the radial electric field at the ring position, as confirmed by the rake probe measurements. It is important to note that the observed correlation patterns are nearly poloidally symmetric.
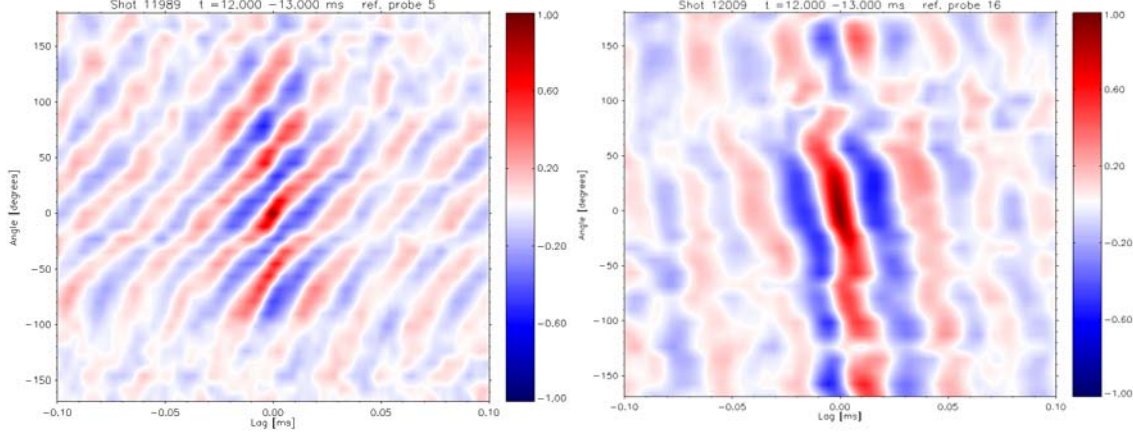

Fig. 3. *Spatial - temporal cross correlation function of potential fluctuations. The reference signal is taken from the plate located at the top of the torus. Left - standard Ohmic discharge, Right - discharge with edge biasing.*

The striking feature is the evident poloidal periodicity of the cross correlation function, with a well-defined poloidal mode number. It is found that the dominant mode number is determined by the magnetic field helicity and is consequently equal to the value of the edge safety factor q, as confirmed by measurements in discharges with the plasma current ramping down [3,4]. A possible interpretation of this observation is that, at a given time instant, only a *single* turbulent structure, elongated along the magnetic field lines, is formed in the SOL. It starts on one side of the poloidal limiter and terminates on the other side. Consequently, its length should be equal to the connection length between the electron and ion side of the limiter, i.e. q2πR. This hypothesis seems to be supported by measurements of the toroidal correlation. The rake probe measurements show that the radial extension of the structure is comparable to the poloidal one. No mode with a similar poloidal mode number has been found by analyzing the Mirnov coils signals, therefore the observed feature seems to be de-correlated from any MHD activities.

The mode analysis, preformed in [3,4] shows also the presence of more poloidal modes (mostly with m < q) on a background of broadband fluctuations. So, the full picture of the SOL turbulence is evidently more complex and its understanding requires further investigations.

The structure of the edge turbulence is dramatically changed with electrode biasing, as demonstrated in Fig. 3. In this particular shot, the biased electrode is located behind the poloidal ring, which consequently happens to be in the region of a strong negative electric field. Therefore, the propagation velocity of the turbulent structure not only increases, but also reverses. As it is seen, the poloidal mode number is significantly reduced down to m = 1-2. This implies, assuming again only a single structure in the SOL, that the toroidal extension of the structure is reduced down to (1-2)*2πR. In this case, however, the turbulent structure would no longer follow a magnetic field line and its parallel wavenumber $k_\parallel$ should differ from zero. Clearly further experimental effort is needed to confirm this picture.

In contrast to poloidally localized electrode biasing, a lower DC voltage (~+20 V) is applied to the 16 plates at the upper half of poloidal ring in a second series of experiments.

Measurements of the turbulent particle flux clearly demonstrate that even relatively low biasing voltages have a strong impact on the edge fluctuations, if a large part of the poloidal cross section is biased. As it is seen in Fig. 4, the local turbulent flux is reduced and, in particular, large bursts, directed outward, are suppressed during the biasing period.
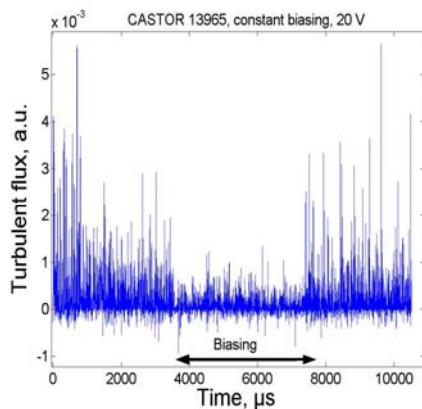

Fig. 4. *Time evolution of turbulent flux in a discharge with DC biasing of 16 poloidal plates located at the top of the torus.*

AC biasing

As a next step, an AC voltage has been applied to the plates. The existing power supply consists of 8 amplifiers, which deliver the AC voltage in the frequency range f = 10-50 kHz. The amplitude of the modulation voltage (<40 V) is comparable to the local plasma potential. A current of several amps can be drawn from each channel. In addition, a DC offset voltage (-20 - +20 V) can be used. Such equipment allows to apply a propagating wave of potential with prescribed poloidal periodicity (spatial-temporal modulation) to the ring of the electrodes.

The aim of this experiment was to provide mode selective synchronization of the edge turbulence. Therefore, the propagation velocity of the potential wave is chosen according to the relationship $\omega = k_\theta v_\theta$, where ω of and k_θ are selected within the wave number and frequency range of the edge turbulence as determined by passive measurements. The resulting spatial-temporal structure of potential fluctuations (measured by Langmuir probes embedded in the array) is shown in Fig. 5.

The potential wave is applied to the 16 top plates of the poloidal ring and propagates in the same direction as turbulent structures. The patterns of the prescribed mode structure (m = 6) and the driving frequency f=12 kHz are clearly visible. Figure 6 documents that the
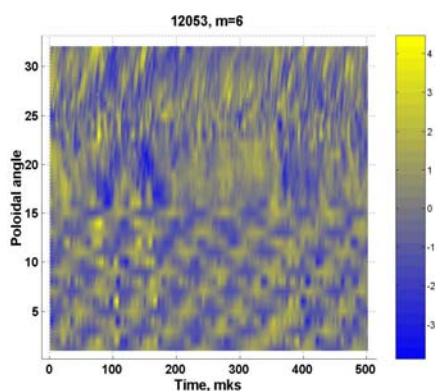

Fig. 5. *Spatial-temporal structure of the floating potential fluctuations with AC biasing, , $V_{amp} = 40$ V, $V_{offset} = 0$ V*
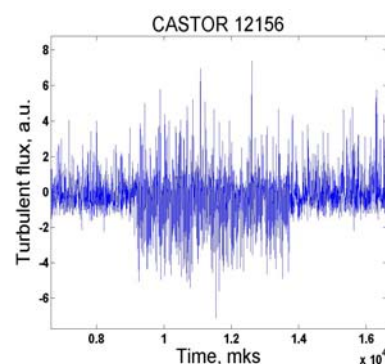
Fig. 6. *Evolution of the turbulent flux in a shot with AC biasing. $V_{amp} = 20$ V, $V_{off} = 20$ V, f = 30 kHz, m = 5*

turbulent flux is significantly modified in this biasing scheme. The large amplitude bursts propagating outwards are not suppressed but inward bursts are amplified, so the net flux is reduced. The reduction is mainly due to de-phasing of the fluctuations of ion saturation current I_{sat} and poloidal electric field fluctuations E_p, while their RMS values remain practically unchanged. It should be also mentioned that counter-rotating waves do not produce any reduction of the local turbulent flux.

In contrast to the DC case, AC biasing does not change the radial electric field, as seen in Fig. 7, where the radial profiles of floating potential are compared. Consequently, the modification of plasma properties occurs in this case due to the interaction of oscillating fields with the turbulent structures.
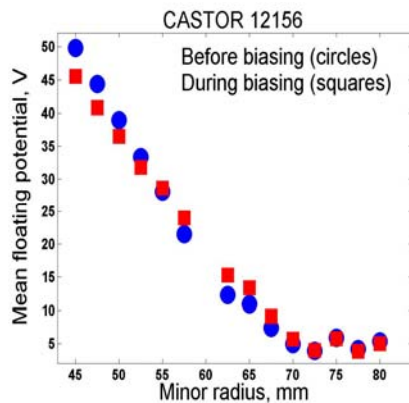
Fig. 7. *Typical radial profile of the time-averaged floating potential with AC biasing.*

Summary
Several interesting features have been observed in experiments with the poloidal ring of electrodes/probes on the CASTOR tokamak:
- formation of steady state poloidal fields in the SOL, if a poloidally localized object (electrode) is inserted there and positively biased;
- a coherent turbulent structure with the poloidal mode number $m \cong q$ is identified in the SOL, if the connection length is much longer than the circumference of the torus;
- manipulation of the SOL turbulence by DC and AC biasing has been demonstrated.

More detailed analysis of the SOL plasma, in particular at AC and DC biasing, will be the subject of future experiments with more sophisticated electronic equipment.

References
[1] C. Schröder et al, Phys. Rev. Lett. **86**, 5711 (2001).
[2] G Van Oost et al, Journal of Fusion Research SERIES, Vol. 4, 29-35, 2001
[3] M. Hron et al., In Proc. of 29th EPS Conf. on Plasma Phys. Contr. Fusion, 2002, Montreux ; P-5.043.
[4] A. Azeroual, et al, In Proc. of, 29th EPS Conf. on Plasma Phys. Contr. Fusion,2002, Montreux , O-3.21.
[5] J P Gunn et al, Czech. J. Phys., Vol. 51, No. 10 (October 2001), p. 1001

Relaxation of plasma potential and poloidal flows in the boundary of tokamak plasmas

M.Hron, I.Ďuran, J.Stöckel

In collaboration with:
C.Hidalgo, Association Euratom/Ciemat, Madrid, Spain,
J.Gunn, Association Euratom/CEA, France

Relaxation times of plasma parameters after a sudden change of electrode voltage have been measured in the plasma boundary during polarization experiments on the CASTOR tokamak. The time evolution of the floating potential after the biasing voltage switch-off can be well fitted by an exponential decay with characteristic time in the range of 10 - 20 µs. The poloidal flow shows a transient behaviour with a time scale of about 10 - 30 µs. These time scales are smaller than the expected damping time based on neoclassical parallel viscosity (which is in the range of 100 µs) and atomic physics via charge exchange (in the range of 100 - 1000 µs). But, they are larger than the correlation time of plasma turbulence (about 5 µs). These findings suggest that anomalous damping rate mechanisms for radial electric fields and poloidal flows may play a role in the boundary of tokamak plasmas.

The mechanisms that control the generation of the radial electric fields E_r and damping of the E_r x B sheared flows represent a key issue for understanding the transition to improved confinement regimes. Neoclassical and anomalous mechanisms have been considered as candidates to explain the generation of sheared flows. Atomic physics, parallel viscosity, and turbulent viscosity are candidates to explain poloidal flow damping.

This contribution reports measurements of relaxation times after electrode biasing switch-off.

Experimental set-up

Poloidal rotation and plasma potential have been modified by means of electrode biasing in the plasma edge region of the Castor tokamak [1]. The electrode, located in the vicinity of the last closed flux surface, was positively biased (U_B = 100 - 230 V) with respect to the vacuum vessel. Typical radial currents drawn by the electrode were about 30 - 40 A.

Relaxation times of both floating potential and plasma rotation have been investigated after a sudden electrode biasing switch-off. The characteristic relaxation time has been determined using two independent measurements: a) the time evolution of floating probes signals and b) the time evolution of poloidal flows.

The floating potential profile was measured using 16 single Langmuir probe tips of the rake probe that are radially separated by 2.54 mm and that cover both the SOL and edge plasma regions (r = 65 - 95 mm). The ion flows were measuremed using the Gundestrup probe [2]. Its ion collecting surface is a nearly continuous cylindrical conductor (a copper tube of diameter 11.7 mm) divided into eight segments that are separated by 0.2 mm gaps. These segments are biased negatively to measure the angular distribution of the ion saturation current.

All signals were digitized at 1 MHz sampling rate.

Relaxation phenomena: Floating potential

Radial profiles of the floating potential and of the radial electric field with and without electrode biasing (i.e. in polarized and ohmic phases of the discharge) show that the maximum of the floating potential at biasing is of similar amplitude as the applied voltage. It appears in the proximity of the electrode possition (r ≈ 75 mm) and the modification extends radially approximately 1 cm both inward and outward the plasma column. The profile of the radial electric field has been computed using the measured floating potential (rake probe) and

the electron temperature profile (measured by a swept tip on the top of the Gundestrup probe).

The autocorrelation time of the floating potential fluctuations, calculated as the width of the autocorrelation function on its half maximum, is shown in fig. 1.
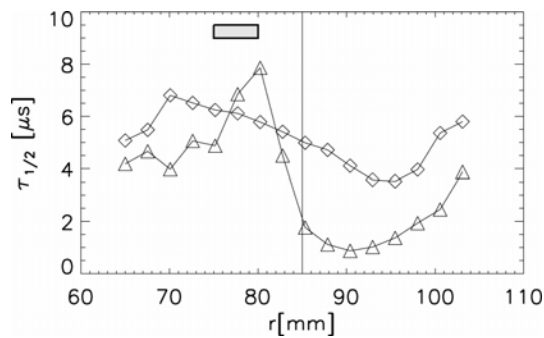

Fig. 1. *Correlation time of U_{fl} fluctuations in the ohmic (squares) and polarized (triangles) phases of a discharge as determined from the rake probe data in #11.099 ($U_B \approx +200$ V). The rectangle denotes the radial position of the polarization electrode.*

The floating potential decay is shown in fig. 2. The time evolution of the U_{fl} decay can be fitted to an exponential function that gives a characteristic time of about 10 - 20 μs.
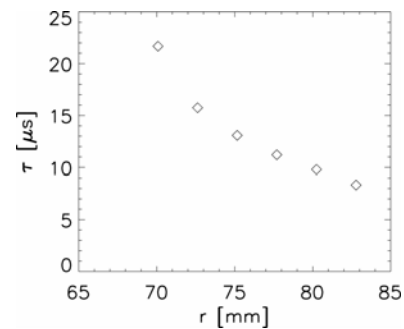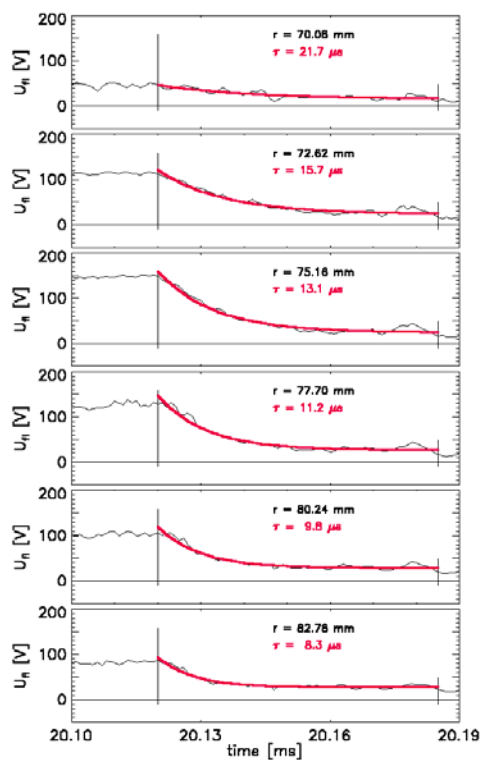
Fig. 2. *Relaxation of the floating potential (from the polarized level to the ohmic) measured by the rake probe tips at different radii after the electrode biasing is turned off (left panel). The radial profile of the characteristic exponential decay time (right panel)*

Conclusions

The present investigation shows that the experimentally measured damping times of the floating potential and of the poloidal flows (10 - 30 μs) are smaller than the expected damping time based on magnetic pumping mechanism (~ 100 μs) and atomic physics via charge exchange (~ 500 μs) and slightly larger than the correlation time of plasma turbulence (5 μs).

This finding suggests the existence of anomalous (turbulent) mechanisms in the damping rate of radial electric fields and poloidal flows in the plasma boundary of the tokamak plasmas.

References

[1] G. van Oost, J. Stockel, M. Hron et al., Journal Plasma Fusion res. Series 4 (2001) 29.

[2] J. Gunn, J. Stöckel, J. Adámek et al., Czech. Journal of Physics 51 (2001)1001.

Publications

M. Hron, C. Hidalgo et al., 30th EPS Conf. on Contr. Fusion and Plas. Phys., 2003, P-1.172

Experiments on Tore Supra
I.Ďuran, R.Pánek, J.Adámek, J.Stöckel

In collaboration with:
J.P.Gunn, J.Bucalossi, T.Loarer, J.-Y.Pascal, B.Pégourie, E.Tsitrone, Association Euratom/CEA, France

Introduction
The CIEL toroidal pump limiter (TPL) was completed and installed on Tore Supra in 2002. This upgrade substantially modifies the edge plasma, compared to the previous operation with the ergodic divertor. There was an active collaboration taking place in the second half of 2002 with the Tore Supra team to characterise and to understand edge plasmas in a new configuration of the Tore Supra tokamak [1]. Particularly, the response of the edge plasma to the new fuelling technique developed on Tore Supra – Supersonic Pulsed Gas Injection (SPGI) - was studied [2]. One of the new results from long discharge operation with CIEL is that a large amount of deuterium is trapped in the walls when regular gas fuelling is used, and about 30% less when supersonic fuelling is used. No estimate of wall trapping is yet available for pellet injection. These results are of great interest in the context of the problem of tritium retention in ITER. Edge measurements are needed in order to understand the mechanisms of gas transport and trapping. Another new result of the edge plasma studies is that the observed toroidal asymmetry of the Tore Supra SOL plasmas properties was linked to the shadow cast by poloidal antenna protecting limiter.

The Langmuir probes system in Tore Supra
The standard set of Langmuir probes mounted on Tore Supra was used as a primary diagnostic tool for the above mentioned studies. It consists from three separate sub-systems:

- **Fast scanning Mach probe** [6]. This oriented Langmuir probe, measuring the toroidal particle flow, is mounted on the fast reciprocating holder and enters the plasma from the top of the torus several times during the discharge.
- **Limiter pop-up probes.** Six arrays of four pop-up probes are mounted in between TPL tiles distributed toroidally every 60°. The arrays are flush with the limiter surface and they are perpendicular to the toroidal direction. Therefore, they measure the poloidal/radial distribution of edge plasma parameters.
- **Fixed pumping throat probes.** There are four radial arrays of fixed probes at the mouths of four out of twelve pumping throats located below the TPL target surface. Each array contains three poloidaly spaced probes mounted at support rods with highs 9.5, 14.5, and 19.5 millimetres with respect to the support plate.

3. Supersonic Pulsed Gas Injection (SPGI)
SPGI is a technique of fuelling of the discharge by an intense pulse of gas with velocity several times higher than the sound speed, by means of a special shaped nozzle [3]. This technique was recently introduced in Tore Supra [4, 5]. A fuelling efficiency in the range of 30-60% what is substantially better than the standard gas puffing, was reached. The technique itself is still technically relatively simple and robust which is the major advantage compared to pellet injection, although the latter offers almost 100% fuelling efficiency. The total plasma particle content in Tore Supra CIEL TPL plasma is plotted in Fig. 1 for the three fuelling techniques, SPGI, standard gas puffing, and pellet injection. The superior fuelling capability of pellet injection is seen. The improved efficiency of SPGI over the standard gas puffing is clearly demonstrated.
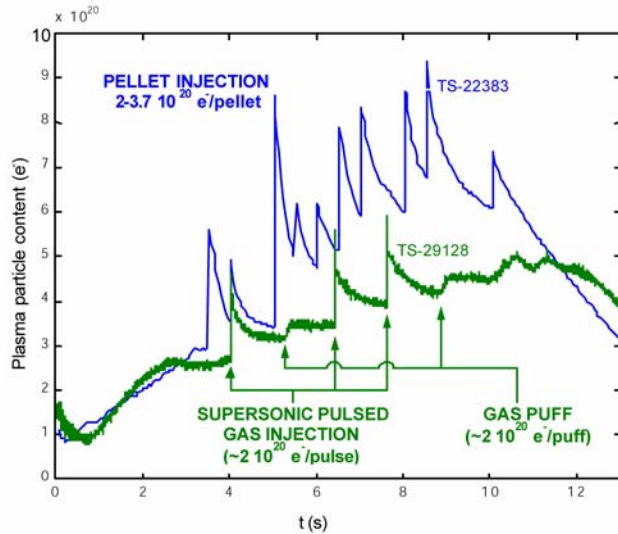
Fig. 1. *Example of the plasma density content evolution during the pellet injection, SPGI and gas puff (from [1]).*

Results

The response of the Tore Supra edge plasmas to the SPGI exhibits following features:

- The plasma edge density, significantly perturbed by the injection of a big amount of gas, comes in a short period back to the values before injection. This period for SOL density, temperature and Mach number lasts about 20-30 ms. On the other hand, relaxation of the perturbed plasma density in confinement region measured by interferometer is in the time scale of second, see Fig. 1.
- The maxima of the relative change of SOL density and absolute change of Mach number are proportional to the amount of injected gas. But, the relative drop of SOL temperature by 40-50% during the SPGI is almost constant. Moreover, the sign of change of Mach number depends whether the gas is injected from LFS or HFS. This is probably caused by the effect of the injection on the position of the stagnation point of flow in SOL. It is in agreement with a simple theoretical model [7].
- The maximum of relative change of the SOL density during SPGI takes place well inside SOL. As a result, we assume that the ionization takes place only in the SOL that would confirm a theoretical model [5].

The toroidal asymmetry of the SOL plasma density measured by fixed TPL pumping throat probes was linked to the magnetic topology of the flux tube associated with the given probe. The measurements with varied position of the poloidal antenna protecting limiter proved that the asymmetry is caused by shadow cast by the limiter onto the bottom part of the torus, where the fixed probes are located. This finding is in agreement with a simple magnetic field line tracking program that was developed for this purpose.

References
[1] E. Tsitrone, et al., Steady state density control in Tore Supra long discharges, proceedings of the 30th EPS conference on Plasma Physics and Controlled Fusion, St Petersburg, July 2003.
[2] I. Duran, et al., SOL Response to Supersonic Pulsed Gas Injection in Tore Supra, proceedings of the 30th EPS conference on Plasma Physics and Controlled Fusion, St Petersburg, July 2003.

[3] Z. Gao, et al., Phys. Plasmas **7** (2000) 2933.

[4] J. Bucalossi et al.: Particle fueling for long pulse with standard gas puff and supersonic pulsed gas injection, in *Proc 19th IAEA Fusion Energy Conferences*, Lyon, October 2002, **EX/P4-04.**

[5] B. Pegourie, et al., Journal of Nuclear Materials **313-316** (2003) 539-542.

[6] J.P. Gunn et al.: Physics of Plasmas **8** (2001) 1040-1047.

[7] E. Gravier et al: Nucl. Fusion **42** (2002) 653-662.

Radial electric field generation due to edge plasma turbulence

R.Pánek, L.Krlín, J.Stöckel, P.Pavlo, V.Svoboda, R.Klíma, V.Petržílka, M.Zápotocký

In collaboration with:

D.Tskhakaya, Institute of Physics, Georgian Academy of Sciences, Tbilisi, Georgia; Association Euratom/ÖAW, Department of Theoretical Physics, University of Innsbruck, Innsbruck, Austria,

S.Kuhn, Association Euratom/ÖAW, Department of Theoretical Physics, University of Innsbruck, Innsbruck, Austria

M.Tendler, Alfvén Laboratory, Royal Institute of Technology, Association Euratom/NFR, Stockholm, Sweden

Introduction

It is generally assumed that tokamak edge plasma turbulence causes anomalous diffusion. The observation shows that the potential structures, formed as a result of plasma turbulence, have in the poloidal plane of tokamaks (e.g., [1], [2]) typical poloidal correlation lengths $\lambda \approx 10 - 20\,\text{mm}$, lifetimes $\tau \approx 10 - 20\,\mu\text{s}$, and amplitudes U < 100 V. Theoretical studies addressing the anomalous diffusion in these fields are usually based on the test-particle drift approximation and on the electrostatic field resulting from the Hasegawa-Mima model (see, e.g. [3]) or the Hasegawa-Wakatani model [4].

In our last works (e.g. [5]), we used a very simplified model of the turbulent potential structures, namely a spatially periodic and time-independent potential. Using a *Hamiltonian* approach (which also takes into account the cyclotron motion), we have found, for impurity ions C^+ and usual potential amplitudes, a substantial increase in the diffusion of these ions (both of the Gaussian and Lévy-walk forms) [6], resulting the generation of a radial electric field [5]. Using a *drift* approximation for this case, no diffusion and no electric field is observed.
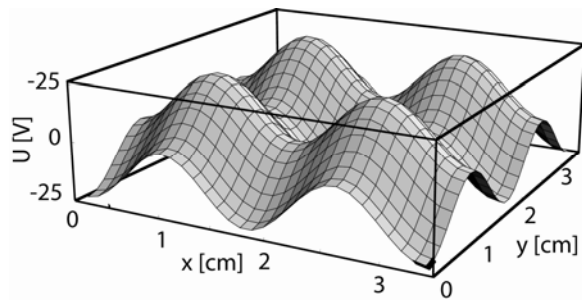

Fig. 1. *Example of the periodic potential.*

Radial electric fields play an important role in the formation of transport barriers in tokamaks (see, e.g., [7]). They give rise to velocity shear, together with strongly reduced turbulence and transport. It seems that in this context our mechanism, resulting from anomalous diffusion of impurities (and not mentioned in [8]), can play an interesting role. Of course, since the turbulence mentioned here appears in the edge plasma, the transport barrier possibly generated can be located only in this region.

Anomalous diffusion of impurities and generation of radial electric field in the Hasegawa-Wakatani potential

Now, we consider a more realistic form of this potential, namely the Hasegawa-Wakatani potential. The Hasegawa-Wakatani (HW) model [9] is based on the numerical solution of mode-coupling equations for the resistive drift-wave instability, modelling in this way the turbulent processes in the edge plasma. Recently, we have followed their approach, using for the numerical simulation the parameters of the Czech CASTOR tokamak [10]. A typical instantaneous potential relief inside a *space sample* with dimensions 4 cm radially × 8 cm

poloidally, taken from the fluid simulation results for the *entire* poloidal cross-section of the tokamak scrape-off layer (SOL), is presented in Fig. 2. In comparison with the periodic relief of Fig. l, the potential amplitudes can be considered as very close.

For this purpose, we use the 2-dimensional Particle-in-Cell (PIC) code BIT2 to follow approximately 10^6 particles (C^+ ions). These particles were initially distributed uniformly in a small rectangular subregion located in the centre of the above-mentioned space sample (first simulation) or over the whole sample (second and third simulations).

Fig. 2. *Example of an HW potential.*

We assume periodic boundary conditions in the poloidal direction. In the radial direction, the boundary conditions are periodic for the calculation of the variance and diffusion coefficient (test-particle case, first and second simulations), and non-periodic for the self-consistent radial electric field generation with particles diffusing in from the plasma outside the simulation region (third simulation). The initial temperature of the impurities is $T = 10$ eV. The electrons and plasma ions are treated as a fixed background and the HW potential is taken from a fluid simulation.

As in the case of the periodic relief, we calculate (in the first and second simulations) the time histories of the average variance $X^2(t)$ and the running diffusion coefficient $D_x(t)$ [4] for the corresponding dynamics (test-particle solution), defined as

$$X^2(t) = \langle (x_j(t) - x_j(t=0))^2 \rangle = \frac{1}{N} \sum_{j=1}^{N} (x_j(t) - x_j(t=0))^2 , \quad D_x(t) = \frac{X^2}{2t}, \quad (1)$$

(and similarly for the *y* direction), where x_j, y_j are the radial and poloidal co-ordinates of the *j*th particle, respectively, *t* is time, and *N* is the number of particles.

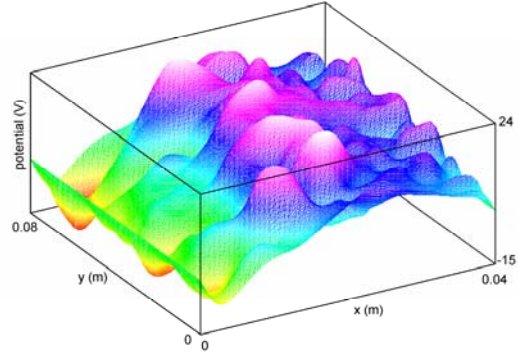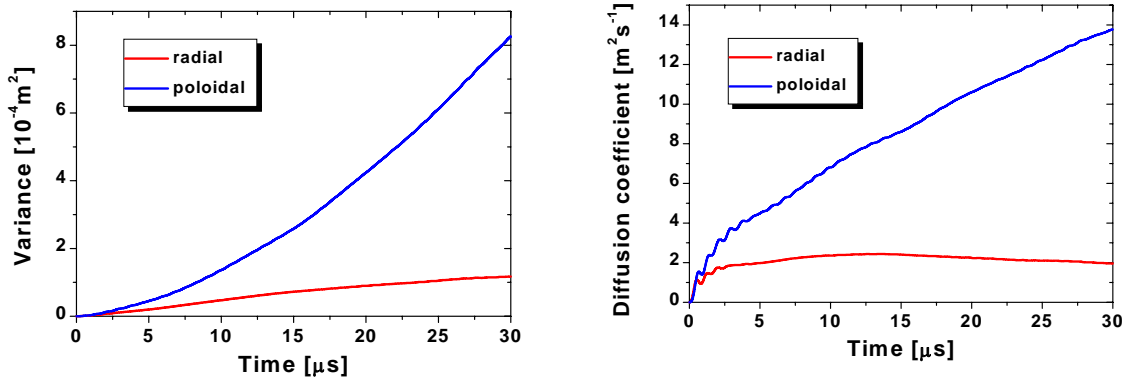The results are presented in Fig. 3. Here, the time traces of the variances and running

Fig. 3. *Variance and diffusion coefficient for C^+ in HW potential.*

diffusion coefficients are presented separately for the radial and poloidal directions. We see that the diffusion is larger in the poloidal direction than in the radial one. This effect has already been noted in [4]. Due to the large number of particles, the variance time traces are practically continuous. Contrary to the results presented in [4], the diffusion in the radial direction is rather Gaussian, and only the diffusion in the poloidal direction has a parabolic-

type variance time trace, thus clearly indicating Lévy-walk dynamics. Comparing this with the diffusion coefficient for the dynamics in the periodic potential relief [6], the enlargement of the diffusion coefficient is much enhanced in the poloidal direction, whereas in radial direction the diffusion is analogous to [6].

Typical time sequences of the spatial diffusion are shown in Fig. 4. Due to the larger diffusivity in the poloidal direction, the form of the initially well defined sample is elongated in the poloidal direction.
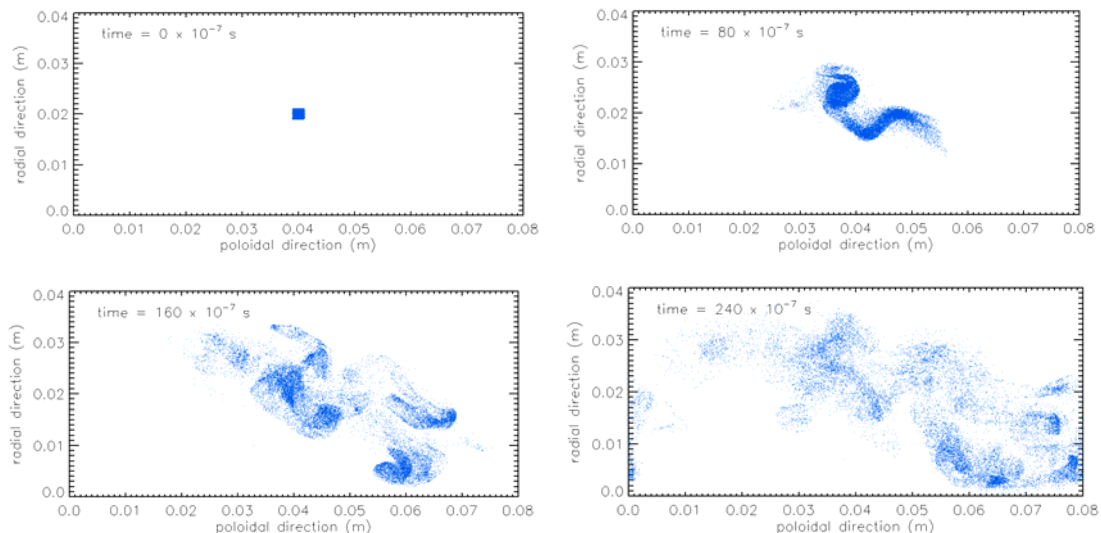
Fig. 4. *Time sequences of the spatial diffusion of C^+*

As already proposed in our recent papers [5] and [11], this anomalous diffusion must (in the self-consistent approach) necessarily result in a positive-charge deficit and, consequently, in the generation of a radial electric field. The profile of this radial electric field, following from our third simulation after $30\,\mu s$, is shown in Fig.5, which indicates that the amplitude is of the order of 10^4 V/m. As in the case of the periodic potential relief, such a field results in a shear of the poloidal plasma rotation.
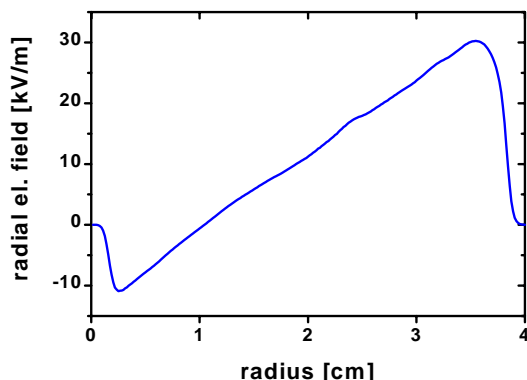

Fig. 5. *Radial electric field after $30\,\mu s$ (poloidally averaged).*

Summary

The paper discusses the anomalous ion diffusion in the Hasegawa-Wakatani model of the low-frequency potential. It has been found that for parameters of the CASTOR tokamak, carbon impurities diffusion is anomalous (in comparison with the collisional diffusion). In the radial direction, the diffusion has Gaussian form, whereas in the poloidal direction it exhibits Lévy-walk character. Due to this diffusion, a radial electric field appears in the turbulence region. Moreover, the same effect can be expected during the injection of non-intrinsic ions from outside. These effects can be of interest in the discussion of thermal barriers. Nevertheless, together with the diffusion of impurities, also the diffusion of plasma ions can appear. This has to be considered in the discussion of the generation of the turbulent potential itself.

References:

[1] W. Horton, Plasma Phys. Contr. Fusion **27** (1985) 937.

[2] M. Endler et al., Nucl. Fusion **35** (19911) 1307.

[3] G. Manfredi, R.O. Dendy, Phys. Rev. Lett. **76** (1996) 4360.

[4] V. Naulin, A.H. Nielsen, J.J. Rasmussen, Phys. Plasmas **6** (1999) 4575.

[5] L. Krlín et al., 27th EPS Conf. on Plasma Phys. Contr. Fusion (Budapest, 2000) Abstracts, p.157.

[6] L. Krlín, J. Stöckel, V. Svoboda, Plasma Phys. Contr. Fusion **41** (1999) 339.

[7] G. Van Oost, Int. J. Amer. Nucl. Soc. **37** (2000) 262.

[8] A.L. Rogister, Transact. Fusion Tech. **37** (2000) 271.

[9] A. Hasegawa, M. Wakatani, Phys. Rev. Lett**. 50** (1985) 682.

[10] K. Dyabilin et al: Czech. J. Phys. **51** (2001) 1107.

[11] M. Tendler et al., Proc. 26th EPS Conf. Plasma Phys. Contr. Fusion (Maastricht, 1999) P4 060.

2 Diagnostics Development

Because of its flexibility and low operational cost, the CASTOR tokamak is a perfect test bed for development of various plasma edge diagnostic techniques. Testing of new diagnostics in a real tokamak environment prior to their use in big machines is an important part of the CASTOR experimental programme. We find that this approach makes the whole progress from a proposal to a working diagnostic significantly faster and more efficient.

The workprogramme for years 2002/2003 was concentrated on the three main tasks:

Probe diagnostics
- Development and extensive testing of several variants of a new Langmuir probe for fast measurement of plasma edge T_e, $T_{i\parallel}$, and $T_{i\perp}$, so called tunnel probe, was done at CASTOR. The PIC simulations of different tunnel probe geometrical configurations and working regimes were an important part of this effort. This work was motivated by Jamie Gunn (CEA Cadarche, France) and performed in close collaboration with the Tore Supra team. The experiments with optimised version of the tunnel probe are currently under preparation on Tore Supra tokamak.
- Magnetic probes based on Hall sensors offer several advantages over the standard magnetic coils, among them smaller size, and the ability to measure the DC magnetic field. The magnetic probe head containing 9 Hall sensors was successfully tested on TEXTOR tokamak. The hybrid magnetic probe having 6 coils and 2 Hall sensors has been constructed recently, and it is prepared for use in TJ-II stellerator. Effort to prepare a prototype magnetic sensor for ITER Steady State Magnetic Diagnostics has been undertaken in collaboration with Lviv Polytechnical University (Ukraine) and ITER International Team.

Spectroscopy
- The ultra soft X-ray multi-monochromator (200-1100 eV), developed in IPP Prague, was used at TCV tokamak to monitor emission from the highly ionised impurities such as Boron, Carbon, and Oxygen. The spectrometer is absolutely calibrated and therefore able to provide information about total impurity content. The measured line intensity ratio between CVI and CV lines was found to be a strong function of perpendicular diffusion coefficient $D_\perp$ in agreement with modelling using STRAHL code. Measurement of line emission radial profile of a single line combined with modelling using the STRAHL code provides information on $D_\perp$ radial profile.
- VUV and XUV spectrometers were calibrated and put into routine operation on the CASTOR tokamak. The first experiments were dedicated to spectroscopic characterisation of various configurations of the CASTOR regimes with edge plasma polarisation.

Microwave reflectometry
- Microwave correlation reflectometry system on the CASTOR tokamak has been upgraded to measure both poloidal and toroidal plasma rotation. Strong modulation of the reflected microwave power amplitude was observed when the position of reflecting layer coincides with expected position of a rational q surface. This work was done in collaboration with Georgian Academy of Sciences.

Development of advanced probes for measurement of the electron and ion temperature
J.Stöckel, J.Adámek, R.Pánek

In collaboration with:
J.Gunn, Association Euratom/CEA, France

Measurements the of the electron and ion temperature at the edge plasma are of principal importance. Especially measurement of the ion temperature performed by the special electric probes is a very difficult task, because it is necessary to remove an electron component of the plasma flux.

Recently, we have developed a new probe, which is called "tunnel probe", which purpose is to measure electron temperature. Later on, other modifications of the tunnel probe, Katsumata Tunnel probe and Segmented Tunnel probe are suggested to measure perpendicular and parallel ion temperature, respectively. The self-consistent, two-dimensional kinetic code XOOPIC is used to understand better the physics of the probes. In this contribution, we describe the design of each configuration, PIC simulation and first experimental result achieved on CASTOR.
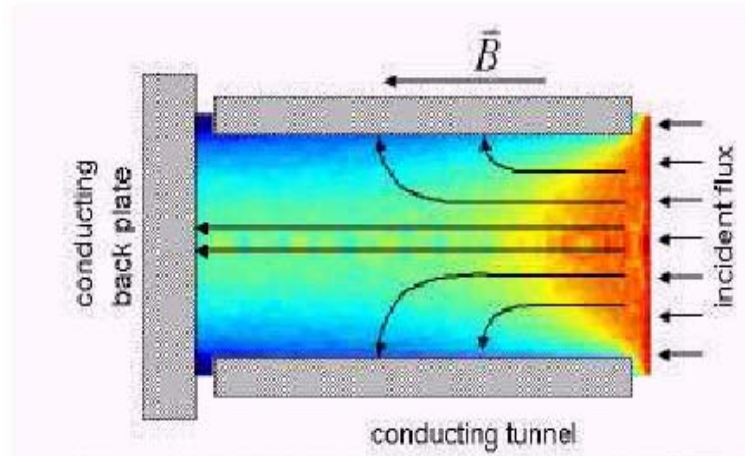

Fig. 1. *Longitudal section of the Tunnel probe with diameter 5 mm. Arrows indicates flux inside the tunnel. Color represents density of the ions.*

Tunnel probe

The tunnel probe (Fig. 1) is a configuration for the simultaneous measurement of the electron temperature and parallel ion current density $J_{//}$ in the SOL. It consists of a conducting tunnel (diameter of 5 mm), which is closed by the electrically isolated conducting back plate. Both tunnel and back plate are biased negatively to collect ions. The tunnel axis and the magnetic field are parallel. The ratio of ion currents distributed on the tunnel and the back plate is determined by the magnetic sheath thickness at the surface of the tunnel and is, therefore, a strong function of the electron temperature. To find the theoretical relation between the current ratio

$$R = \frac{I_T}{I_{BP}}$$

(I_T, I_{BP} is the ion saturation current of the tunnel and the back plate, respectively) and electron temperature, the XOOPIC code is used.

The results of PIC calculation is seen in Fig. 2, where the ratio R is plotted as a function of $J_{//}$, the electron temperature is a parameter. PIC calculations are for two potentials (-100V, -200V) of the tunnel and back plate.
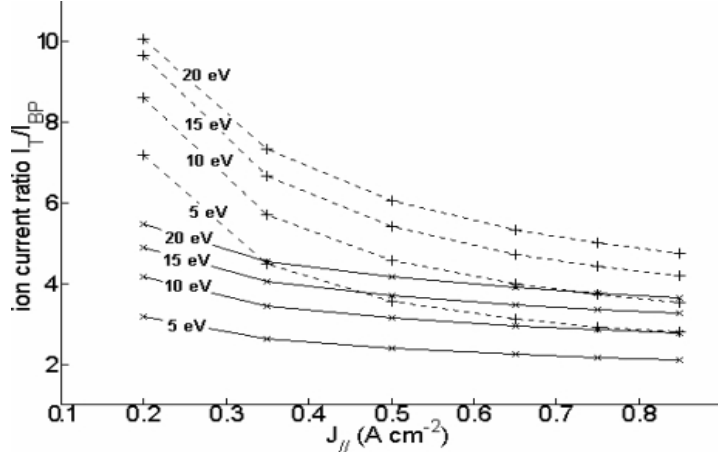
From Fig. 2 it is apparent the ratio R does not depends only on Te and $J_{//}$, but also on the potential applied to the tunnel surfaces. Consequently, using results of the PIC simulations we find the analytical expressions for T_e as an function of J_{par} and R for different values of J_{par} and applied voltage, which are finally used for processing of experimental data :

$$T_e = 1.0204 J_{//}^{1.2633} R^{2.0454} \; (0.15 Acm^{-2} < J_{//} < 0.3 Acm^{-2}) \; - 200V$$

$$T_e = 0.8435 J_{//}^{0.6197} R^{2.5236} \; (0.3 Acm^{-2} < J_{//} < 2.0 Acm^{-2}) \; \; -100V$$

$$T_e = 0.8421 J_{//}^{0.70193} R^{2.5237} \; (0.15 Acm^{-2} < J_{//} < 0.3 Acm^{-2}) \; -100V$$

Example of the measurement is shown in Fig. 3. The radial profiles of the electron temperature T_e is plotted. The measurements was performed for two values of applied voltages (-100V,-200V). It is seen the electron temperature calculations for both cases are nearly identical, in particular in the SOL (r > 60 mm).

Tunnel probe can also operate as a concave Langmuir probe when the tunnel and the back plate are connected to each other and their potential is swept. Electron temperature is determined from the exponential fit of I-V characteristics. It is evident, for two operating regimes (concave Langmuir, ratio R) different profiles of the electron temperature are obtained. The mutual multiplication constant is about 3.
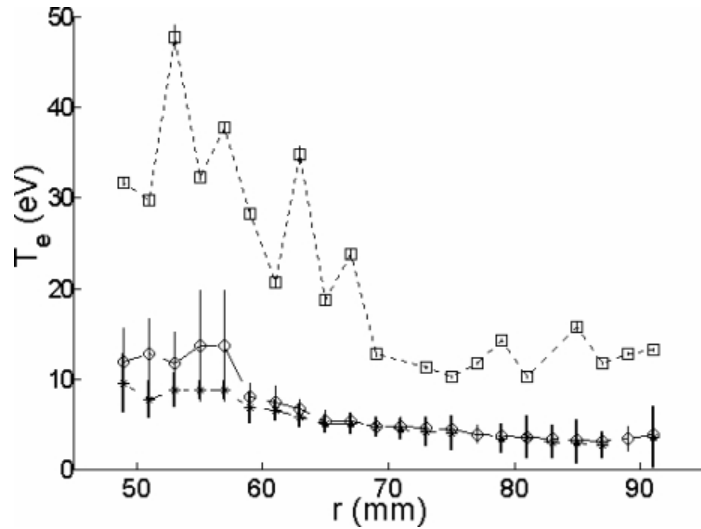

Fig. 3. *Radial T_e profile, obtained using the composed characteristics of shots #16200 - #16221. Langmuirn probe analysis (squares), Tunnel probe –100V (circles), Tunnel probe –200V (stars).*

55

Segmented-Katsumata Tunnel Probe

The Katsumata Tunnel probe is created by the adding of a small diaphragm on front of the orifice, which shields the tunnel surface from the electrons as apparent from the left-hand side of the probe head shown in Fig. 4. A retarding voltage is applied to the conductors in order to determine the perpendicular ion energy distribution and, consequently, the perpendicular ion temperature $T_{i,\perp}$. If the tunnel is divided axially into two parts, in addition, the parallel ion temperature $T_{i \parallel}$ can be obtained from the ratio between the ion saturation current of the first and second

Fig. 4. *Schematic picture of the Segmented-Katsumata Tunnel probe with 5 mm tunnels.*

segments. The experimental set-up, which combines the Katsumata tunnel probe and the Segmented tunnel probe, is depicted in Fig. 4.
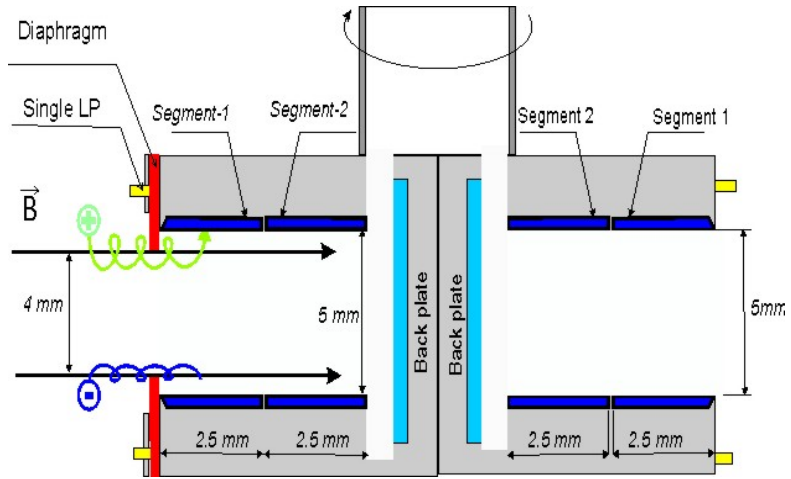
Katsumata Tunnel Probe

In this contribution we show how a slight modification of the tunnel probe transforms it into a kind of Katsumata probe, thereby providing access to measurements of the perpendicular ion temperature $T_{i,\perp}$. The addition of a small diaphragm in front of the orifice shields the concave tunnel surface from electrons. This probe geometry presents the advantage that it can be simulated easily using the XOOPIC code. We report on the first measurements using such a configuration in the CASTOR tokamak and compare them with kinetic simulations of the ion current characteristic, Fig. 5.

In principal, retarding voltage V_s is applied to the tunnel in order to scan the perpendicular ion energy distribution from which $T_{i,\perp}$ can be determined. When the retarding
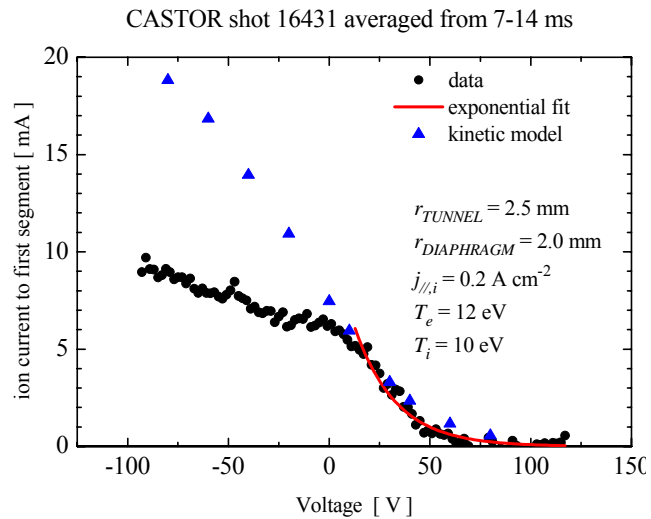

Fig. 5. *Real IV characteristic (solid circles) of the first segment and simulated characteristic (triangles) obtained from an XOOPIC code simulation with the parameters indicated. The solid line shows the exponential fit from which a value of $V_d \cong 30\ eV$ was determined.*

voltage V_s increases from negative values, the ion current decays approximately linearly. For V_s higher than the floating potential (see Fig. 5) the ion currents start to decay exponentially approximately like $I_{i,1} \approx \exp(-V_s/V_d)$. V_d is a characteristic constant of exponential decay. It is seen that the electron screening by the diaphragm works properly only for the first segment, where the current decays to almost zero as it was expected.

Unfortunately, however, a non-negligible electron current is seen to reach the second segment. Consequently, the indicated values of $V_d \cong 14.1$ eV for the ohmic and $V_d \cong 14.9$ eV for the biased part of the discharge were determined only from the characteristics of the first segment. In general theses two values are very similar.

The I-V characteristic of the first segment is plotted in Fig. 5. We apply two approaches to estimate the perpendicular ion temperature $T_{i,\perp}$. The exponential fit of the decay of the ion current to the first segment yields the factor $V_d \approx 30$ eV. The results given by the PIC simulation, which are plotted in Fig. 5, are also in a good agreement with the experimental data for the positive applied voltage. However, the ion temperature T_i which is an input parameter for the PIC simulation is equal to 10 eV.

Fig. 6 shows radial profiles of exponential decay V_d in a range of $57 < r < 92$ mm, with the position of the biased electrode at $r_E = 60$ mm. The radial position of the **l**ast **c**losed **f**lux **s**urface (LCFS) is 73 mm. The solid squares show always the values for the ohmic part of the discharges, whereas the solid circles show the values taken during the biased part of the discharge. In the biased part of discharge the plasma column is polarized by the constant electric field using the massive electrode. It is interesting the V_d decreases towards to the plasma core, which is an unexpected.

Fig. 6. *Radial profiles of the slope of the exponential decay V_d , which gives a measure for the perpendicular $T_{i\perp}$.*

Segmented Tunnel Probe

When the tunnel is segmented axially into two parts, see right-hand side of the probe head in Fig. 4, the probe can also measure the parallel ion temperature $T_{i,//}$. This can be gained from the ratio between the ion saturation current $I_{i,1}$ to
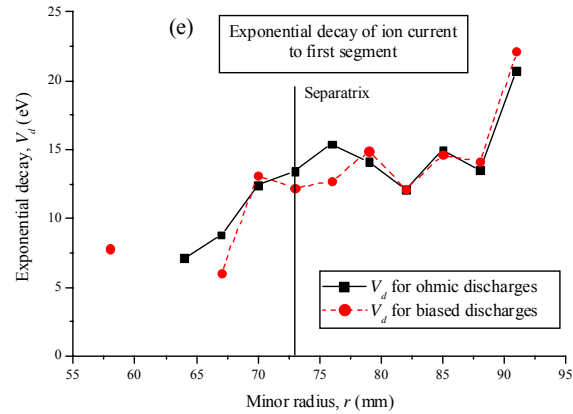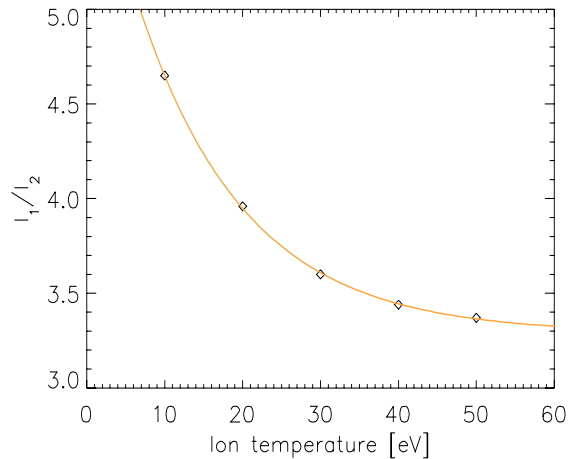

Fig. 7. *Results of a PIC simulation for $T_e = 20$ eV and $J_{//} = 2500$ A/m^2 .Current ratio is inversly proportional to the parallel ion temperature $T_{i//}$.*

the first segment and $I_{i,2}$ to the second one. The rationale is that ions with a high parallel velocity component can make it to the second segment, whereas those ions with a small parallel velocity (having on the other hand a large perpendicular velocity component) will mainly be attracted by the first segment. It has been confirmed by PIC simulation as seen in Fig. 7.

The current ratio of the first and the second segments is inversly proportional to the parallel ion temperature $T_{i\,//}$. Assuming that $J_{//}$ and the electron temperature are close to the condition in a PIC simulation we can estimate parallel ion temperature using the experimental data in Fig. 8.
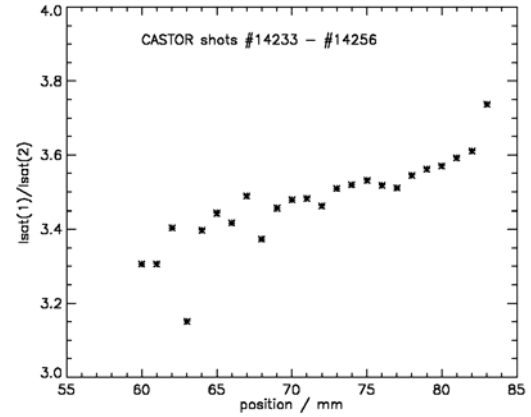

Fig. 8. *Radial profile of the ratio of the ion saturation currents of the segments 1 and 2. Paralel ion temperature is increasing towards to the plasma core.*

Spectroscopy on CASTOR
Vojtěch Piffl, Vladimír Weinzettl

In collaboration with:
A.Burdakov, S.Polosatkin, Budker Institute, Novosibirsk, Russia

VUV Imaging Seya-Namioka Spectrometer

Introduction
Spatially resolved measurements of plasma vacuum ultraviolet (VUV) emission spectra are a valuable diagnostic technique in studies of high temperature plasma [1]. This is because the radiation of plasma, namely emitted from the plasma periphery, at tokamak temperatures, falls in the VUV part of the spectrum. As a consequence, spatially resolved observations of VUV emission provide a possible (natural) method of studying the many characteristics of plasmas in tokamaks and in certain other fusion devices. Such observation can be used profitably in the study of the plasma impurities behaviour (diffusion coefficient, effective charge, etc.). The magnitude and VUV spectrum of the radiation flux from a plasma are directly related to the plasma density and plasma impurities content. Furthermore, the plasma temperature could be evaluated analysing the spatial intensity distribution of the selected lines, whose excitation rate coefficient is sensitive to the electron temperature in the needed energy range.
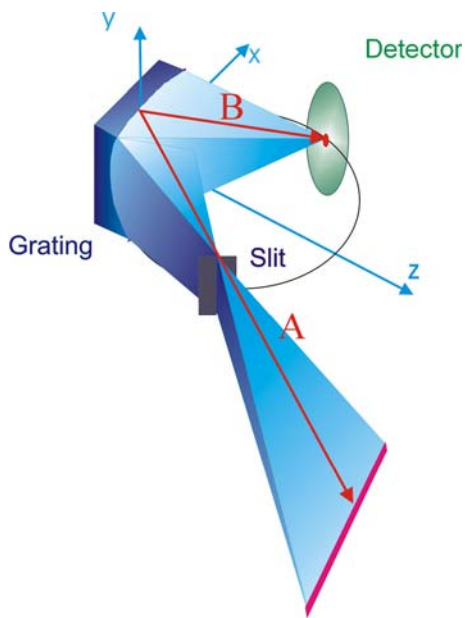

Fig. 1. *Formation of the image in spectrograph. The linear source located in vertical focus of the device, is represented as a point in a plane of registration*

Instrument's design
The spectral instruments equipped with curved diffraction gratings have been used elsewhere for getting common information on spectrum in VUV emission range, where the use of the optical elements like lenses, prisms is undesirable due to the high absorption of VUV radiation in such elements [3].

Spectrometer beam line arrangement
The design of the spectrometer was based on vacuum spectrometer BM-3, product of Ioffe Institute, and assembled according to the Seya-Namioka scheme. In Fig.1 the optical scheme of the Seya-Namika spectrometer is shown. The spherical dispersion grating with gold cover, radius of curvature $\rho=0.5$ m, 1200 grooves per mm, was installed in this instrument. The angle between incident and diffraction rays is $70^o15'$. The incident angle is smaller than the diffraction angle and the spectrum is obtained in negative orders. The incident radiation is coming through the input slit and after the diffraction at the grating is focused on the output window displaced near to the Rowland circle. The spectrum scanning is done by turning the grating body around the central axis.

The calculation method of the geometrical displacements, inclusive the important distances between the radiation source, grating and output screen, has used the derivations of the common grating equation. It could be shown that for the best spatial resolution of the image the vertical and horizontal focal lengths have to be equal and the distance A, between the radiation source and the gratings, can be expressed as:

$$A = \frac{\rho \cdot \cos\theta}{2\cos^2\theta \cdot \sqrt{1 - \left(\frac{m\lambda}{2d\cos\theta}\right)^2} - 1}$$

If mλ<2d.cosθ ≈1000 nm the dependence of the focal length versus the wavelength is weak. We notice here, that the radiation object should be situated at the distance much longer than the distance from input slit to the grating (as minimum three times). Therefore, if the radiation source is placed at the distance A from the grating, the image of the emission spectrum is created on the detector surface at Rowland circle. In the horizontal direction (meridian plane) the wavelength spectrum is created and the spatial dependence of the line intensity is displayed in vertical direction.

According to the formula, the distance A=1300 mm, between the centre of the plasma and diffraction grating, has been chosen in our configuration, which allowed the spectra measurements for mλ=50÷400 nm with spatial resolution better than 5 mm. The height of the input slit is 14 mm now, the width of the slit could be changed without breaking the vacuum. The spectrometer views the central part of the plasma column along the horizontal chord in most of the experiments.

Detector - converter system
The two dimensional detector system of the spectrometer, we have operated on CASTOR tokamak, consists of set of two channelplates of working area diameter, 38 mm. The front of the first channelplate is covered by CsI. The output electrons are accelerated onto the scintillator of the fiberoptic lightguide, which is consequently used as a vacuum throughput. The DC or impulse voltage, up to -1200V, is applied on channel plates set, while the electrons leaving the channelplate converter are accelerated up to 3100V before impact the scintillator. The spectra could be taken during the whole plasma discharge in 1÷10 ms exposition time, if the spectrometer detection system is operated in the pulse regime.

CCD camera
The image of the spectrum is recorded by CCD camera equipped with Tevidon 1.4/25 objective. The CCD element contains 165 x 192 pixels of rectangular form of 1.17 aspect ratio. The Image_Grab programme allows recording of the pixels content in the own 16 bit format and conversion in common formats like tiff, bmp, png.

Spectrum and line intensity measurements
The theoretical limit of spectral resolution of the instrument is roughly equal to the number of illuminated grooves of grating. In our case, the spectral resolution could be expressed as the product of the tokamak input slit size, 20 mm, and grows line density, 1200/mm, so it has been found: mλ/δλ=24000.

The real instrument spectral resolution is basically determined by the width of the input slit and defocusation effect of the plane detector at the curved focal surface. The deviation of the

flat detector from the focal surface grows with wavelength λ. For λ=200nm this deviation represents 1.5 mm at the frame edge [4], [5].
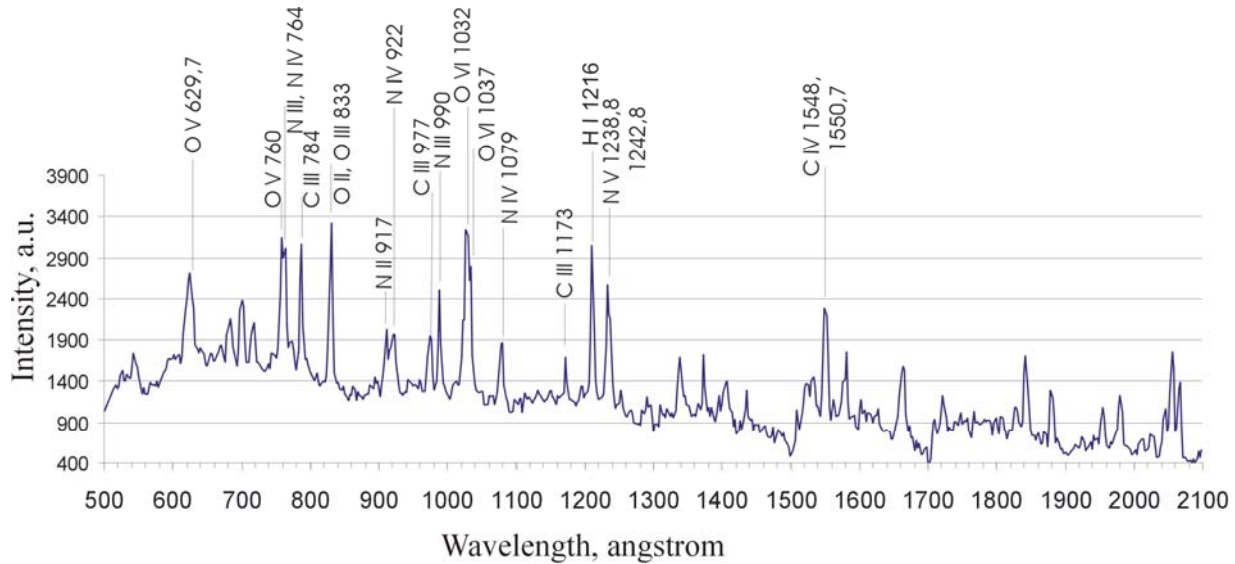

Fig. 2. *Spectrum of VUV plasma radiation.*

Spatial calibration

The spatial calibration of the VUV spectrometer was done that the vertically symmetric steel screen of 10 mm in height was put inside the diagnostic port so that its shadow on a CCD image was imaged in the time of a tokamak discharge. The dependence of the shadow center position on the spectrometer tilting was linearly fitted, so the position of the pixel corresponding to the tokamak chamber center and the pixel spatial resolution (0.536 mm on plasma per pixel) were computed for the current position of the CCD camera and the current spectrometer position.
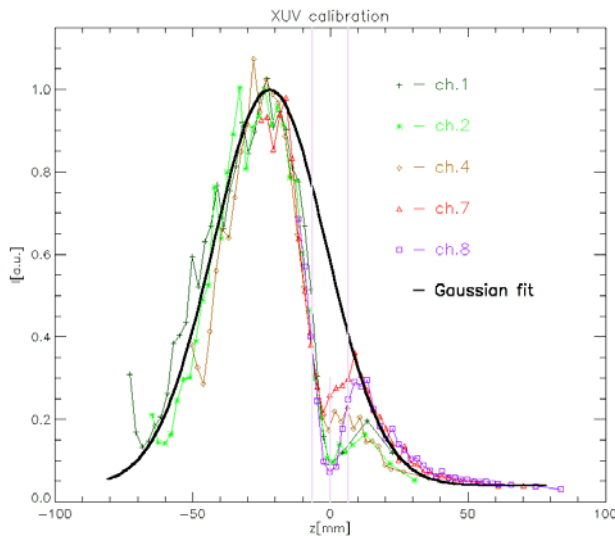

Spatial calibration of XUV spectrometer

The spatial calibration of the XUV spectrometer has been done in a similar way as in the VUV case. The vertically symmetric steel screen of 10 mm in height was put inside the diagnostic port such that its shadow could be seen on the measured spatial profile, see Fig.3.

Fig. 3. *Spatial calibration of the XUV spectrometer. Notice the off axis profile of C V radiation, that suggest a plasma column vertical shift.*

Spectroscopic investigation of edge plasma biasing experiments on the CASTOR tokamak
The edge plasma biasing has been investigated on the CASTOR tokamak since 1998. The impact of the edge plasma biasing on the discharge parameters on the plasma periphery and electrostatic turbulence suppression was demonstrated. Such research was mainly directed to electric and magnetic field fluctuation analysis. On the other hand, advanced spectroscopic tools like XUV monochromator and VUV Seya-Namioka imaging spectrometer were developed on the CASTOR tokamak in the meantime. Both spectrometers allow to reconstruct spatial profiles of a chord-integrated line intensity by tilting of spectrometer on a shot-to-shot basis.

The dependence of plasma parameters like electron density and H_α line radiation on the combination of the biasing electrode position and voltage has been found. As a result three different biasing regimes – so called "radiating regime", "non-radiating regime", and "reduced H_α regime" have been identified and characterized using an available set of spectroscopic tools.

Plasma biasing "radiating regime"
The high biasing voltage (beyond +200 V) often leads to a dramatic increase, mostly about 100 %, of the electron density, soft X-Rays and all carbon radiation during biasing, see **Fig.5**. After that period all plasma parameters, including radiation return to their pre-bias level. The possible reason is a sputtering of the biasing electrode, what strongly increases the carbon content in plasma. This regime can be suitable for particle transport studies, especially its "decay part".

Plasma biasing "non-radiating regime"
The most common type of the biased discharge is so called "non-radiating regime". Low biasing voltages (~ +50-100 V) cause visible changes in a floating potential profile near the edge, however, the effect on electron density and radiation is very weak. The spatial profile of C V 4.03 nm radiation becomes flatter with time, see **Fig.4**. Fluctuation measurements show a decorrelation of edge turbulent structures [2], what indicates a decrease of particle transport near the edge. However, a strong influence of a weak edge biasing is not indicated by other spectroscopic data analyzes.
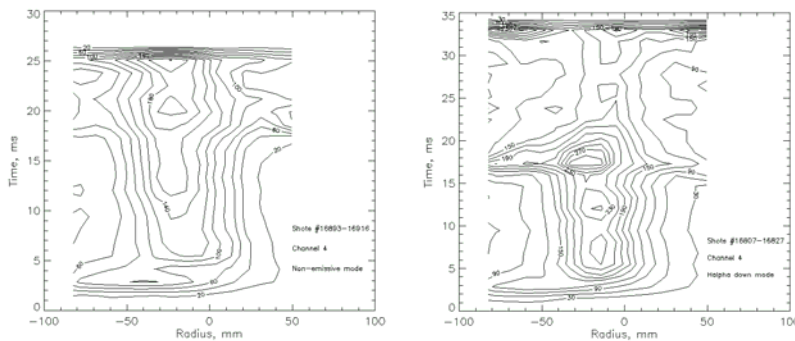

Fig. 4. *Contour plot of C^{4+} 4.03 nm radiation in a "non-radiating" (left) and "reduced $H\alpha$"(right) regime*

Plasma biasing "reduced H_α regime"
Deeper electrode positions (r_B~55 mm) combined with higher biasing voltages (>100-200 V) often lead to the next biasing type called "reduced H_α regime". However, the exact conditions for this type of biasing vary, and must be found for each session experimentally.

This regime with a significant enhancement of particle confinement time is characterized by an electron density increase together with an $H\alpha$ line radiation decrease. The form of the $H\alpha$

intensity drop is nearly rectangular, see **Fig.5**, what corresponds to very fast transitions between the regimes of a low and high confinement. A weak decrease of the C III line radiation was observed during a biasing phase. The confirmation of the improved confinement can be also the fact that the highly ionized state like O^{5+} shrinks its profiles. On the contrary, after a switching-off of the biasing voltage, plasma column profiles quickly become very wide.
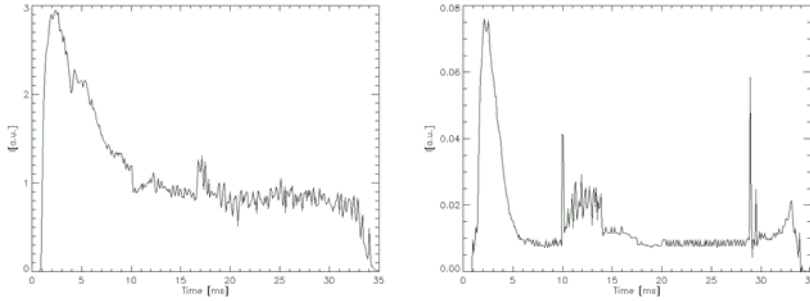

Fig. 5. *Typical Hα line intensity evolution in "reduced Hα regime" (left), and CIII 464.7 nm line evolution in "radiating regime" (right)*

Publications

[1] V.Piffl et al.**,** Trans.Fus.Sci.Tech., January 2003, Vol. 43, No.1T, p. 231 – 236

[2] V.Piffl et al., Czechoslovak Journal of Physics, vol. 52(2002), Suppl. D, p. 70-76

[3] V.Piffl, Vl.Weinzettl, A.Burdakov, S.Polosatkin: "VUV Imaging Spectroscopy on CASTOR Tokamak**"**, 29th EPS Conference on Plasma Phys. And Contr. Fusion Montreux, 17-21 June 2002 ECA Vol.26B**,** P-4.123(2002)

[4] A.V.Burdakov, V.Weinzettl, V.Piffl, S.V.Polosatkin, V.V.Postupaev, 10th Russian Conference on High-Temperature Plasma Diagnostics, 8-13 June 2003, Troick, Russia, contrib. N5, p. 77-78

[5] A.V.Burdakov, V.Weinzettl, V.Piffl, S.V.Polosatkin, 30th Zvenigorod Conference on Plasma Physics, 24-28 February 2003, Zvenigorod, Russia, contrib. MS-2-16, p. 81

USX-ray spectroscopy and transport effects
on light impurity ionisation equilibria in TCV
V.Piffl

In collaboration with:
H.Weisen, A.Zabolotsky, CRPP, Lausanne, Switzerland

USX-ray spectroscopy in TCV

The TCV tokamak is equipped with an ultra-soft X-ray multi-monochromator allowing low energy resolution (E/δE≈30) measurements in the energy range 200 – 1100 eV. Its purpose is to monitor emission from the main resonance lines of highly ionized light impurities such as Boron, Carbon and Oxygen. Energy selectivity is achieved by using of synthetic multilayer mirrors (MLM) having 30 – 50 alternate layers with layer period in the range from 30 to 70Å depending on wave-range to be investigated. The instrument can provide the direct measurements of radiation losses from the main lines of hydrogen-like and helium-like of Boron, Carbon and Oxygen impurities, which have clearly been identified. Since the absolute transmission and sensitivity data are available for all of the USX Spectrometer components a determination of the absolute impurity levels is possible. The absolute line emission from hydrogen-like impurity ions is consistent with coronal equilibrium modeled using IONEQ code for $n_{Carbon}/n_e≈2\%$, $n_{Boron}/n_e≈1\%$, $n_{Oxygen}/n_e≈0.1\%$ (before

Fig. 1. *USX Spectrometer built by IPP Prague for TCV*

boronization). The strongest lines accessible to the instrument are responsible for about two third of the total radiated power of H- and He- like ionization stages of these light impurities. USX measurements and absolute emissivities from soft X-ray tomography are used together with the emission-transport code to determine the impurity levels.

Modeling of ionization equilibria using STRAHL code

- Establish the sensitivity of the line intensity ratios to the transport effects in low- and high- confinement regimes

Very first experience with the USX Spectrometer built by IPP Prague for TCV has shown that ionization equilibria for light impurities differ from those expected from pure coronal equilibrium without transport. This is particularly the case for the line ratios of H-like and He-like emission lines of light impurities. An absolute determination of impurity levels from intensity measurement of H-like and He-like lines appears to be difficult without knowing of the spatial variation of transport coefficients. (Relative impurity level proportions may probably be estimated from similar ionization stages of different impurities.)

Line intensity ratio and transport effects (Code STRAHL use)

The modelled radial profile of the line emission density, W/m3, is sensitive to the radial variations of the diffusion coefficient $D_\perp$. With increasing $D_\perp$ the shape of the profile is broader and the maximum is displacing towards the central part of the plasma

The ionisation and radiation code STRAHL uses measured electron temperature and density profiles and calculates power intensity profiles of selected main lines of each charge state of

the impurity ion species under consideration. According a simulation we have done for H- and He-like Carbon, it could be expected that the lines intensity ratios are sensitive to $D_\perp$, especially for $D_\perp \leq 2m^2/s$ at outer diameter of a plasma at TCV.

An experimental proof of line intensity ratio sensitivity to the changes of plasma diffusion coefficient at the plasma periphery is carrying out at tokamak TCV in series of shots in L-mode, H-mode discharges, with and without additional heating, as well as in different plasma configurations (triangularity, elongation).

The impurity transport affects the chord integrated line intensity, W/m^2, and consequently the line intensity ratio of two selected lines. In dependence on experimental conditions, it is possible to select the spectral lines (in our case: CVI line at 367 eV and CV line at 308 eV), which specific emissions, W/m^3, are predominantly sensitive to the transport phenomena as result of their location near the "transport barrier" effects (steeper density gradient ect.). Remarkable increase of the CVI/CV intensity line ratio was observed during the transition from the L- to H-mode. It seems the appearance of the transport barrier influences the ionization equilibria and consequently

Fig. 2. *The experimentally measured ratio of CVI/CV line chord intensities in L and H modes for different q95.*

the line power emission of the high ionized stages of the impurity ions.
There is an attempt to include the above described idea in the model and perform the simulation of near experimental conditions to explain the observed increase of the CVI/CV intensity line ratio.

Transport effects on ionisation equilibrium of light impurities

- Determine the dependence of the impurity transport parameters on the edge plasma conditions

In some TCV plasma regimes, the ion recombination time is long enough, of the order of tens milliseconds, thus being comparable to the characteristic times of the particle transport. This fact leads to a distribution of ionised states, which is not in equilibrium with the electron temperature, as it would be expected according to the corona model [private communication]. The broadening of the radial profile for each ionised species is the typical effect of transport phenomena and can
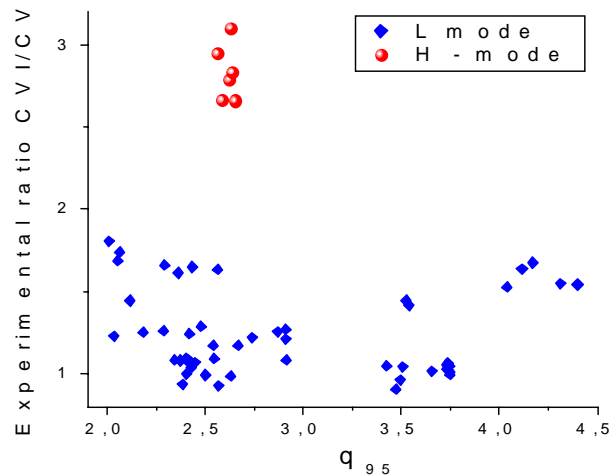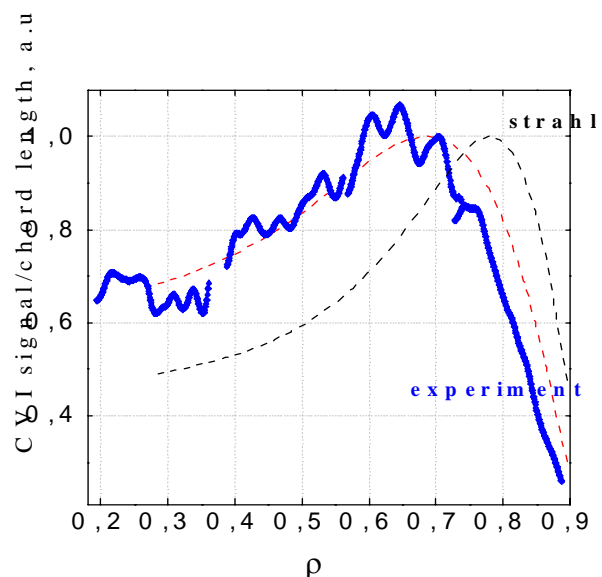

Fig. 3. *The experimental profile of CVI line chord intensity at 367 eV is plotted together with simulated profile.*

be checked by radial profile measurements of the intensity of the chosen line. Moreover, it is well known, the neo-classical and anomalous transports are stronger in the plasma edge.

Radial profile measurements of CVI (367.5eV) emission by USX Spectrometer in tokamak TCV (first results)

The emission profiles of the main H-like and He-like lines of carbon impurity have been measured in edge plasma region using reconfigured USX Spectrometer (Multichromator) during the swept OH L-mode plasma in tokamak TCV.

There was the idea to change the shape or move the plasma in such a way that each chord of USX Multichromator sees the different regions of the plasma in order to obtain the complete scan along the radii in a single shot. The main plasma parameters: Te, n_e, q_{edge}, are kept as constant as possible during the plasma shift in chamber space.

Only two shots with Ip=150 kA and Ip=200 kA with changes of plasma shape have been performed during the half day session. Both disrupted after 0.5 s. In spite of this, some information on CVI emission profile could be obtained.

The first attempts can be considered as promising: the emission radial profile of CVI (367.5 eV) was obtained. The emission was simulated by fitting the radial dependence of the diffusion coefficient $D\perp(\rho)$. The problem of relative high value of $D\perp$ near the edge can't be solved without additional data of the other important diagnostics (XTOMO,XBOLO, MPX and DNBI). We are going to try this method in low density OH regime and in discharge with ECH heating in next sessions in August September 2003.

Summary

Spatially resolved measurements of plasma ultra-soft x-ray emission (USX) seems to be really a valuable diagnostic technique in the study of the impurity transport processes in tokamak plasma periphery, if the central electron temperature is high enough. The combined method of the radial profile measurement of the USX line emission and STRAHL code simulation provide the radial dependence of the diffusion coefficient. The method was first successfully employed for the tokamak TCV during the two weeks Piffl's mission to CRPP Lausanne in March / April 2003.

Reflectometric measurements on CASTOR
J.Preinhaelter,J.Zajac

In collaboration with:
S.Nanobashvili, Institute of Physics, Georgian Academy of Sciences, Tbilisi, Georgia

Microwave reflectometric measurements of plasma investigation are broadly used in the present thermonuclear devices. A substantial progress took place especially during the last decade when the technique of highly fluctuating signals elaboration has been mastered.

Advantage of the reflectometry is unambiguous. It is a non-intrusive, contactless method and it can give data about the fast plasma density fluctuations deeply in the hot plasma center as well as in many parts of the periphery, hardly accessible by other diagnostic methods due to the vessel limitations.

Many types of reflectometers have been developed and are used in tokamaks both for determination of plasma density profile as well as for plasma density turbulence. For the measurements in tokamak CASTOR a correlation reflectometer working in 8mm region has been developed and constructed, see photograph on Fig.1. It can work on three fixed frequencies: 29, 33 and 35GHz. To analyze the fast fluctuations of reflected signal, a sin-cosin interferometric schema has been chosen. There are two identical antenna systems installed in CASTOR (the second one quite recently). Each system consists of 3 horns placed in one poloidal plane from LFS direction. The central horn is transmitting. The two other horns, placed symmetrically around the central horn by angle 22°, are receiving - see Fig.2. In this way correlation measurements of plasma rotation in the poloidal direction are possible. The other 3-horn antenna system, fed by the same generator, is placed 90° toroidally away from the first one and, in this way, correlation measurements in the toroidal direction are possible as well. The construction of the microwave circuit allows to change the mode of reflectometer operation from poloidal to toroidal correlation between two successive tokamak discharges. The both systems can operate in O- or X-mode by changing the antenna systems (inside of the device, i.e. opening of the device is needed).

A new interesting result obtained by a single receiving horn with O-polarization quite recently is demonstrated in Fig.3. Namely, because
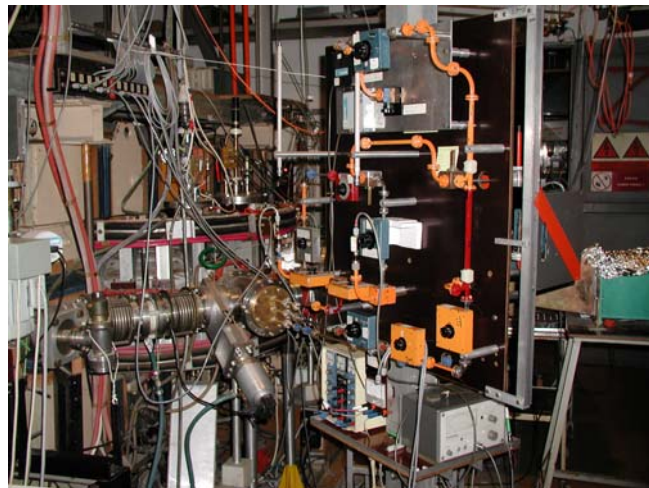

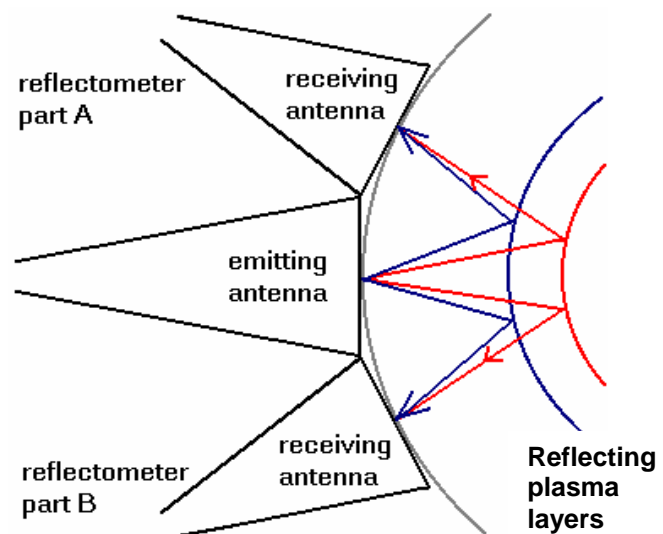**Fig.1.** *Photograph of the CASTOR reflectometer.*

Fig.2. *Poloidal geometry of horn antennas.*

a substantial modulation of power reflected from the plasma is usually observed during the CASTOR pulse, an attempt to explain this phenomenon by existence of rational q in the reflecting region, has been done. The upper part of the Fig.2 shows time course of radial position r_c of the wave reflection (cut-off of the wave) for the frequency 29GHz used, evaluated from the value of line averaged density (measured by 4mm interferometer through the central chord) under assumption of a symmetrical parabolic density profile. The shift of r_c over a substantial part of the CASTOR radius during the discharge has been realized by a controlled plasma gas puffing. Radial position of magnetic surfaces r_q with

Fig.3. *Upper part – time course of the radii of reflecting surface r_c and some rational magnetic surface r_q; lower part – time course of the reflected power.*

several rational values q, determined from the measured toroidal magnetic field and total plasma current (under assumption of a squared parabolic current density profile) are brought in this figure as well. The lower part of the Fig.2 shows the time course of measured reflected power amplitude P_r. Note that only fluctuating part of this amplitude is shown in the figure for the better comparison with the curves r_c and r_q given the upper part of the Fig.2. The time coincidence of the P_r peaks with the moments when the reflected surface r_c crosses those radii of rational surfaces r_q is striking. It may be concluded from this fact that the density current profile supposed in CASTOR (a parabolic with square power) is taken properly and maybe that reflectometry could be used as a very simple method of radial current distribution estimate in this tokamak.
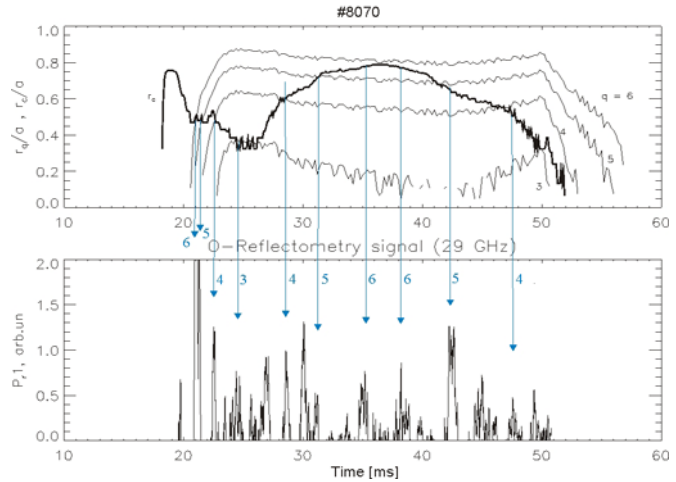
Development of magnetic diagnostics based on Hall sensors

I.Ďuran, M.Hron, J.Stöckel

In collaboration with:
K.H.Finken, M.Lehnen, G.Fuchs, Association Euratom/IPP, TEC partner, Jülich, Germany,
C.Hidalgo, M.A.Pedrosa, Association Euratom/CIEMAT, Madrid, Spain,
G.Van Oost, Ghent University, Gent, Belgium,
I.Bolshakova, R.Holyaka, Lviv Polytech. Nat. University, Lviv, Ukraina

Introduction

Present probe measurements of the magnetic field in fusion devices are almost exclusively realised using various set-ups of inductive loops (see e.g. [1] for CASTOR tokamak). The advantage of this approach is a technical simplicity, good sensitivity and excellent frequency response. However, this technique allows only measurement of the magnetic field changes but not the absolute value itself, which is the desired quantity in most of cases. To obtain the absolute value of the magnetic field, the loop's signal has to be integrated. Demanding requirements on the stability of integrator's circuits are set, especially when the precise measurement is required for long time sequences as it will be in ITER. One of the alternative methods is the use of Hall sensors. These semiconductor elements measure directly the absolute magnitude of the magnetic field. Because of their small size (typically a few millimetres) and their good frequency response up to a few tens of kHz, they can be used with some advantages over the standard coils also in the present devices. The main limitations are lower sensitivity 10-100 mV/T, and rather low maximum operational temperature that is typically not higher than 150 °C for commercially available Hall transducers. With respect to their possible use in steady state magnetic diagnostic for ITER, the radiation hardness (esp. neutrons) is presently the main open issue. The use of specially doped semiconductor materials is foreseen to satisfy the requirement for reliable operation even under ITER harsh radiation environment.

Experiments on TEXTOR tokamak

A radial array of nine Hall sensors was successfully used to monitor magnetic fluctuations up to 100 kHz in the edge plasmas of TEXTOR tokamak [2]. The improved edge magnetic diagnostic is essential for study of the TEXTOR edge plasma with Dynamic Ergodic Divertor, which was recently installed on TEXTOR. The set-up of the measuring system and the analysis of absolute calibration were published in [3]. The main results from the diagnostics development point of view may be summarized as follows.
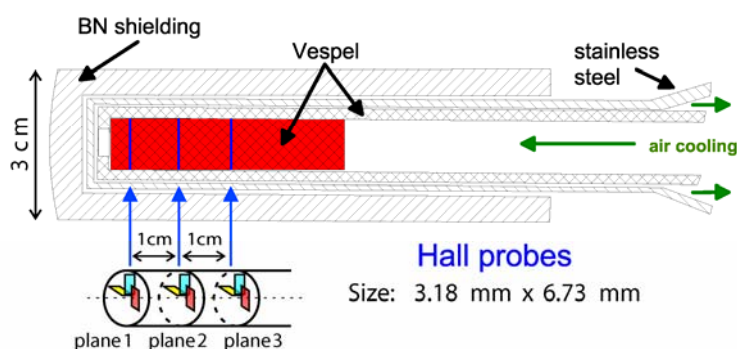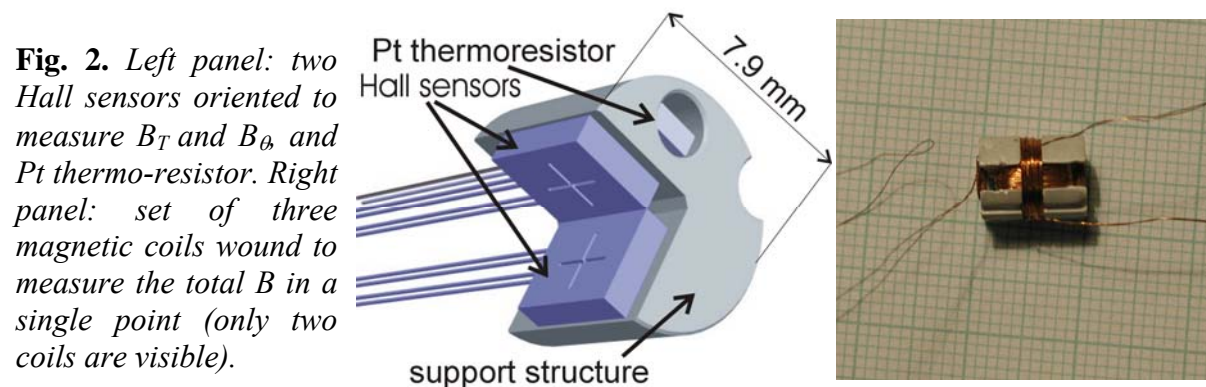

Fig. 1. *Schematic layout of the probe head containing 9 Hall sensors used on TEXTOR.*

- It has been shown that a diagnostic based on Hall detectors does allow measurements of magnetic fluctuations with amplitude < 0.1 mT within the frequency range 1 - 100 kHz with sufficient sensitivity.

- Careful avoiding of any inductive loops (as small as 1 mm^2) in the measuring circuit is critical for the measurements of the magnetic field oscillations in the kHz range of frequencies. If such loops cannot be avoided completely, one may think of compensating them by artificial ones.
- The response time of the Hall detector to the measured magnetic field via Hall effect was found to be immediate in the frequency range 1-60 kHz.

Development of the magnetic probe head for TJ-II stellerator

A new probe head designed to address a complex picture of the electromagnetic turbulence in stellerator TJ-II is presently developed. It contains two parts: electrostatic with 3 Langmuir probes to measure fluctuation induced flux, and a combined magnetic probe head containing two sets of triple coils (one triple coil see Fig. 2 right panel) and two Hall sensors (Fig. 2 left panel). The temperature near the Hall sensors will be monitored by platinum thermo-resistor. The magnetic part that will monitor magnetic turbulence and the local topology of magnetic field lines was designed and developed in IPP Prague. Calibration of the probe and the first experiments on TJ-II are under preparation.

Fig. 2. *Left panel: two Hall sensors oriented to measure B_T and B_θ, and Pt thermo-resistor. Right panel: set of three magnetic coils wound to measure the total B in a single point (only two coils are visible).*

Irradiation tests of the Hall sensors in LVR-15 (10 MW) fission reactor

The need for steady-state magnetic field detectors for the future thermonuclear fusion reactor is evident. The primary magnetic diagnostics for ITER are based upon coils with the subsequent analog integration. For pulse length $\geq$ 1000 s this approach becomes difficult. A possible solution is the use of Hall detectors that measure the absolute value of magnetic field directly. However, the quality of performance of the Hall sensors in the harsh reactor-like environment is still uncertain, esp. vulnerability to radiation damage has to be tested (high neutron fluxes). A neutrons (>0.1 MeV) flux density of 2×10^{16} n/(m^{2}s) is expected inside the ITER vacuum vessel (behind the blanket, where the magnetic sensors will appear) for a possible maximum fusion power of 700 MW [4]. Recently, the irradiation tests of specially doped Hall sensors proved their stable operation (decrease of sensitivity < 1%) up to fast neutron fluence of $3.1 \ 10^{20}$ n/m^2 (15 ITER shots each 1000 s long) (see [5]). Irradiation tests of these specially doped sensors and also commercially available ones are prepared in the fission research reactor LVR-15 (10 MW) placed in Nuclear Research Institute in Řež (member of Ass. EURATOM/IPP.CR). The flux of the fast neutrons (>1 MeV) of ~ 10^{17} n/(m^{2}s) is provided in the test chambers. Under these conditions, the irradiation of 10^{19} n/m^2 (equivalent of 500 s of ITER discharge) will be reached in 100 s, and the irradiation of 10^{20} and 10^{23} n/m^2 (equivalent of 5 – 5000 ITER shots) in 16 minutes and 11.5 days respectively.

References

[1] I. Duran et al., Coherent modes and broadband magnetic turbulence on the CASTOR tokamak, proceedings of 1998 ICPP combined with the 25th EPS Conf. on Controlled Fusion and Plasma Physics, Prague, p. 714-717, 1998.

[2] I. Duran et al., Czech. J. Phys., **52**, 2002, Suppl. D, D38-D48.

[3] I. Duran et al., Review of Scientific Instruments, Vol. **73**, Issue 10, page 3482, October 2002.

[4] ITER Joint Central Team and Home Teams, Fusion Engineering and Design **55** (2001).

[5] I. Bolshakova et al., Stable Semiconductor Magnetic Field Sensors Under Dozes of High Radiation, proceedings of the 30th EPS conference on Plasma Physics and Controlled Fusion, St. Petersburg, July 2003.

3   Wave Interactions in Plasmas

Study of RF field-plasma interaction in IPP Prague has a long tradition both in the field of theory as well as an experiment. The effort during 2002/2003 years has been concentrated on several following tasks:

- **Numerical simulation of particle nonlinear dynamics:** using a simple toroidal model with a spatially localized Lower Hybrid Waves (LHW) and numerical solution of a transcendent Hamiltonian equation, an intensive stochastization of particles motion and their successive acceleration has been found in the region of large LHW powers. This result could explain the well known LHCD problem of the spectral-gap.

- **Quasi-neutral particle-in-cell (QPIC) simulation of the tokamak edge plasma response to the LH antenna electric field:** a new QPIC code dispensing with the Poisson equation has been developed for assessment of fast toroidal streams of particles formed in front of the LH grill antennas.

- **Electron Bernstein Waves (EBW) transformation:** A 3D model of Electron Bernstein Waves propagation, absorption and X- and O-mode conversion has been developed and used to optimize the 60GHz RF antenna and to determine ECE emission from the MAST plasma.

- **Measurement of radiation from CASTOR tokamak using a 32-channel radiometer:** significantly enhanced radiation corresponding to converted EBW has been detected in some regimes of CASTOR operation.

- **Effects of plasma fluctuations and LHW spectra width on the fast particle generation and CD efficiency in Tore Supra tokamak:** a participation on the measurement of hot spots (produced by accelerated particles), LHCD efficiency and signal of the RF probes (designed and partially delivered by Czech side) in TS has been realized.

- **Generation of Hot Spots on JET divertor by LHW:** in a broad international cooperation the Hot Spots located on JET divertor apron in the places magnetically connected to the JET grill mouth were observed and analysed.

- **Probe measurements of plasma fluctuating characteristics in front of the CASTOR tokamak grill:** a movable probe with two toroidally spaced tips allowed a direct measurement of fluctuating toroidal electric field in front of the CASTOR LH grill antenna.

CASTOR Radiometer Measurements
J.Zajac

Microwave radiometry became a standard diagnostic tool in almost all fusion experiments. The electron temperature measurements by means of ECE (Electron Cyclotron Emission) is well-used radiometer application. The ECE frequency is 28 GHz for $B_t = 1$ T and is anisotropically emitted. The width of the ECE spectrum depends on the magnetic field variation along the line of sight. Typically the tokamak plasma is not transparent for the fundamental cyclotron frequencies due to the density-dependent plasma frequencies so the 2nd harmonic range is usually used.

Microwave frequency scanning radiometer has been constructed in 2002 - see the flow chart and the picture. It consists of two heterodyne receivers built-up from solid-state circuits. A mechanical waveguide switcher at the input selects one of two frequency bands. The low band is 17 – 27 GHz while the high band is 27 – 40 GHz. The toroidal magnetic field during an ordinary CASTOR shot varies from 0.8 T at the low-field side (LFS) to 1.7 T at the high-field side (HFS). Radiometer bands cover the whole ECE spectrum of fundamental harmonic frequencies if B_t is slightly reduced.
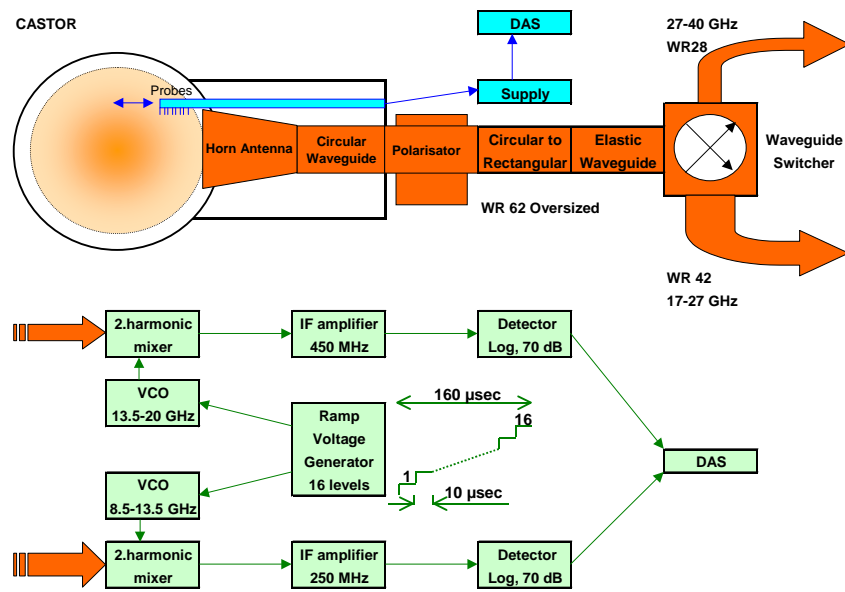

Fig. 1. *Radiometer flow chart.*

Each band is divided into 16 sweeped frequency channels. The sweep time cycle is 160 μs. If better time resolution is needed an arbitrary single frequency can be picked with 1 μs sampling of the Data Acquisition System (DAS). The waveguide part consists furthermore of a horn antenna placed inside tokamak from the LFS and a polarizator which selects polarization of the received microwaves. Besides, near
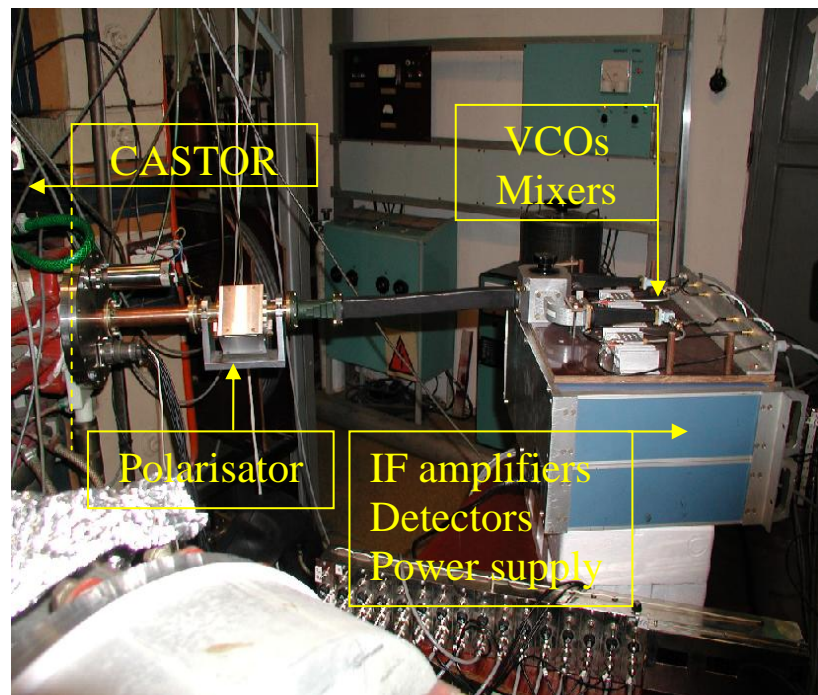

Fig. 2. *Picture of the radiometer in situ.*

the horn antenna, a movable rake of Langmuire probes allows to determine plasma density profile at the plasma edge.

The main object of the investigation is to verify experimentally Electron Bernstein Wave (EBW) conversion. EBW are electrostatic waves excited in the electron cyclotron range of frequencies. A linear mode conversion mechanism between electromagnetic wave and EBW at the Upper Hybrid Resonance (UHF) layer enable to use EBW for plasma heating. Commonly used electron cyclotron heating collides with reflective cutoffs inside plasma. Higher harmonics must be used. The problem is more acute for spherical tokamaks as the plasma frequency can exceed a few cyclotron harmonics. On the other hand EBW has no high density propagation limits. The conversion techniques, which are theoretically well predicted, combine coupling and passing wave modes at some layers inside plasma or near the plasma edge.

Numerical calculations take into account plasma density and its gradient and magnetic field together with wave frequency, polarization and angle of incidence. Density fluctuations at the plasma edge are included, too. As an example see figure 3. Measured density
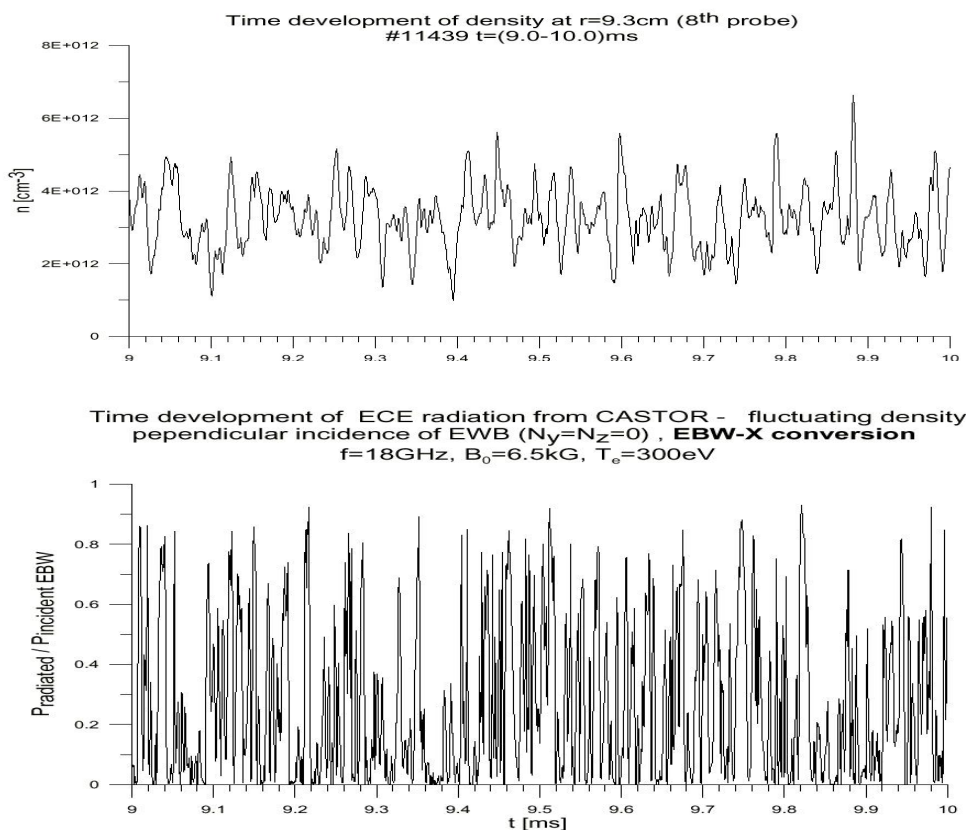

Fig. 3. *Top – Edge plasma density fluctuation.*
Bottom – Calculated EBW-X conversion efficiency.

fluctuation during 1 ms and computed conversion efficiency at promising conditions are shown. Strong changes of calculated amplitude are typical when the propagation is perpendiculat to the plasma surface.

A few experimental series have been done. The point is to find optimal conditions to see converted EBW. Usually lower magnetic fields are used to satisfy predicted conditions. Plasma density is controlled by means of gas puffing. Some experiments with plasma polarization by the biasing electrode, which strongly influences the plasma edge properties and the density gradient, have been done, too.

An example of measured data is shown in figure 4. A density boost during 10–17 ms, caused by a gas puff, is seen on the top diagram. The next diagram demonstrates course of HFS, central and LFS fundamental cyclotron frequency during the shot. In the next diagram there are two signals - a Lagmuire probe checking the density fluctuation in the edge plasma and the radiometer 18 GHz with 1 μs resolution. Except unstable beginning of the shot there is a part of the radiometer signal above the radiation background during the 14th ms. In the detailed window in the bottom diagram one can compare the amplitude modulation with the numerical model in figure 3. The character is the same and indicates the EBW-X conversion influenced by plasma fluctuations.
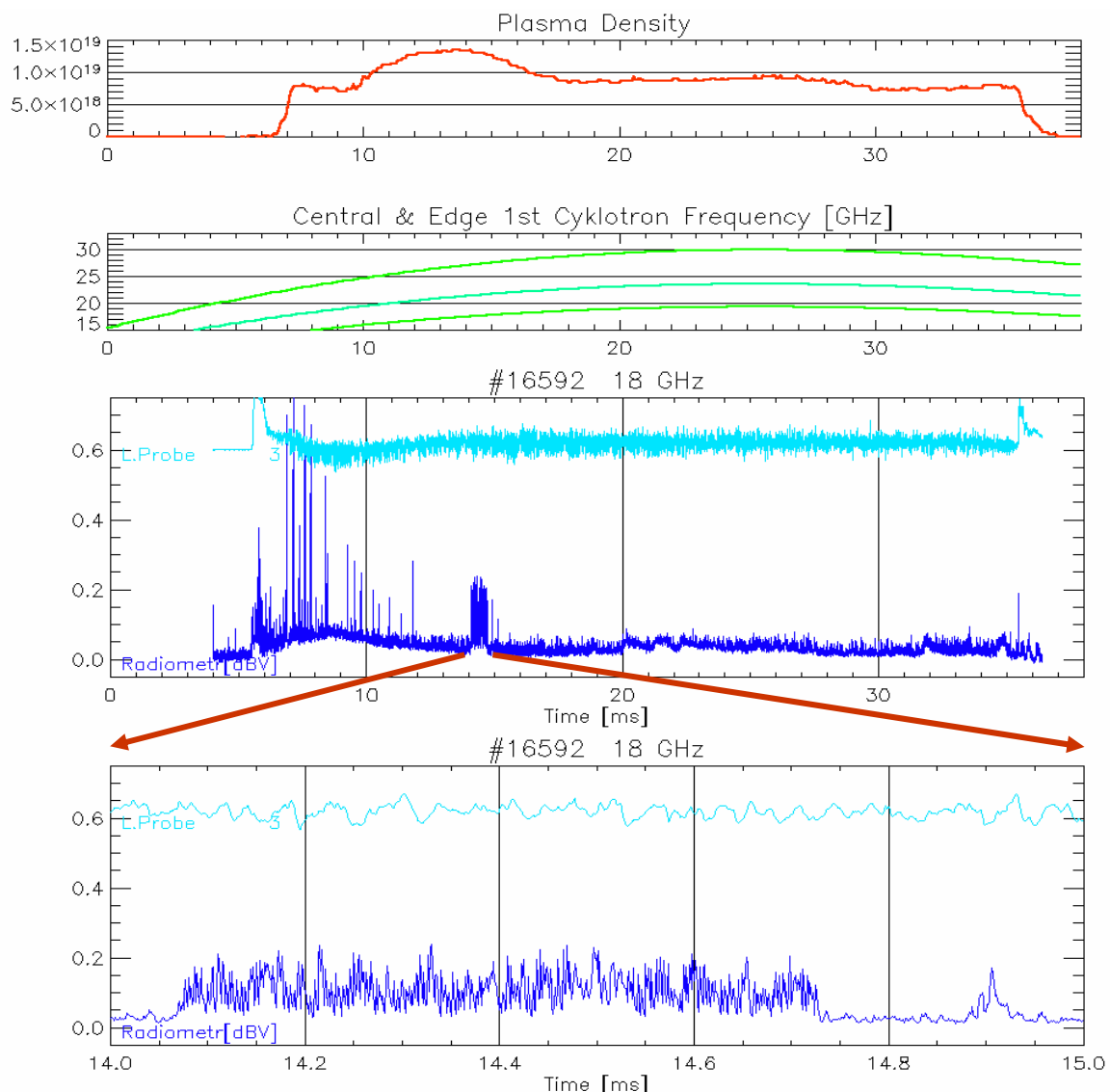

Fig. 4. *Observation of EBW-X conversion in the 14th ms.*

In figure 5 there are shown signals of the radiometer in low band sweeping mode, so there are time courses of 16 frequencies. Again during impulsive gas puffing a signal bursts appeared in the frequency up to 23 GHz. But as a normal magnetic field was used in this shot, these signals are under cyclotron frequency.

The nature of bursts in the last example, as well as of the strong background radiation, have been under examination. Suprathermal runaway electrons are considered. An antenna for oblique radiation should allow us to get more efficient EBW-O conversion in the future. Investigation of the EBW has been carrying out in cooperation between CASTOR and spherical tokamak MAST, Culham.
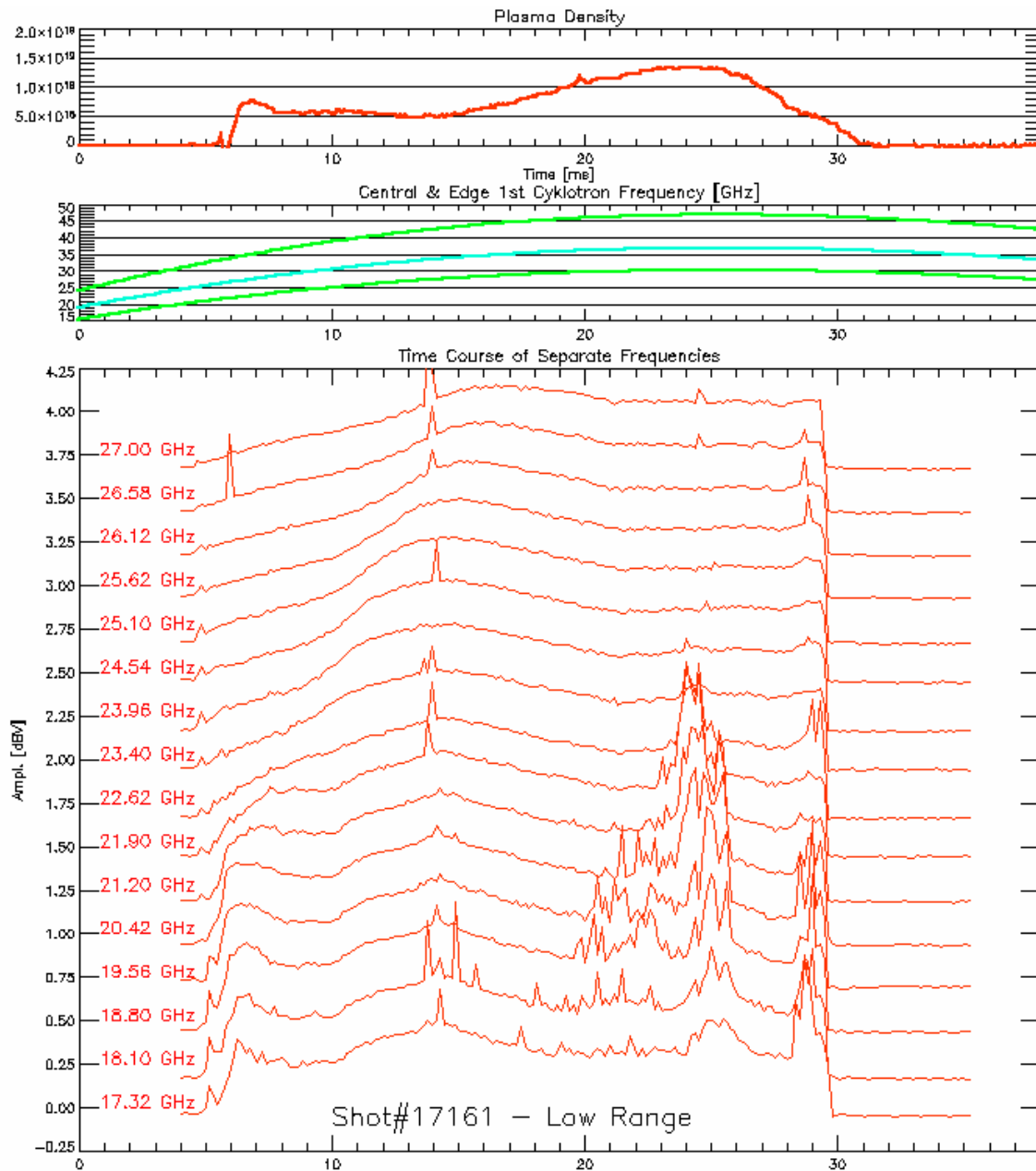

Fig. 5. *Radiometer in sweeping mode, low band 17 – 27 GHz.*

Collaboration between UKAEA, Culham and IPP, Prague
J.Preinhaelter

In collaboration with:
V. Shevshenko,UKAEA, U.K.

During last five years, Culham Laboratory and our Institute were engaged in an intensive collaboration on ECR program.

With the help of V. Shevshenko from Culham, we have developed a radiometer working in 16-40 GHz for the detection of electron cyclotron emission from CASTOR. Results of the experiments and the radiometer itself are described in other place of this report.

In the theory we have concentrated on two main problems:

- Prospects of the envisaged RF heating and current drive experiments on MAST with 60GHz 1MW system which was used in previous experiments;
- Interpretation of the experimental results of electron cyclotron emission measurements on MAST.

In spherical tokamaks, such as MAST, high density and the low magnetic field prevent to use simple strategy of heating plasma by e.g. a normally incident X-mode and its direct absorption on higher harmonics of electron cyclotron frequency. Incident radiation must be converted in the upper hybrid resonance region to the electron Bernstein waves, which can easily penetrate to dense plasma and are fully absorbed at the electron cyclotron harmonics.
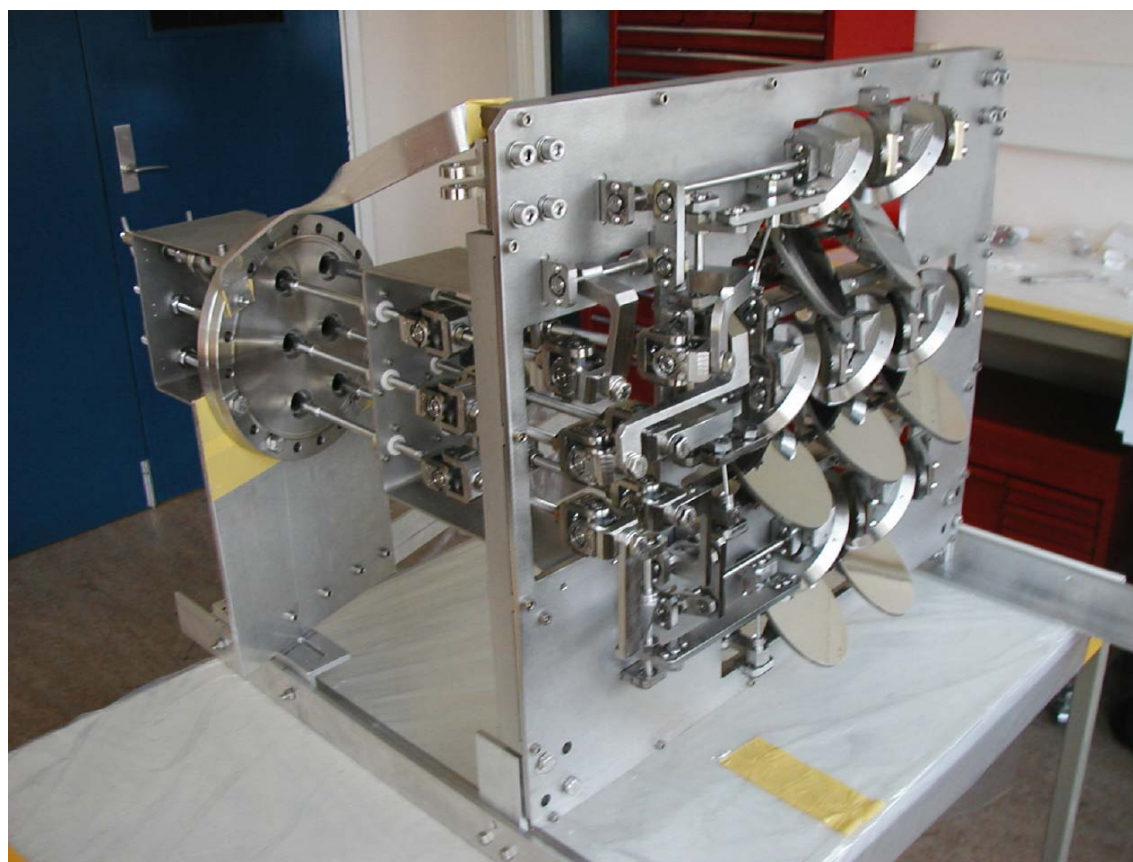

Fig. 1. *Steerable antenna system for the launch of 7 beams of RF power. Each beam corresponds to one from seven gyrotrons (60GHz, 300kW).*
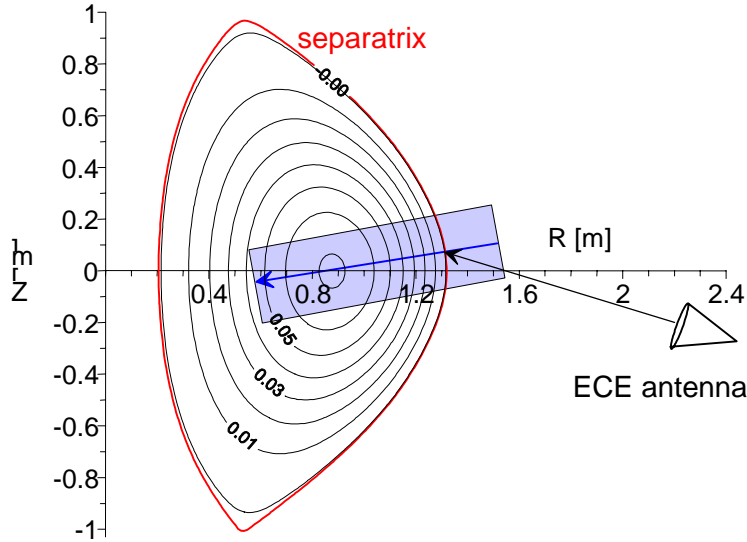
Fig. 2. *Antenna position*

We investigated the efficiency of the mode conversion in MAST with the help of our analytic formulas and also using full wave solution of wave equation in tokamak plasma [1-8]. We found that, for MAST parameters, the direct conversion of X mode to EBW at normal incidence is very inefficient and that the 60GHz wave can be converted to EBW only if it is incident obliquely as elliptically polarized O mode. In this case, the O mode is first converted to the X mode at the plasma resonance and this X wave than propagates back to rarefied plasma and it is fully converted to EBW at the upper hybrid resonance. We emphasized that the requirements on the angular divergence of the incident beam of circularly polarized wave are for 60GHz wave in MAST very stringent. V. Shevshenko than designed a steerable antenna system consisting from 7x3 adjustable mirrors (one with grooves) allowing to launch narrow beams of arbitrary polarization (see Fig. 1).

Interpretation of the electron cyclotron emission in spherical tokamaks is rather difficult. On MAST, ECE measurements serve mainly to finding the window, which can be used for the launch of power to heat plasma and generate the current. To simulate the ECE from MAST we attempted to build up the model of MAST plasma which would be as near as possible to the experiment [8-11].

A 3D model of Electron Bernstein Waves propagation, absorption and X- and O-mode conversion has been developed and used to determine ECE emission from the MAST plasma.. The instantaneous magnetic field and its spatial derivatives are reconstructed from a 2D splining of two potentials determined by an EFIT equilibrium reconstruction code. The plasma density and temperature profiles in the whole *RZ* cross-section of the plasma are obtained from mapping the high spatial resolution Thomson scattering measurements on magnetic surfaces.

The intersection of the antenna pattern with the separatrix determines both the spot position (at which the antenna is aimed) as well as the components of the wave vector of the outgoing waves. The auxiliary plane-stratified plasma slab is used to determine the mode conversion efficiency by a numerical full wave solution of the wave propagation (see Fig.2). Because the conversion region is only several centimeters thick the plane-stratified model is adequate. From a cold plasma model we obtain the values of the global conversion efficiency. It represents the conversion efficiency of both processes: the direct EBW-X conversion as well as the process in which an obliquely incident EBW is first converted to an X mode which subsequently mode converts to an O-mode at the plasma resonance.

To determine the radiative temperature we must study the propagation of EBW in 3D. For this purpose we adopt standard ray tracing (see Fig.3). The antenna beam is supposed to be Gaussian and is replaced by a set of rays. An angular divergence of the rays is determined from the geometry of experiment.
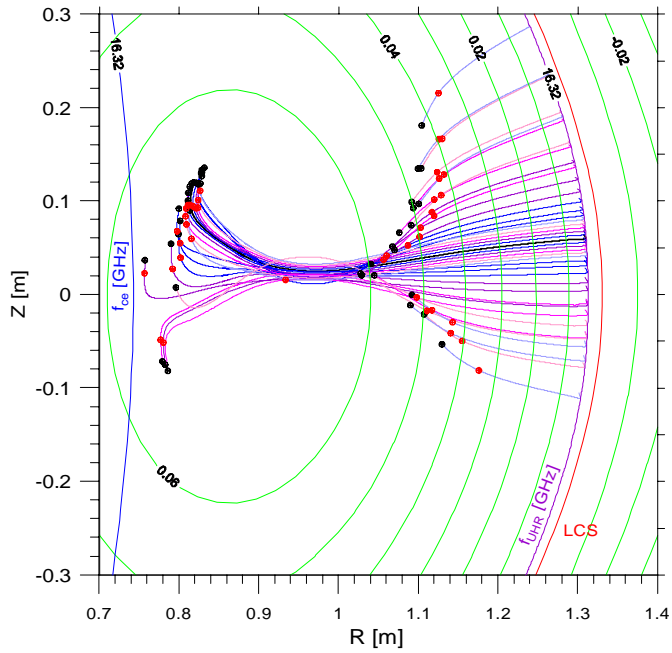
Fig. 3. *Rays in R_Z plane. Red spots mark the start of absorption, at black spots all incident power is absorbed.*

The ray equations describe the motion of the EBW wave packet. To obtain power absorption we integrate the time evolution equation for power simultaneously with the ray. Absorption along the ray is non-local with reabsorption of the radiation playing an important role. To determine the radiative temperature we must solve the radiative transfer equation simultaneously with the ray evolution equation. Radiative temperature stands in the Rayleigh-Jeans black body radiation intensity.

The total power detected by ECE antenna is obtained by summing the contributions from all rays starting at the area visible by antenna on the last closed flux surface. Using this procedure we are able to determine the ECE power incident on our antenna (Figs. 4).
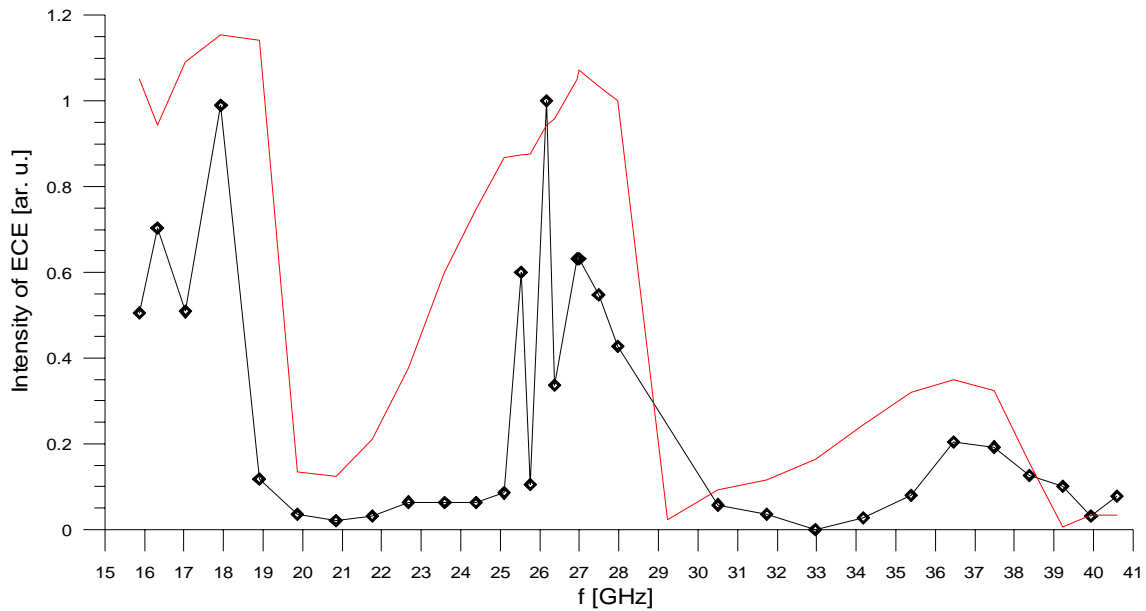
Fig. 4. *ECE from MAST, shot #4958, t=120ms. Black diamonds are experiment data and the thick full line is numerical simulation of ECE power incident on antenna. Reference frequency f=26.16GHz, for which $I_{ECE}=1$.*

References

[1] J. Preinhaelter, V. Shevchenko, M.A. Irzak, L. Vahala, G. Vahala: ECRH in Spherical Plasmas: O-X-EBW Mode Conversion in MAST. Rep. UKAEA FUS 444, Culham Science Centre, UK (November 2000).

[2] J. Preinhaelter: O-X-EBW mode conversion of 60GHz wave in MAST H-mode twin peak density profile. MAST OPS NOTE No: 00.36, UKAEA Fusion, Culham Science Centre, UK (November 2000).

[3] J. Preinhaelter: Estimates of the performance of a new 60ghz RF antenna for MAST. MAST OPS NOTE No: 01.08.[

[4] J. Preinhaelter, M.A. Irzak, P. Pavlo, L. Vahala, G. Vahala: Exitation of Electron Bernstein Waves in MAST. 27th EPS Conf. On Contr. Fusion and Plasma Physics, Budapest, (2000), ECA **24B** (2000) , editors: K.Szego, T.N. Todd, S. Zoletnik, p. 1204.

[5] J. Preinhaelter, M.A. Irzak, L. Vahala, G. Vahala: Electron cyclotron resonance heating in spherical plasmas: O-X-EBW mode conversion in MAST. 13th Topical conference on High-Temperature Plasma Diagnostic, Tucson, Arizona June 2000. Rew. of Sci. Instruments**, 72**, 391 (2001)

[6]. J. Preinhaelter, M.A. Irzak, E. Tregubova, L. Vahala, G. Vahala: ECE and ECRH from O-x-EBW mode Conversion in Sperical Plasmas, Quebec City, Canada, October 2000. Bulletin of APS, **45**(2000) MP1 159, p. 254.

[7] J. Preinhealter, M. A. Irzak, L. Vahala, G. Vahala: Mode Conversion Processes
for Electron Bernstein Wave Excitation in Spherical Tori, ICOPS, Las Vegas 2001,6585

[8]. J. Preinhealter, V. Shevchenko, M.Valovic, P. Pavlo, L. Vahala, G. Vahala and the MAST team: Interpretation of ECE measurement on MAST.29th EPS Conf. on Contr. Fusion and Plasma Physics, Montreux, (2002), ECA Vol **26B** P_5.095 (2002), editors:R.Behn, C. Vandaras.

[9] J. Preinhealter, P. Pavlo, V. Shevchenko, M.Valovic and MAST team, L. Vahala, G. Vahala: Electron Bernstein wave-X-O mode conversion and elefctron cyclotron emission in MAST. 14th Topical conference on High-Temperature Plasma Diagnostic, Madison 2002. Rew. of Sci. Instruments, **74**, No3 (2002), in print

[10] J. Preinhealter, V. Shevchenko, M.Valovic, P. Pavlo, L. Vahala, G. Vahala: EBW-X-O and ECE in MAST.Presented at 44th Annual Meeting of the Division of Plasma Physics, Orlando, Florida , November 11-15, 2002. Bulletin of APS **47** (2002) KP1 107, p. 211.

[11] J. Preinhealter, V. Shevchenko, M.Valovic, P. Pavlo, L. Vahala, G. Vahala and the MAST team: ECE in MAST: theory and experiment. 15th Topical Conf. on Radio Frequency Power in Plasmas, Jackson Lake Lodge, Wyoming, May, (2003), in print.

Probe Measurements of Plasma Fluctuating Characteristics in Front of the CASTOR tokamak Lower Hybrid Grill antenna

F.Žáček, V.Petržílka

In collaboration with:
P.Devynck, M.Goniche, Association Euratom/CEA, France

Detrimental phenomenon of particle acceleration in front of tokamak RF antennas represents a real danger for plasma-facing components connected with the region of particle acceleration by magnetic field lines (so called "hot spots" have already been observed in tokamaks JET and Tore Supra) [1]. Theory suggests a mechanism of the particle acceleration by absorption of higher spatial harmonics in the antenna spectrum [2] and enhancement of this acceleration or even acceleration without presence of the high LHW harmonics by formation of random toroidal electric fields [3]. Experimental assessment of the relative magnitude of these two mechanisms has not been done yet.

A small tokamak CASTOR operating in IPP Prague offers, due to the short pulse and low plasma energy density, unique possibility to carry out direct probe measurements in front of the lower hybrid antenna. As it has been shown already in [4], radially very narrow layer (several mm only) with a dip in floating potential up to –200V (potential "well") is formed just in this region (nothing like that is observed outside of the grill mouth), see Fig.1. Note that the maximum of V_{fl} drop (and apparently also the maximum particle acceleration) is slightly shifted from the grill mouth (r=86mm in CASTOR) into the plasma. This is in accordance with the JET measurement [1b], exhibiting maximum hot spots brightness at the divertor apron for a grill slightly retracted behind the limiter.
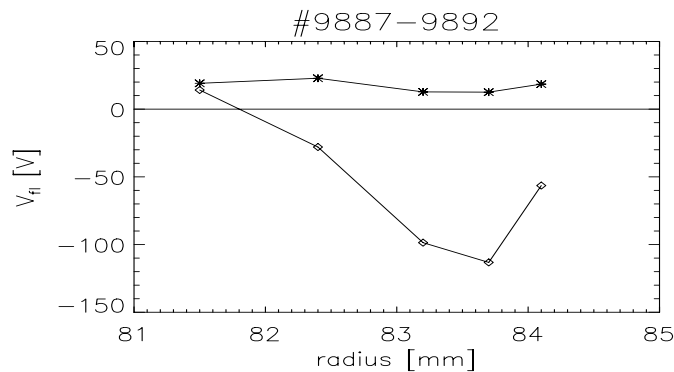

Fig. 1. *Comparison of radial dependence of the time averaged floating potential in front of the CASTOR grill in OH (asterisks) and RF (diamonds) discharge phases.*

A double probe with two tips, movable in all three directions, has been used for such experiments in CASTOR. Correlation and frequency analyses of the probe signals have been done and changes during the RF application have been investigated. Two probe systems with the tips separated by 3.5mm toroidally or poloidally have been used. The both tips are measuring either the plasma floating potentials only (to estimate the electric fields and the plasma rotation) or one of the tips is measuring the plasma floating potential while the second the ion saturated current (to estimate changes in the plasma particle transport).

In the first case of the tips separated toroidally, an assessment of the toroidal electric field E_{tor} (supposed to be responsible for the particles acceleration), is possible. The characteristics of this field in CASTOR (up 500kHz) has been done [5]. The main results of the correlation measurements can be summarized as follows:
(i) generally, there is a significant difference in character of the cross-correlation between

floating signals of the both tips during OH and RF discharge phases;
(ii) frequency spectrum of floating potential exhibits in certain radially very narrow layer (located just in the plasma potential "well") an expressive component ~50kHz during RF application;
(iii) a well observable time shift between the both signals appears in this layer during RF (about 1μs, indicating formation of toroidal rotation with velocity of several km/s in this layer).

A significant difference during OH and RF discharge phase has been found in behaviour of the toroidal electric field E_{tor} itself:
(i) E_{tor} is highly enhanced during RF phase in all radial positions, see Fig.2;
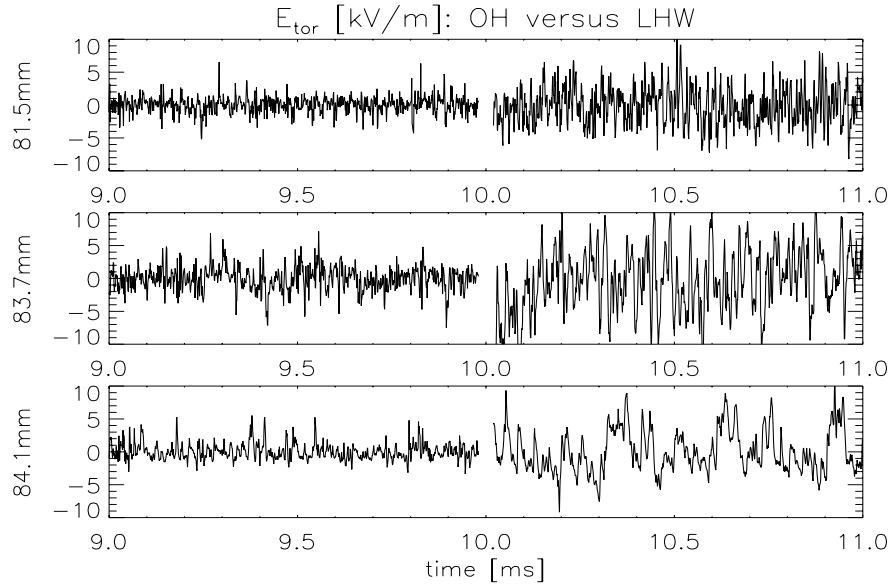
Fig. 2. *Comparison of the toroidal electric field measured at three different radial positions during OH and RF discharge phases (RF switched on at t=10ms).*

(ii) while E_{tor} has character of a broad-band noise during OH (especially deeper in the plasma), its spectrum exhibits a "massive" low frequency part in RF, see Fig.3;
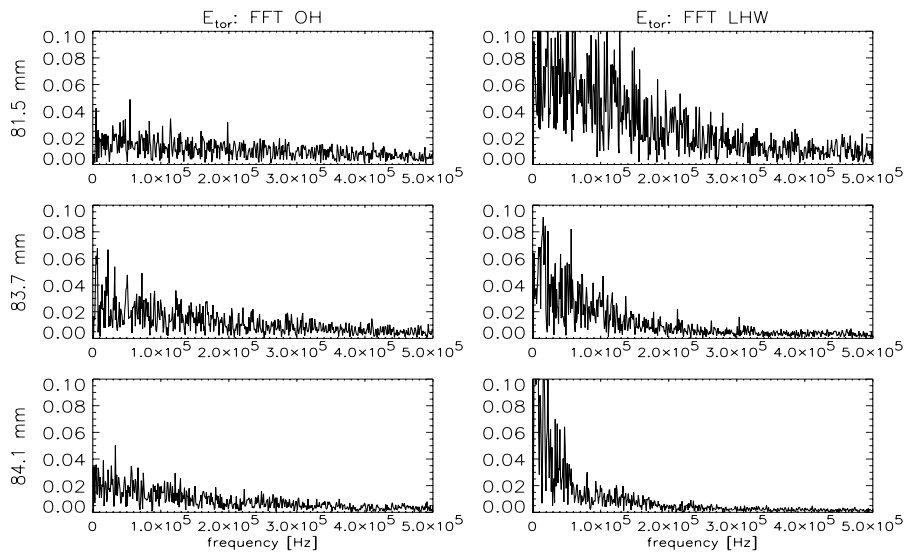
Fig. 3. *Comparison of radial dependence of toroidal electric field frequency spectra for OH and RF discharge phases.*

(iii) this distinct difference is not in any case more expressed in the "well"; this fact could indicate that the fluctuating toroidal electric field, detected in the experiment, participates in the particle acceleration in the very narrow layer in front of the grill mouth and, in this way, it is absorbed there. This would be similar to the absorption of the high LH field harmonics observed in numerical simulations [6] just in this very narrow layer.

References:
[1] a) M. Goniche et al., Nucl. Fus. 38 (1998) 919,
    b) K. Rantamaki et al., 30th EPS Conf. on Contr. Fus. and Plasma Phys., Petersburg 2003
[2] V. Fuchs et al., Phys. Plasmas 3 (1996) 4023.
[3] V. Petrzilka et al., 18th IAEA Conf., Sorento 2000, paper CN-77 EXP4/07
[4] Zacek F., et al.: Proc of 28th EPS Conference on Controlled Fusion and Plasma Physics, Funchal, Portugal, 18-22 June 2001, ECA Vol. 25A (2001), p. 325-328
[5] F. Zacek et al, 30th EPS Conf. on Contr. Fusion and Plasma Physics, Petersburg 2003
[6] K. Rantamaki et al., Nucl. Fus. 40 (2000) 1477

LH Driven Plasma Density Variations and Flows in Front of LH Grills and Resulting Reflection Coefficient Changes and Thermal Loads

V.Petržílka, F.Žáček, V.Fuchs L.Krlín

In collaboration with:

A.Ekedahl, M.Goniche, J.Gunn, Association Euratom/CEA, France,
S.Kuhn, D.Tskhakaya, University of Innsbruck, Austria,
K.Rantamäki, Association Euratom/VTT, Finland

The lower hybrid (LH) power dependence of plasma density perturbations and plasma flows resulting from the fast particle production in front of LH launchers is explored. Consequences for the reflection coefficient R of the LH wave are estimated and compared with measured R variations as a function of LH power for Tore Supra grill modules [1].

We demonstrate that owing to the local electron acceleration in front of a lower hybrid (LH) grill mouth by the LH wave [2], an appreciable inhomogeneous plasma outflow arises in both directions along the grill. For the modeling, we have developed an advanced version of our 3d two fluid numerical code [3]. It is shown that, when the plasma sources S are sufficiently intense, the plasma density n in front of the grill mouth increases in the center of a wave-guide row with growing LH power P_{in}, while it decreases in front of the boundary modules. We note that the primary plasma expulsion from in front of the grill by the LH wave along magnetic field lines also leads to significant secondary poloidal and radial plasma flows, as well as toroidal, radial and poloidal charge separation electric fields. By using test particle simulations of electron acceleration for parameters relevant to conditions of the Tore Supra LH grills, it is possible to determine an effective potential $W_{pond} = W$, which expels and accelerates the electron fluid with the ensemble averaged kinetic energy W [4]. The source term S depends on the LH power, $S = (W_{mid}/W_0)\,S_0$, where W_{mid} is the ponderomotive potential (cases 1-3 in what follows, Figs. 1-2) normalized to the maximum value of the ponderomotive potential W_0 of case 4 in what follows, Figs. 1-2. We assume that $S_0 = Dn/(L_n)^2 + S_i = C\,Dn/(L_n)^2$, where the term S_i and/or the value of C represent ionization, L_n is the unperturbed density radial scale length and D is the diffusion coefficient. The value $W_{pond} = 400$ eV (case 4) corresponds to the LH field electric field intensity E at the grill mouth of about $E = 3$ kV/cm, which in turn corresponds to the LH wave power flux of about 20 MW/m^2. The computed density n_{max} in the grill center grows with rising LH power (Fig. 1 –
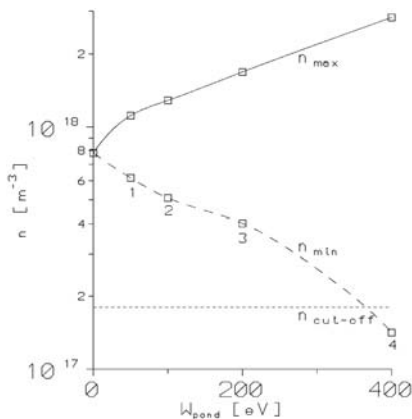

Fig. 1. *C2 grill: Dependence of the plasma density at the wave-guide row center (n_{max}) and at its toroidal boundary (n_{min}) on W_{pond}.*
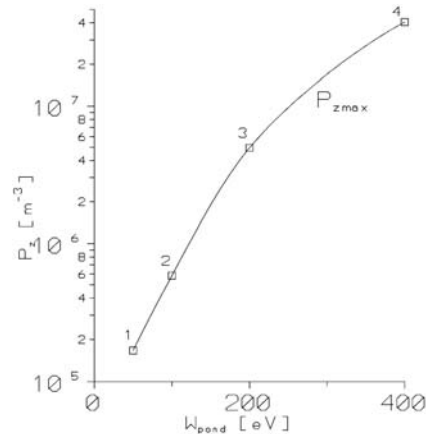
Fig. 2. *C2 grill: Dependence of the maximum plasma outflow power flux density P_z on W_{pond}.*

solid line), which will not deteriorate the LH wave coupling. On the other hand, the density decreases at the toroidal boundary of the wave-guide row, cf. the curve n_{min} - dashed line in Fig. 1. The dashed line even crosses the cut-off density, and therefore an increase of the reflection coefficient in the boundary grill modules can be expected, when the LH power grows. The Tore Supra measurements (Fig. 3) correspond to these simulations. The plasma density is strongly inhomogeneous both poloidally and toroidally, Fig. 4 a-f.

P_{in} (kW)
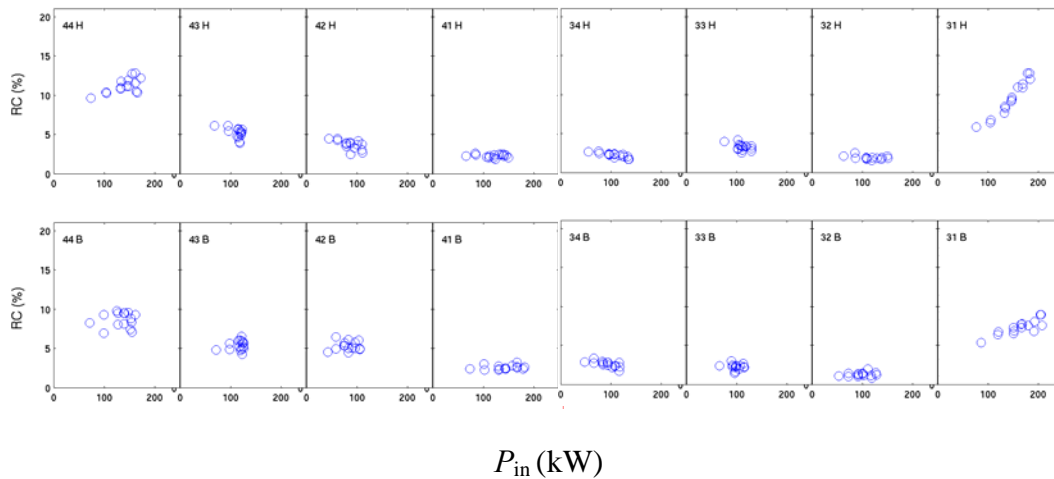
Fig. 3. *Reflection coefficient vs incident power for each module on the Tore Supra grill C3; P_{in} = 200 kW in one module corresponds to ~ 20 MW/m². *
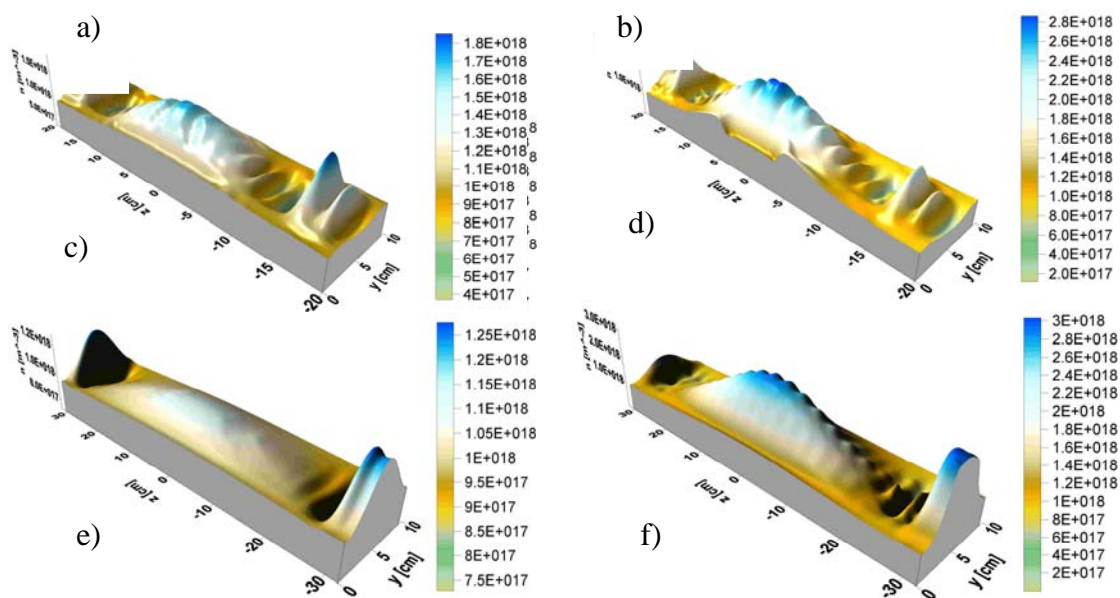
Fig. 4: *Plasma density n [m⁻³] profiles in front of the grill in dependence on W_{pond} ;C2 grill: 4a – 4d correspond to cases 1-4 in Fig.1, respectively; C3 grill:4e-4f correspond to W_{pond} of 50 and 400 eV, respectively.The grill (wave-guide row) boundaries are at z = -15 and z = 15 cm for C2, and at z = -28.5 and z = 28.5 cm for C3. Note different plasma density n scales in 4a –f.*

In the computations, we assumed that $C = 10$, and $D = 10$ m^2/s. The plasma density variations in front of the grill mouth at growing LH power, resulting from the fast particle production in front of the LH grill, agree with measured variations of the reflection coefficient in Tore Supra. A more exact comparison by using a coupling code is difficult because of the LH induced poloidal and toroidal nonuniformity of the plasma density . The power flux P_z carried by the plasma outflow toroidally from the grill grows approximately as $(W_{\text{pond}})^3$. As, in turn, the average electron energy W (or W_{pond}) grows approximately as $E^{3/2}$ [2], P_z grows as $E^{9/2}$, or $P_{\text{in}}^{9/4}$. As found in Tore Supra, the heat flux on the bottom limiter BL5 can grow even more steeply, namely as P_{in}^3 [2b].

References
[1] V. Petrzilka, A. Ekedahl, V. Fuchs, M. Goniche, J. Gunn, L. Krlin, S. Kuhn,
K. Rantamäki, D. Tskhakaya and F. Zacek, EPS St. Petersburg 2003.
[2] a) V. Fuchs et al., Phys. Plasmas 3 (1996) 4023; b) M. Goniche et al., Nuclear Fusion 38 (1998) 919; c) K.M. Rantamäki et al., Nucl. Fusion 40 (2000) 1477.
[3] V. Petrzilka et al., Proc. 29th EPS Conference, Montreux, June 2002, paper 2.105.
[4] V. Petrzilka et al., 18th IAEA Conference, Sorrento 2000, paper CN-77/EXP4/07.

Effects of plasma fluctuations and LH wave spectra width on fast particle generation and current drive efficiency

V.Petržílka

In collaboration with:
M.Goniche, Asociation Euratom/CEA, France

Our association IPP.CR participated in the Tore Supra experiments "Largeur du spectre hybride" suggested together by our association (V. Petrzilka) and CEA Cadarache (M. Goniche), and in the evaluation of results of these experiments [1]. The fast acquisition system of the two RF probes mounted on the C3 launcher (which were prepared in our IPP Prague Institute by the group headed by F. Zacek) was ready at this time and it was possible to undertake a study of the correlation between the intensity of thermal loads due to fast particle effects and between the turbulence level. In addition, the current drive efficiency in dependence on the LH spectrum width was evaluated. It was found that, by decreasing the powered grill length to one half at the same LH power, the current drive efficiency increases by about ten percent. The analysis of the hot spot IR images on C2 launcher guard limiters, fluctuation spectra up to 50 MHz, and density and temperature data from probes mounted on C2 and C3 launchers are contained in an internal report „Short review of some recent Tore Supra shots", by V. Petrzilka, F. Zacek, M. Goniche and P. Devynck. No detectable correlation between RF probe 1 and 2 was found, Fig. 1.
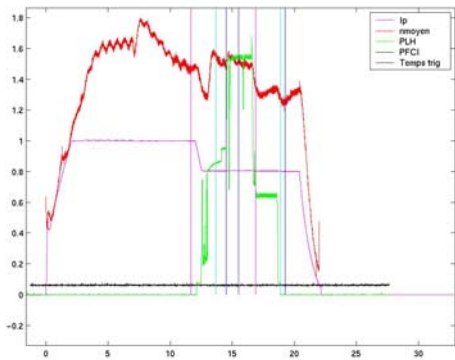
1st trigger in the LH (green curve) ramp up phase
2nd trigger at full LH power
3rd trigger just after LH switch off
red:density; magenta: Ip; blue: triggers;
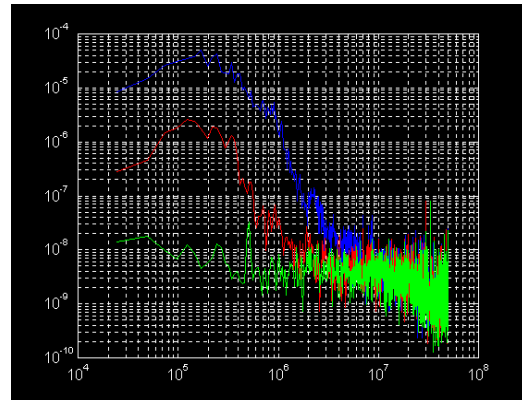
1st trigger: blue   2nd trigger: red   3rd rigger: green
#30541, probe 1 spectrum

Fig. 1. *Typical fluctuations spectra up to 50 MHz, probes LH launcher C3: Apparently not much difference between (i) probes 1 and 2, (ii) shots, and (iii) various triggers.*

Also, no correlation between the intensity of thermal loads, as illustrated in Fig. 2, due to fast particle effects and between the turbulence level was found. However, the hot spots temperature is strongly growing with decreasing klystron number at about the same LH power, when the density (also as measured on the launchers) remains about the same, Table 1.
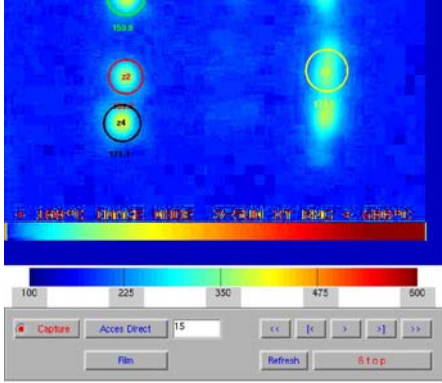
IR image of the C2 launcher guard limiters
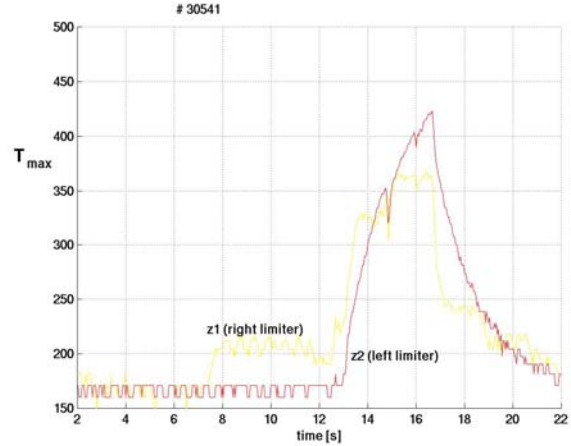
C2 guard limiter temperatures

Fig. 2. *Tore Supra shot #30541 – phase 0 deg, 3 klystrons.*

Table 1. *The hot spots temperature is strongly growing with decreasing klystron number at about the same LH power, the density (also as measured on the launchers) is also about the same.*

Shot #	# of klystrons	total LH P[MW]	ΔT [deg C] right limiter	ΔT [deg C] left limiter
Phasing 0 deg				
50538	8	2.0	125	110
39	6	2.0	120	170
		in the 2nd half 1.7		
40	4	1.85	140	265
41	3	1.53	200	355
phasing –60 deg				
50542	8	2.0	100	125
43	6	2.02	115	190
44	4	1.85	145	250
phasing +60 deg				
50545	8	2.02	150	130
46	6	2.0	120	180
47	6	2.0	130	175

A correction +45 deg Celsius is applied for the left limiter – the temperature at the shot beginning is not 165 deg Celsius (on the graph), but 120 deg Celsius (temp of cooling water).

We assume to perform test particle modeling of the particle acceleration for the real LH wave spectra of these experiments, in order to understand better this rather unexpected result. Some of the results were also presented at the seminar of the Tore Supra group, and are contained in an internal report "Spectre LH et efficacité de génération de courant", authors M. Goniche, V. Petrzilka, A. Ekedahl. The stochastic nature of the acceleration process leads to non predictable results for the mean energy of the electrons when the number of active waveguides is changed at constant launcher power. Whereas we found a reasonable agreement between the mean RF electric field and the heat flux, two explanations could explain this discrepancy between the mean energy gained by the electrons and this measured heat flux. First, in order to maintain plasma quasi-neutrality, a static potential arises and 3D convection flows occur [2]. The particle flux is inhomogeneous and locally underestimated. Secondly, velocity of fast particles

may be enhanced by random fields resulting from wave diffusion on plasma fluctuations[3]. This process is expected to be more important at high electric field.

References

[1] M.Goniche, V.Petržílka, A.Ekedahl, V.Fuchs, J.Laugier, Y.Peysson, and F.Žáček, 15th RF Topical Conference, Moran, USA, May 2003.

[2] V.Petržílka. et al. "A 3-D model of the plasma vortex in front of LH grills" "in *Proc of the 28th EPS conference on Cont. Fus. and Plasma Phys.,Funchal,* edited by European Phys. Soc., Genève, 2001, Vol.25A,pp289-292.

[3] V.Petržílka et al. Czech. Journ. Phys. **S3**, 127 (1999).

Simulations and theory of electron behavior in the vicinity of LH grills

Quasi-neutral particle-in-cell simulations of the tokamak edge plasma response to the LH antenna electric field

V.Fuchs, V.Petržílka

In collaboration with:
J.Gunn, M.Goniche, Asociation Euratom/CEA, France

We report here on two activities, both dealing with the **edge plasma response to Lower Hybrid (LH) antennas**. In 2002 V. Fuchs discontinued cooperation with Cadarache on a project dealing with **LH-supported internal transport barriers in JET**, the results of which were published in Ref. [1].

Simulations and theory of electron behavior in the vicinity of LH grills.

It is now well established, both experimentally and theoretically, that electrons in front of a LH grill heat up but mainly accelerate thus forming toroidal fast streams which can damage tokamak wall and/or divertor components. This constitutes a potential hazard during LHCD.

We have reported test electron simulations in the Czech. J. Phys. [2], and published a paper dealing with the electron distribution function and the Langevin (i.e. diffusive) representation of electron dynamics in Nuclear Fusion [3].

The Langevin (or Monte-Carlo) representation of electron dynamics is made possible by the electron diffusive response nature of their interaction with the LH antenna electric field. Thus, instead of solving Newton's equations which has the rapid LH frequency time scale, we solve the Langevin equation which has a much slower (by about a factor of 10) diffusive time scale. For simulations with about 10^5 to 10^6 electrons this results in substantial CPU time savings. We derived the electron diffusion coefficient used in the Langevin method from the quasi-linear approximation. In Figs. 1 and 2 we show, respectively, the electron temperatures and densities computed from the electron Newton and Langevin equations for a 32 - waveguide Tore Supra grill.

Furthermore, in Ref. [2] we analytically solved the electron kinetic quasi-linear equation with parallel flow, thus obtaining an approximation for the electron velocity distribution function along magnetic field lines near the LH grill. In accordance with the LH grill spectrum, the distribution is composed of one-sided Maxwellians, characterized by parallel (to the magnetic field) temperatures depending on the electron velocity space diffusion coefficient.

Quasi-neutral particle-in-cell simulations of the tokamak edge plasma response to the LH antenna electric field.

Particle-in-cell (PIC) simulations of the tokamak edge electron response to the Lower Hybrid (LH) antenna electric field were pioneered by the Helsinki group (K. Rantamäki et al.). In these simulations ions formed a frozen background. Even so, because of restrictions on CPU time, the simulation region was restricted to a fraction of the grill length.

In order to simulate the electron **and** ion response along magnetic field lines along the grill to a distant target, we have developed a quasi-neutral PIC (QPIC) code which dispenses with the Poisson equation. Instead, quasi-neutrality is imposed via a charge separation (i.e. ambipolar) electric field calculated from the electron momentum fluid equation. The Langevin method developed previously in Refs [1,2] is particularly useful in the present context, since the simulations now proceed on the much larger ion transit time scale along the simulation region. More importantly, the Langevin method leads to a spatially much

smoother electron response than that from the spatially discontinuous grill electric field structure which is explicit in the Newton representation. Correspondingly, the number of simulation cells needed for spatial resolution is greatly reduced in the Langevin representation. We have presented encouraging preliminary QPIC results at the 2002 EPS conference [4]. In Figs. 3-5 we show more recent results for a 32 – waveguide Tore Supra grill. In Figure 3 we see the spatial profiles of electron and ion density. Quasi-neutrality is seen to be approximately preserved everywhere along the simulation region. Figure 4 shows the electron and ions temperatures along the simulation region. As expected, the electron heating along the grill is comparable to the results of Fig. 2 from the test electron simulation. Ions do not exhibit an appreciable response. Finally, Fig. 5 then shows the temporal oscillations of electron density around the ion density at one of the grill ends.

Future planned work

The continuing work on QPIC involves much code development, and particularly the development of a fast and accurate integration scheme for forces dependent on velocity , as is the case for the Monte – Carlo Langevin representation of electron dynamics. The "Langevin" results shown here were obtained using a 2nd order Runge Kutta scheme.

Of particular interest is the development of Langmuir probe diagnostics for the generated supra-thermal electrons. For this, we will also need to analyze the effect of electrons reflected from the first wave-guide on the electron distribution function at the probe. The reflected electrons are expected to significantly contribute to the probe signal.

References

[1] L. Eriksson, C. Fourment, V. Fuchs, et al., Phys. Rev. Lett. **88** (2002) 574.
[2] V. Fuchs, V. Petržílka, J. P. Gunn, M. Goniche, Czech J. Phys. **52** (2002) 45.
[3] V. Fuchs. J. P. Gunn, M. Goniche, V. Petržílka, Nucl. Fusion **43** (2003) 341.
[4] V. Fuchs. J. P. Gunn, M. Goniche, V. Petržílka, "*Removal of the lower hybrid (LH) frequency time scale in quasi-neutral PIC simulations of LH-induced tokamak edge plasma flow*"**,** in Proceedings. of the 29th EPS Conference on Plasma Physics and Controlled Fusion , Montreux, 17th – 21th June 2002, Editors: R. Behn, C. Varandas, **Vol. 26B**.
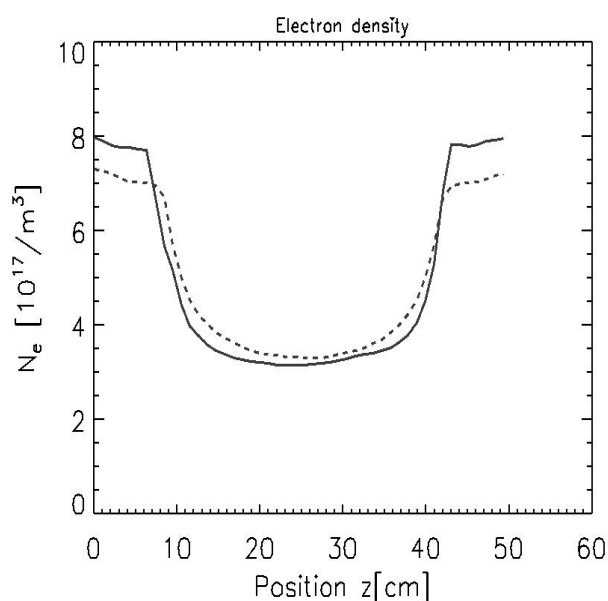
Fig. 1. *Test electron result: the electron density along simulation region. Newton: full line and Langevin: dashed line.*

Electron temperature
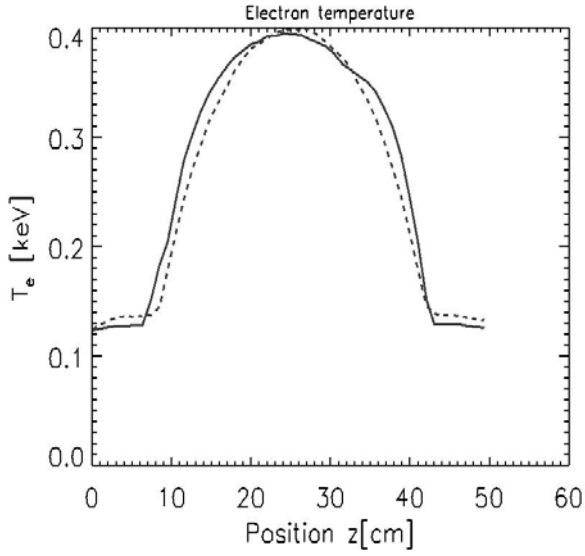
Fig. 2. *Test electron result: the electron temperature along simulation region. Newton: full line and Langevin: dashed line.*
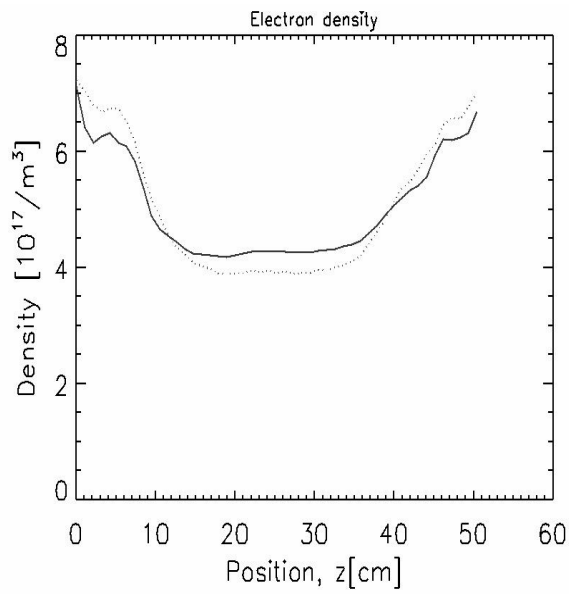

Electron density

Fig. 3. *QPIC result: electron (full line) and ion (dashed) density along simulation region.*
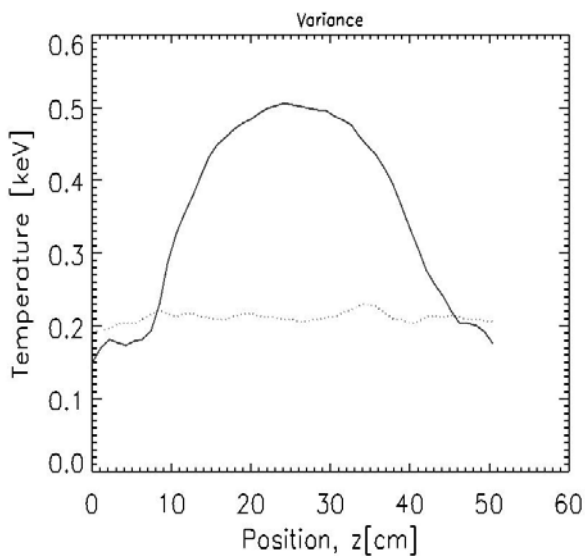

Variance

Fig. 4. *QPIC result: electron (full line) and ion (dashed) temperature along simulation region.*
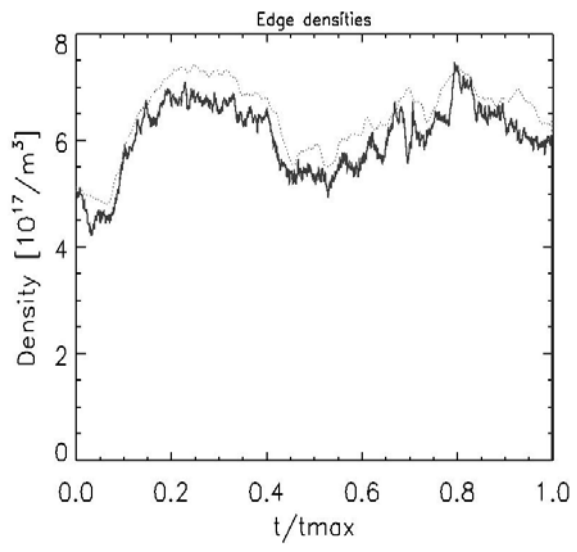
Fig. 5. *QPIC result: temporal oscillations of electron density around ion density.*

Lattice Boltzmann Modelling
P. Pavlo

In collaboration with:
A.Macnab, College of William & Mary, Williamsburg, USA
G.Vahala, L.Vahala, Old Dominion University, Norfolk, USA

Computer simulations of dynamic physical phenomena have become a valuable tool for scientists in all disciplines. Hand-in-hand with the steady increase of the computing power available, new methods, algorithms and simulation techniques are being developed. Lattice Boltzmann methods (LBM) provide a novel kinetic simulation technique for systems governed by nonlinear conservation laws. The strengths of LBM lie in the avoidance of the nonlinear convective derivatives that typically consume most of the computation time in standard finite difference, finite volume or finite element simulations, their ability to model systems in complex physical geometries, and especially in the simple computational algorithms which lend themselves to ideal parallelization on multiprocessor computers.

Lattice Boltzmann methods use the linearized Boltzmann equation with a simple Bhatnagar, Gross and Krook (BGK) collision term to temporally evolve particle distribution functions on a discrete lattice,

$$N_k(\vec{x} + \vec{e}_k, t+1) - N_k(\vec{x}, t) = -\frac{1}{\tau}\left(N_k - N_k^{eq}\right) \tag{1}$$

where $N_k(\vec{x}, t)$ is the density of particles moving in the direction $\vec{e}_k$ (cf. Fig.1) at time t and spatial node $\vec{x}$, and $N_k^{eq}(\vec{x}, t)$ are the equilibrium distribution functions. These are chosen so as to recover (in the low frequency, long wavelength approximation, using Chapman-Enskog expansion of Eq.(1)) the desired macroscopic equations.

Numerical procedure consists of two steps – the particle distributions are freely moved to the next node, and then collisions are performed:

(i) $N_k(\vec{x}, t) \rightarrow N_k(\vec{x} + \vec{e}_k, t)$;   (ii) $N_k(\vec{x}, t+1) = N_k(\vec{x}, t) - \frac{1}{\tau}\left(N_k - N_k^{eq}\right)$.

Our effort in development of LBM in the past period has been directed to modeling of compressible fluid flows and magnetohydrodynamics. The work has proceeded in a close and long-lasting cooperation with George Vahala, Angus MacNab (*Dept. of Physics, William & Mary*) and Linda Vahala (*Dept. of Electrical & Computer Eng., Old Dominion University*).

Energy-Dependent Octagonal Lattices

One of the problems encountered in simulations of compressible flows by conventional LBM is the numerical instability which limits the applicability of the models to rather low Reynolds and Mach numbers and a narrow range of temperature. We have shown earlier that higher-isotropic lattices improve considerably the accessible range of these parameters. Recently, we have introduced an energy-dependent octagonal lattice (see Fig.1) which effectively removes the limit on the temperature range. We performed a
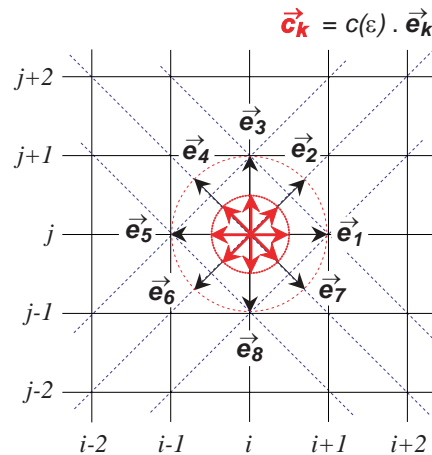

Fig. 1. *Energy-dependent octagonal lattice.*

number of test runs which proved integrity of the approach. In simulations of a channel flow, we were able to achieve Mach numbers of about 0.5. More details can be found in [1].

LBM Models for Resistive MHD

Following the approach suggested by P.J. Dellar [*J. Comput. Phys.* 179 (2002) 95], but using the highly isotropic octagonal grid, we have constructed a 2D scalar-vector model for resistive MHD simulations.   In this model, a scalar distribution function is used to recover the density, the velocity field and momentum flux tensor, and a vector distribution function to recover the magnetic field and magnetic flux tensor. Thus, the viscosity is decoupled from the resistivity. This scalar-vector distribution function approach also allows greater freedom in choosing expansion coefficients for the distribution functions resulting in better numerical stability.

We have tested the code by simulations of standard problems (Orsag-Tang vortex [*J. Fluid Mech.* 90 (1979) 129], and Biscamp-Welter [*Phys. Fluids B* 1 (1989) 1964] vortex – a less symmetric variant of the former). .   The initial conditions are characterized by two alternating X and O points of vorticity and four varying current layers, and give rise to most of the notable features of MHD turbulence such as magnetic reconnection and the formulation of jets. Good agreement with the previous simulations has been confirmed [2-4]. An example is shown in Fig. 2.
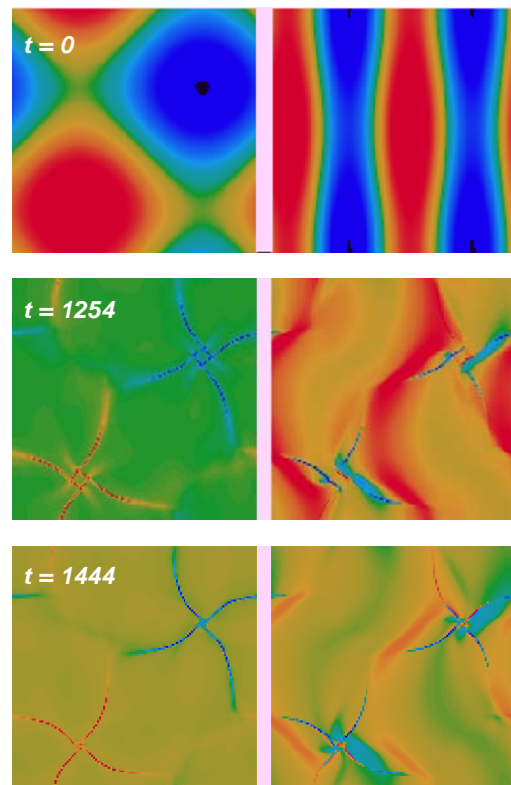
Fig. 2. *Biscamp-Welter vortex simulations (left -vorticity, right – current density) [3].*

Grid refinement in LBM models

While multi-grid algorithms are quite common in standard Computational Fluid Dynamics (CFD), they have not received as much attention in LBM. The incorporation of non-uniform grid methods resolves the regions containing shocks and current sheets with higher precision so that dynamic behavior on a fine scale can be examined. (The necessity of such approach for highly nonlinear problems is obvious also from Fig. 2.)

In [5], we have proposed an algorithm for grid refinement in LBM, and applied it to the 1D Burger's equation which is a 1D analogue of the Navier-Stokes equation. Fig. 3 shows the benefit of such approach – the shock region is perfectly resolved, without the unphysical oscillations which appear in conventional fixed grids. Application of the procedure to the 2D MHD model is in progress.
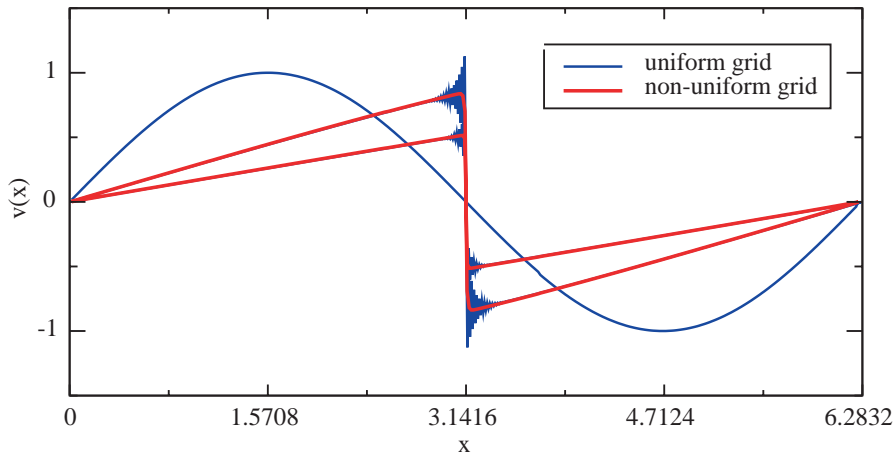
Fig. 3. *A comparison of simulations of Burger's equation using a uniform (blue) and coupled nonuniform (red) LBM [5].*

References

[1] Pavlo P., Vahala G., Vahala L.: J. Stat. Phys. 107: No.1/2 (2002) 499-519.

[2] Macnab A., Vahala G., Vahala L., Pavlo P., Soe M.: Czech. J. Phys. 52, Suppl. D (2002) D59-D64.

[3] Macnab A., Vahala G., Vahala L., Pavlo P.: 29th EPS Conference on Contr. Fusion and Plasma Phys., Montreux, Switzerland, June 17- 21, 2002, ECA 26B (2002) P1.111.

[4] Macnab A., Vahala G., Vahala L., Pavlo P., Soe M.: Bull. Am. Phys. Soc. 47:9 (2002) 51.

[5] Macnab A., Vahala G., Vahala L., Pavlo P.: 30th EPS Conference on Contr. Fusion and Plasma Phys., St Petersburg, Russia, July 7- 11, 2003, in production, P3.188.

Nonlinear Effects in LH Wave - Plasma Interaction

R. Pánek, L. Krlín, P. Pavlo, R. Klíma, V. Petržílka

Introduction

Lower hybrid wave (LHW) is launched by a grill whose area Γ constitutes only a very small fraction (< 0.01) of the plasma surface S. Consequently, the power density in the region actually filled with RF field much exceeds the power density averaged over the magnetic surface. The dynamics of particles in this RF region can be therefore strongly nonlinear, and the description of the interaction using the quasilinear approximation (based on averaging the RF effect over the magnetic surfaces) can be inadequate. Indeed, we have found [1-5] a strong discrepancy between the numerical simulation with a discrete spectrum of LH waves, and results of the quasilinear description for the equivalent continuous spectrum.

We discuss the mechanism of stochastization of particle motion in a spatially localized monochromatic lower hybrid wave of high amplitude. Such a model of interaction enables simple analytic formulation and numerical elaboration; the mechanism of the stochastization is caused by the non-integrability of the corresponding Hamiltonian. We take advantage of the simplicity of such model for a more detail discussion of the acceleration mechanism, diffusion of electrons in velocity space, and estimation of the stochasticity threshold of the interaction.

Description of the model and the analytical background for the numerical simulation

A simplified geometry of the interaction is presented in Fig. 1. Here, the region Γ represents the cross-section of the LHW cone with a chosen magnetic surface.

We assume the interaction of electrons with a monochromatic electrostatic wave $E_z = E_0 \sin(kz - \omega t)$ with $E_0 = const. \neq 0$ for $0 < z < L$. Here, ω is the angular frequency of the wave and k is the parallel (z component) component of the wave vector **k** of the wave. For simplicity we assume only 1D motion of electrons along magnetic filed lines (z direction).

The Hamiltonian of a particle in the RF field in the laboratory coordinate system z, p_z is

Fig.1. *Model arrangement*

$$H_0 = \frac{1}{2m} p_z^2 - e\varphi_0 \cos(k.z - \omega.t + \psi_0),\qquad(1)$$

where φ_0 is the amplitude of the potential of the electrostatic wave. After transformation into the coordinate system of the wave, we obtain the Hamiltonian of the mathematical pendulum, the dynamics of which is completely describable by means of the elliptic functions and integrals (e.g. [6], [7]). From this Hamiltonian we obtain finally following transcendental equation for ΔQ

$$\frac{\omega}{k}\frac{\pi}{\omega_t}\frac{1}{K(\frac{1}{\kappa^2},\frac{\pi}{2})}(F(\frac{1}{\kappa^2},\frac{kQ_m}{2}) - F(\frac{1}{\kappa^2},\frac{kQ_0}{2})) + \Delta Q = \Delta z\qquad(2)$$

where P, Q are new coordinate in the coordinate system of the wave, $\Delta Q = Q_m - Q_0$, Q_0 and Q_m are taken at the moment when the particle enters and leaves the RF region, respectively, and $F( )$ is the elliptic integral. Similar expression can be derived for the trapped particles.
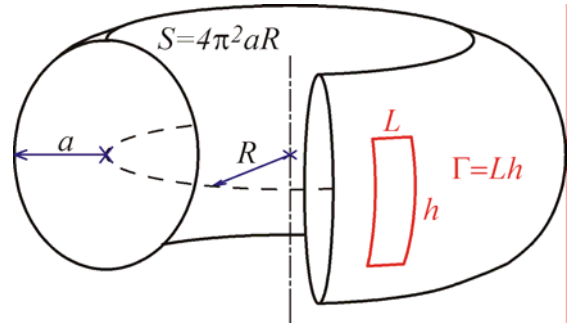
In the field-free region (inertial motion), the Hamiltonian is simply

$$H_0 = \frac{1}{2m} p_z^2 \qquad (3)$$

The velocity v_{out} with which the particle leaves the RF region follows from the energy conservation.

The transcendental equation (2) is solved numerically. This model offers the calculation of particle trajectory with any desired precision, since we need only to calculate the values of the elliptic functions and integrals, and to solve the transcendental equations (2). There is therefore no numerical integration of the equations of motion at all.

Simulation results

The numerical simulations are performed for following parameters: $N = 1.85$, $\omega = 3.7$ GHz, $h = 0.3$ m, $L = 0.3$ m and $R = 3$ m and the amplitudes of electric field $E_0 = 30$ kVm^{-1} and 200 kVm^{-1}. In Fig. 2 we show the time dependence of the electron velocities during repeated electron transitions through the RF region. Different colours correspond to the different initial electron velocities in the range from 0.2×10^8 m.s^{-1} to 1.4×10^8 m.s^{-1}. The corresponding phase velocity of the wave is $v_{ph} = 1.62 \times 10^8$ ms^{-1}.

We can see that for the amplitude $E_0 = 30$ kVm^{-1}, there is no change of the velocity for initial velocity values $v_0 < 1.2 \times 10^8$ m.s^{-1}. However, for $E_0 = 200$ kVm^{-1}, the acceleration of particles is dramatic even for $v_0 \approx 0.5 \times 10^8$ m.s^{-1}.

The typical dependence of the numerically determined diffusion coefficient $D^*(v)$ on the electric field amplitude E_0 is presented in Fig. 3. Whereas the threshold of the stochasticity of phases seems to be around 10^5 Vm^{-1}, the threshold for the acceleration of particles appears to be higher; this may be due to the fact that the diffusion coefficient is, at 10^4 Vm^{-1}, too small, and the acceleration would become apparent only after a longer time.

Fig. 2. *The velocity of particles when leaving the RF area, for various initial velocities in the range from 0.2×10^8 m.s^{-1} to 1.4×10^8 m.s^{-1} and for $E = 30$ kVm^{-1} and $E = 200$ kVm^{-1}.*

Summary

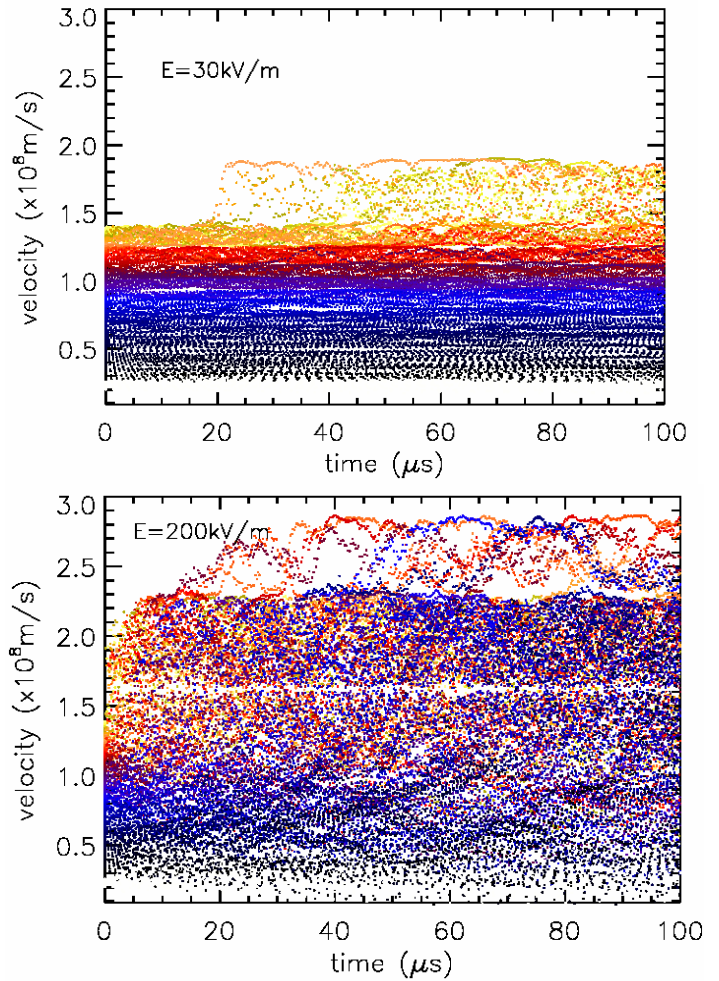Broadening of the interaction region in the velocity space, acceleration and deceleration of particles around the phase velocity of the wave and the resulting change of the distribution function in this region, are the most important results of this work.

Needless to say that the inclusion of the self-consistent fields (see e.g. [8], [9]) and collisions can significantly alter the physical picture. Moreover, the described effects are strongly connected with the sharply defined rectangular spatial envelope of the RF field. This is a good approximation close to the grill. Here, the differences from the quasilinear description will be most apparent.

The step-like spatial profile of the beam is connected with high harmonics of its Fourier representation. A rather fast absorption of higher harmonics in the k-spectrum will lead to a change of the (initially rectangular) spatial shape of the electric field envelope [4]. This will result in a reduced interaction of slower particles with the LH wave.

Fig.3. *Numerically determined diffusion coefficient as a function of velocity for different amplitudes of the electric field.*

The effects we have found have to be further discussed in a more accurate model, which includes 3D ray tracing simulation and the study of the absorption of LHW along its path deeper in the plasma column. Assuming that the change of the envelope will be not critical, and for an effective focusing of LHW cone, the mentioned effects can help to explain the k-spectrum gap problem.

References:

[1] Pavlo P and Krlín L : *Plasma Phys. Control. Fusion* 1999 **41** 541

[2] Pavlo P, Krlín L, Klíma R, Petržílka V, and Pánek R: *26th EPS Conf. Control. Fusion and Plasma Phys.* Maastricht, 1999 ECA **23J** 541

[3] Krlín L, Klíma R, Pavlo P, Petržílka V, Svoboda V, and Tataronis J A: *Plasma Phys.* 1999 62 203

[4] Pavlo P, Krlín L 2000 *Czech. J. Phys.* **50** 25

[5] Pánek R, Krlín L, Pavlo P, Klíma R, and Petržílka V: *27th EPS Conf. Control. Fusion and Plasma Phys.* Budapest 2000, Abstracts, 403

[6] Lichtenberg A.J., Lieberman M.A.: *Regular and Stochastic Motion*, Springer-Verlag 1983

[7] Sagdeev R.Z. et al.: *Nonlinear Physics*, Harwood Academic Publisher, Chur 1988

[8] Califano F, Lontano M: *Phys. Rev. Lett.* 1999 **83** 96

[9] Rantamaki KM et al: *Nuclear Fusion* 2000 **40** 1477

4   Atomic Physics and Data for Edge Plasma and Plasma Wall Interactions

Detailed knowledge of the total and differential cross-section characteristics of dissociative recombination and other molecular processes is essential for optimization of the operation of plasma power and particle exhaust in large fusion devices. When the cooling processes in the divertor lower the plasma temperature down to a level of about 1-2 eV the possibility for recombination reactions in plasma arises. The molecular processes in tokamak divertor therefore resemble those studied in low-temperature plasma and hence similar experimental methods can be applied [1].

The H_3^+ ion and its deuterated analogues play important roles in the fusion plasmas at walls (tokamak divertor [2,3]). Rate coefficients (cross sections) for recombination at higher energies are necessary for understanding and modeling of phenomena in fusion edge plasmas [4]. One such recombination mechanism including H_3^+ ion that can occur in tokamak divertor could be the reaction chain [5]

$$H_2 + H_2(v) \longrightarrow H_3^+(v') + H^- \tag{1}$$
$$e + H_3^+(v) \longrightarrow H_2 (v>=5) + H^*(n=2), \qquad (E> 1eV) \tag{2}$$
$$\longrightarrow 3H \qquad\qquad\qquad (E<1eV)$$
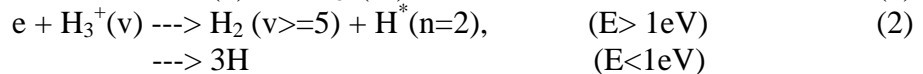
The rate coefficient of reaction (1) is not known, but at temperatures below 2eV it could be high. The recombination (2) produces vibrationally excited $H_2(v)$ required for reaction (1). Therefore at low electron temperatures (between 1 and 5 eV) reactions (1) and (2) form a closed recombination cycle. Therefore we attempted to study the reaction (2) with ion H_3^+ and with its deuterated analogues H_2D^+, HD_2^+ and D_3^+.

The critical fusion reactor design issue of tritium codeposition in tokamaks with carbon as wall material is further closely linked with the plasma chemistry involving hydrocarbons, see e.g. [6,7,8]. There is a general need for data on behavior of small hydrocarbon ions ($C_1 - C_3$ hydrocarbon ions) of energies 10-100 eV in collisions with surfaces.

References

[1] S. Takamura, N. Ohno, D. Nishijima, Y. Uesugi, *Generation and characteristics of a detached recombining plasma and its dynamic behaviour-a bridge between fusion plasmas and low-temperature ionized gases*, Plasma Sources Sci. Technol. 11 (3A) (2002) A42-A48.

[2] R.K. Janev, *Atomic physics and plasma wall interaction issues in divertor plasma modeling*, Atomic and Plasma-Mater.Interaction Data for Fusion, IAEA, vol. 9, (2001) 1-10.

[3] R.K. Janev, *Alternative mechanisms for divertor plasma recombination*, Physica Scripta T96 (2002) 94-101.

[4] R.K. Janev, Proceedings of the 1999 Conference on Dissociative recombination, *Theory, Experiment and Applications IV*, editors M. Larsson, J.B.A. Mitchell, I. F. Schneider, World Scientific, Singapore, (1999), p.40.

[5] R.K. Janev, *Atomic and molecular processes in SOL/divertor plasmas*, Contrib. Plasma Phys. 38(1998) 307-318.

[6] R.K. Janev, D. Reiter, *Collision processes of CHy and CHy+ hydrocarbons with plasma electrons and protons*, Physics of Plasmas 9 (9) (2002) 4071-4081.

[7] R.K. Janev, D. Reiter, *Unified analytic representation of hydrocarbon impurity collision cross-sections*, Journal of Nuclear Materials 313 (2003) 1202-1205.

[8] A. Kirschner, J.N. Brooks, V. Philipps, P. Wienhold, A. Pospieszczyk, R.K. Janev, U. Samm, *Modelling of the transport of methane and higher hydrocarbons in fusion devices*, Journal of Nuclear Materials 313 (2003) 444-449.

Study of recombination of H_3^+ and D_3^+ ions with electrons in He-Ar-H_2 stationary and flowing afterglow plasma

J.Glosík, R.Plašil, P.Kudrna, M.Tichý

Introduction

The three-atomic ions H_3^+, H_2D^+, HD_2^+ and D_3^+ have been the subject of a number of studies. The H_3^+ ion and its deuterated analogues play important roles in the fusion plasmas at walls (tokamak divertor [1]) and also in laboratory produced and space plasmas. Rate coefficients (cross sections) for recombination at higher energies are necessary for understanding and modeling of phenomena in fusion edge plasmas [2]. Because of their importance these ions have been extensively studied. The kinetics of formation of H_3^+, H_2D^+, HD_2^+ and D_3^+ ions, and their reactions with neutrals are well understood [3,4]. Equally important for the hydrogen and deuterium containing plasmas is to understand the processes of destruction of these ions in collisions with electrons. However, despite enormous efforts the results of studies determining the rate of recombination of H_3^+ (or D_3^+) ions with electrons gave values that varied by at least one order of magnitude; in recent studies from 1×10^{-8} to 3×10^{-7} cm^{3}s^{-1}.

To address discrepancies between different experiments and between experiments and theory we recently designed and built new afterglow experiment - Advanced Integrated Stationary Afterglow (AISA) utilizing advantages of both the stationary and the flowing afterglow techniques [5,6,7]. In addition our formerly developed and described High Pressure Flowing Afterglow (HPFA) system [8] has been applied for this purpose.

In our recent studies of recombination of H_3^+ [5,6,7,] made in frame of the EURATOM program we observed in the He-Ar-H_2 afterglow dependence of "apparent" recombination rate, α_{eff}, on number density of H_2 (which we denote by square brackets, i.e. [H_2]). We concluded that the observed recombination is likely to be three-body process proceeding via formation of long-lived neutral H_3^* which is stabilized against reverse autoionisation by a collision with neutral H_2. This stabilization process is very fast and it is saturated already at [H_2] $\sim 2 \times 10^{12}$ cm^{-3} [6]. At [H_2] $\sim 5 \times 10^{10}$cm^{-3} we obtained $\alpha_{eff} \sim 3 \times 10^{-9}$cm^{3}s^{-1}, in fact this value is given by a limitation of the present experimental arrangement. Because the binary dissociative recombination is just one reactive process that can lead to observed recombination in the afterglow, we concluded that at 260 K the rate of dissociative recombination $\alpha_{DR} < \alpha_{eff} \sim 3 \times 10^{-9}$ cm^{3}s^{-1}. We used AISA to study recombination of D_3^+ ions with electrons. On the basis of our study of H_3^+ and of previous results from literature it was reasonable to expect slower recombination of D_3^+, as compared to that of H_3^+, and also its dependence on [D_2].

Experiment and data analysis

The main part of AISA is the cylindrical stainless-steel UHV discharge chamber (40 cm long with diameter 40 cm) [5,6,7] cooled to below -40 ºC during the measurements. Purified He was used as a buffer gas (impurity level <0.1 ppm). The plasma was periodically generated by pulses of microwave power (~1kW, 0.2 ms pulses, repetition period 40-100 ms). The electron number density (n_e) was determined from Langmuir probe measurements. The cylindrical probe was 18 μm in diameter and 8mm in length; for experimental details see e.g. Ref. [6,9]. The plasma composition was monitored by a mass spectrometer [9]. The experimental precision was limited by imperfect reproducibility of the plasma parameters in each impulse, fluctuations of He temperature (230±40K), presence of traces of impurities and less precision in measuring flow at very low flow rates of deuterium. The HPFA apparatus depicts following picture (for more detailed description of the HPFA system see [8]).

Mechanism of D_3^+ ions creation in both systems is similar; only the time variable in stationary afterglow is replaced by length in flowing afterglow system. To convert virtually all ions formed in the active discharge to D_3^+ ions in the early afterglow period it is necessary to make a "suitable" mixture of He-Ar-D_2. The ion chemistry is well understood and the rate coefficients involved are well established. The pressure of He has to be over 1.5 Torr to enhance the three-body association of non-recombining atomic He^+ and D^+ ions to form He_2^+ and HeD^+. In the presence of Ar (5-20mTorr), the Ar^+ ions are formed in the sequence of reactions of Ar with helium ions and

Fig. 1. *Schematic diagram of the AISA system.*

helium atom metastables produced in the active discharge and during the very early afterglow. In the presence of trace amounts of D_2, the Ar^+ ions react in sequence of ion-molecule reactions to produce the D_3^+ ions (see discussion of formation of H_3^+ in refs. [6,7]). The set of differential equations describing these reactions was numerically solved to obtain

Fig. 2. *Schematic diagram of the HPFA system.*

the time evolution of the ionic composition for the different gas mixtures. Measured time resolved mass spectrum confirm the validity of this model for our experiment. After 5-15 ms, for nearly all of the D_2 flows employed, the chemistry forming D_3^+ is complete and the plasma can be characterised as a D_3^+/e^- plasma. For the lowest D_2 flows, complete conversion to D_3^+ ions is slower.

If losses of D_3^+ due to the recombination, diffusion and reactions are characterised by α, ν_D (see e.g. [10]) and ν_R, respectively, the balance equation can be in the first approximation written:

$$\frac{dn_e}{dt} = -\alpha[D_3^+]n_e - \nu_D n_e - \nu_R n_e = -\alpha f n_e^2 - \nu_D n_e - \nu_R n_e = -\alpha_{eff} n_e^2 - \nu_D n_e - \nu_R n_e \qquad (1)$$

102

Here we assume that in formed plasma there is fraction $f = f(t) = [D_3^+]/n_e$ of recombining D_3^+ ions and other ions are "not recombining" (predominantly Ar^+, ArD^+, He_2^+). The fraction $f(t)$ can be estimated from the ionic composition as determined by the calculations and mass spectral data. For $[D_2] > 2 \times 10^{11} cm^{-3}$ the D_3^+ ions are formed within 5 ms and $f \sim 1$ can be used to obtain α. If the plasma is governed by recombination of D_3^+ then the solution of this equation is $1/n_e = 1/n_{e0} + \alpha f t$, this formula is usually used to obtain α from the slope of the plot of $1/n_e$ versus t, under assumption $f = 1$. Introduced $\alpha_{eff} = \alpha f$ represents the rate coefficient of the processes in which loss of charged particles is proportional to the n_e^2. We will use the symbol α_{eff} to stress this fact. Because of the high precision of our data, dn_e/dt can be calculated and equation (1) can be rewritten to the form suitable for evaluation of α (using n_e' for dn_e/dt):

$$-\frac{n_e'}{n_e^2} = \alpha_{eff} + \frac{(v_D + v_R)}{n_e} \qquad (2)$$

The plot of $-n_e'/n_e^2$ versus $1/n_e$ should be linear with slope given by $v_D + v_R$). Because of the high purity of the system, the term $v_R n_e$ in equation (1) represents just a small correction. For $[D_2] < 2 \times 10^{11} cm^{-3}$ the formation of D_3^+ is slow and $f < 1$ at small t.

Results

In a mixture of He, Ar and D_2, we measured the total "de-ionisation rate", α_{eff}, in the plasma containing D_3^+ ions. The obtained α_{eff} as a function of $[D_2]$ is plotted in Figure 3. Also included are the previous results of Gougousi et al. [11] and Laube et al. [12].

Conclusion

We measured the rate coefficient of the overall recombination of D_3^+ with electrons (α_{eff}) in a decaying plasma in He-Ar-D_2 mixture. We observed that α_{eff} depends on the D_2 number density, indicating that the recombination of D_3^+ is a three-body process. Since only three-body recombination has been observed we concluded that the binary channel that corresponds to dissociative recombination is negligible in comparison with the three-body one, even at low deuterium densities. Our data place an upper limit on the binary recombination of D_3^+ with electrons of $\alpha_{DR} < 4 \times 10^{-9}$ cm^{3}s^{-1}, at temperature $\sim(230 \pm 40)$K. The obtained $\alpha_{eff} = \alpha_{eff}([D_2])$ is important for many deuterium containing plasmas, where the effective recombination rate coefficient governing the loss rate of D_3^+ ions in the interaction with electrons can reach values up to $\alpha_{eff} \sim 7 \times 10^{-8}$ cm^{3}s^{-1} due to the presence of significant concentrations of deuterium. Our data has also enabled us to estimate the contribution of "effective recombination" proceeding via formation of D_5^+ that is, however, only important at large $[D_2]$ and He densities.
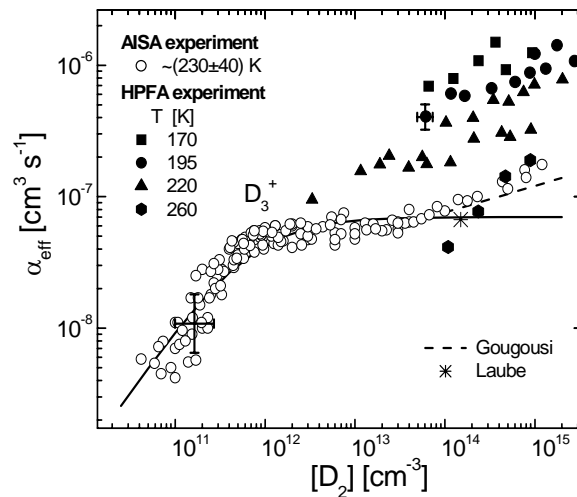
Fig. 3. α_{eff} vs deuterium number density measured on AISA (open symbols) and on HPFA (full symbols).

References

[1]   R.K. Janev, *Atomic physics and plasma wall interaction issues in divertor plasma modeling*, Atomic and Plasma-Mater.Interaction Data for Fusion, IAEA, vol. 9, (2001) 1-10.

[2]   R.K. Janev, Proceedings of the 1999 Conference on Dissociative recombination, *Theory, Experiment and Applications IV*, editors M. Larsson, J.B.A. Mitchell, I. F. Schneider, World Scientific, Singapore, (1999), p.40.

[3]   D. Smith and P. Španěl, Acc. Chem. Res., Vol. 25, No. 9 1992, 414.

[4]   V.G. Anicich, J. Phys. Chem. Ref. Data, Vol. 22, No. 6, (1993) 1469.

[5]   P. Kudrna et al., Czech. J. Phys., 50/S3 (2000) 329.

[6]   J. Glosík et al., J. Phys. B.: 34(2001)L485-L494.

[7]   J. Glosík et al., Chem. Phys. Letter, 331 (2000) 209

[8]   J. Glosík et al., Int. J. Mass Spectr. Ion Proc., 149/150, 187-197, 1995

[9]   R. Plašil et al., Int. J. Mass Spectrom., 218(2002)105-130.

[10]   E.W. McDaniel, J.B.A. Mitchell, M.E. Rudd, Atomic collisions, Heavy Particles Projectiles, A Wiley Interscience, New York, 1993.

[11]   Gougousi, R. Johnsen, M.F. Golde, Int. J. Mass Spectr. Ion Processes, 149/150,(1995) 131.

[12]   S. Laube, et al., J. Phys.: At. Mol. Opt. Phys., **31** (1998) 2111.

Energy transfer and chemical reactions in collisions of ions with surfaces and in the gaseous phase

Zdenek Herman

Lack of data on molecular collision processes in plasma edge and in plasma-wall interactions has been repeatedly stressed. There is a general need for data on behavior of small hydrocarbon ions (C_1 – C_3 hydrocarbon ions) of energies 10-100 eV in collisions with surfaces.

In close cooperation with the Institute of Ion Physics, Leopold-Franzens University Innsbruck (prof. T.D. Märk), the effect of initial internal energy on the extent of surface-induced fragmentation on a hydrocarbon-covered stainless steel surface was investigated in a tandem mass spectrometer for CH_3^+ and CH_4^+ ions prepared in different ion sources [1]. The different initial internal energy content had a considerable effect on the extent of fragmentation of the surface-excited projectile ions: ions from a Nier source with a large amount of initial internal energy (b) fragmented at much lower collision energies than internally relaxed projectile ions from a Colutron source (a). A quantitative estimation of this effect showed that the initial internal energy content of the projectile ions was entirely preserved in the projectile ion during the ion/surface collision.
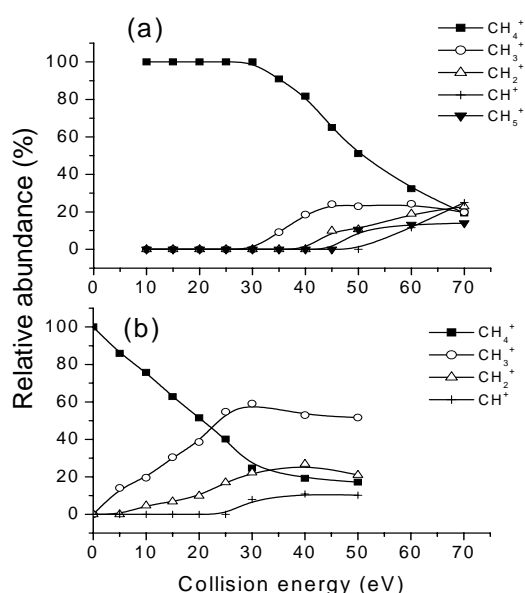
Fig. 1. *Relative abundances of various ions in dependence on the collision energy for the projectile CH_4^+*

For instance, for the projectile CH_4^+ the dissociation thresholds and characteristic crossings of relative concentrations of various ions in dependence on the collision energy (Fig. 1) were shifted by about 30-35 eV. Taking into consideration the earlier established value of collisional-to-internal energy transfer on this surface of 6%, this corresponds well to the estimated internal energy content of the unrelaxed CH_4^+ ion, formed by electron impact. The studies have been recently extended to collisions of other small hydrocarbon ions (CH_5^+, $C_2H_4^+$, C_2H_5 $C_2H_6^+$) and the effect of their internal energy on the extent of fragmentation in collisions with hydrocarbon-covered surfaces has been investigated [2].

A new beam scattering apparatus was developed in Prague to study collisions of slow ions with surfaces (Fig. 2). Projectile ions are formed by bombardment of suitable target molecules in the ion source by 120 eV electrons. The ions are extracted, accelerated to about 200-330 eV, mass analyzed by a 90^0 permanent magnet, and decelerated to a required energy in a multi-element deceleration lens. The resulting beam has an energy spread of 0.2 eV, full-width-at-half-maximum (FWHM), angular spread of 2^0, FWHM, and geometrical dimensions of 0.4x1.0 mm^2. The beam is directed towards the carbon target surface under a pre-adjusted incident angle Φ_N. Ions scattered from the surface pass through a detection slit (0.4x1 mm^2), located 25 mm away from the target, into a stopping potential energy analyzer. After energy analysis the ions are focused and accelerated to 1000 eV into a detection mass spectrometer (a magnetic sector instrument), and detected with a Galileo channel multiplier. The primary beam exit slit, the target, and the detection slit are kept at the

same potential during the experiments and this equi-potential region is carefully shielded by µ-metal sheets. The primary beam - target section could be rotated about the scattering center with respect to the detection slit to obtain angular distributions.

The carbon target surfaces in the experiments can be kept either at the ambient temperature or at an elevated temperature of about 600^0 C. For this purpose, the carbon surface could be resistively heated up to about 1000^0 C; its temperature is measured by a thermocouple and by a pyrometer. Practical absence of chemical reactions with surface hydrocarbons indicated that heating the surface to 600^0C decreased the concentration of hydrocarbons on the surface more that 100-times. This temperature was then regarded as sufficiently high to essentially remove the hydrocarbon layer that covered the HOPG surface at the room temperature.

The scattering chamber of the apparatus is pumped by a 2000 l/s diffusion pump (Convalex polyphenyl ether pump fluid), and the detector by a 65 l/s turbomolecular pump; both pumps were backed by rotary vacuum pumps.

Using this apparatus, we undertook a program of investigating collisions of small hydrocarbon ions with carbon surfaces to obtain data on ion survival in ion-surface collision, on surface-induced dissociation processes and on chemical reactions with the surface material. Also, the data should serve to elucidate energy transfer in collisions with surfaces and the extent of inelasticity of the collisions and degree of incident-to-internal energy transfer for ions of increasing complexity. In the first part of the work, we report on interactions of C_1-hydrocarbon ions with carbon surfaces at room temperature and surfaces heated to about 1000 K [2,3].
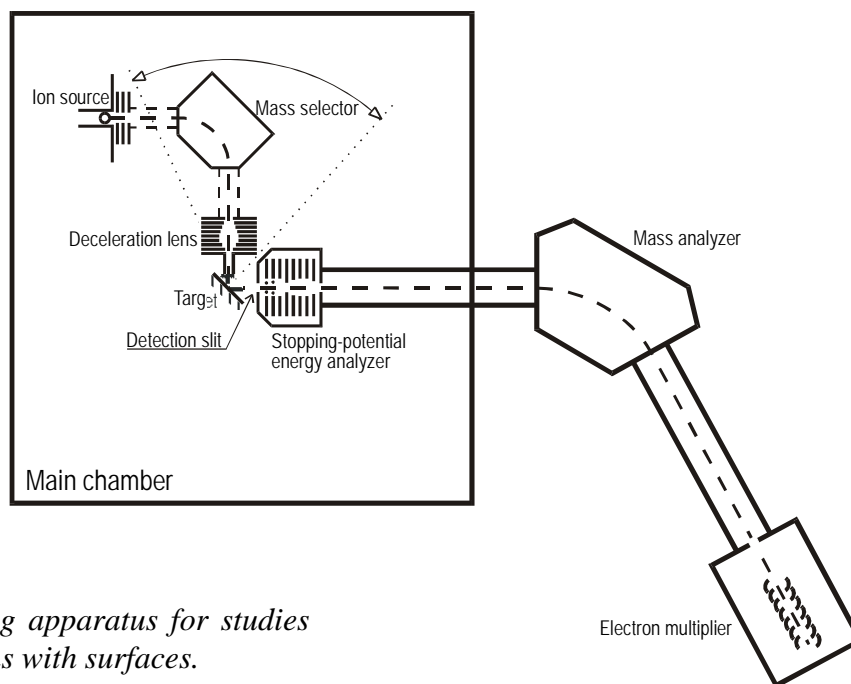
Fig. 2. *Beam scattering apparatus for studies of collisions of slow ions with surfaces.*

Interaction of small hydrocarbon ions CD_3^+, CD_4^+, CD_5^+ and their isotopic variants CH_n^+ and $^{13}CH_n^+$ (n=3,4,5) with room temperature and heated carbon (highly-oriented-pyrolytic-graphite, HOPG) surfaces was investigated over the collision energy range 16-52 eV. Mass spectra, translational energy distributions, and angular distributions of product ions were determined. Collisions with room temperature surfaces showed both surface-induced dissociation of the projectiles and chemical reactions with the surface material. All projectiles showed formation of $C_2X_3^+$ (X=H,D) in interaction of the projectiles

with terminal CH_3- groups of surface-adsorbed hydrocarbons, small amount of C_3 product ions, and collisions of CD_4^+ led, in addition, to CD_4H^+ by H-atom transfer from surface hydrocarbons. The surface collisions were inelastic with 41-55% of incident energy in product ion translation (incident angle 60^0 with respect to the surface normal). Heating of the surface to 600^0 C practically removed the surface hydrocarbon layer. Interactions of the projectiles with the heated surface showed then only dissociation of the projectile ions (no chemical reactions) in inelastic collisions with about 75 % of the incident energy in product ion translation. The ion survival probability was estimated to about 12 % for the closed-shell ion CD_5^+ and about 30-60-times smaller (0.2-0.4 %) for CD_3^+ and $CD_4^{+\cdot}$

The experiments have been recently extended to collisions of $C_2H_n^+$ ions ($C_2H_2^+$, $C_2H_3^+$, $C_2H_4^+$, $C_2H_5^+$) with heated and room-temperature carbon surfaces. Data on dissociation of these projectile ions in surface collisions have been obtained in dependence on the collision energy (5-50 eV). The ion survival probability is similar as stated above, i.e. considerably higher for closed-shell projectile ions. The main chemical reaction of the projectile ions with the hydrocarbons on the surface leads to the formation of $C_3H_3^+$ product. The experiments have been carried out again in close collaboration with the Institute of Ion Physics of the Leopold-Franzens University in Innsbruck.

References
[1] A. Quayyum, T. Tepnual, C. Mair, S. Mat-Leubner, P. Scheier, Z. Herman, T.D. Märk, Chem. Phys. Letters (in print)
[2] A. Quayyum, Z. Herman, T. Tepnual, C. Mair, S. Mat-Leubner, P. Scheier, T.D. Märk, J. Phys. Chem (submitted).
[3] J. Žabka, Z. Dolejšek, J. Roithová, V. Grill, T.D. Märk, Z. Herman, Int. J. Mass. Spectrom. 213 (2002) 145-156.
[4] J. Roithová, J. Žabka, Z. Dolejšek, Z. Herman, J. Phys. Chem. B, 106 (2002) 8293-8301.

5 Collaboration with JET

Association IPP.CR contributes to the JET work programme since 2001. Recently, several experts were seconded to JET to participate on the programme of task forces E and H during the year 2002 – beginning of 2003 (i.e. campaigns C5-C9).

Task force E (Exhaust)

In frame of TF E, two topics were evaluated. First, the probe measurements were covered by participation of M.Hron and I.Ďuran on campaigns C6, C8-C9 and C9 respectively. Second, the modelling activities were a topic for a stay of R.Pánek on JET during the C8.

Probes are used for edge plasma parameters measurements on JET – first, fixed Langmuir probes are mounted on the target, limiter, and RF antenna, next, two reciprocating probe systems with exchangeable probe heads are on the top of the machine.

During the campaign C9 I.Ďuran joined the ion temperature measurement using a bi-directional retarding field analyser (RFA) that was placed on one of the two reciprocating probe systems (in Octant 1). In frame of this work the edge profiles of ion temperature and Mach numbers were measured in JET reversed field configuration. Significant difference of the ion temperature measured on the upstream and downstream side was found. Relation of this asymmetry to plasma flows was investigated. This activity was performed in collaboration with the Swiss and UKAEA Associations.

Further, M.Hron participated on the edge plasma parameters measurements using Langmuir probes: first, radial profiles of the edge plasma were measured using the turbulent transport probe (TTP) on the other reciprocating probe system (Octant 5). A coupling between turbulent transport and parallel flows in the plasma boundary has been investigated. The work was done in collaboration namely with the CIEMAT, IST, and UKAEA Associations. Together with the TTP experiments, training for the KY3 reciprocating probe systems manipulation has been performed. Further, a brief analysis of divertor probe response to type I ELMs was done. Latest, a general programme for the target probe data analysis was prepared. This programme processes the KY4D probe data between individual shots, calculates the spatial-temporal evolution of the ion flux on the target, the field line angle at individual probes, the projected area of the probes, the maximum and total ion fluxes on the individual parts of the divertor etc., and regularly stores these results in the public PPF database. Preparation of this analyses was done in collaboration with the Association FZJ.

Concerning the modelling activities, R.Pánek, joined in 2003 the modelling group within TF E. In frame of this topic, the Scrape-Off-Layer of the JET tokamak is simulated using EDGE2D code. Main aims of the work are to perform a benchmark of the EDGE2D and SOLPS codes and to try to simulate ELMs in Helium discharges.

Task force H (Heating)

Within TF H the Association IPP.CR participated in preparation of a parasitic experiment concerning fast particle production in front of LH grills and ensuing hot spots. The experiment was proposed by our association and CEA Cadarache and, independently, by the Finnish association. Unfortunately, the water leak in JET, disallowed the realization of the experiment. Therefore, the existing JET shots that exhibit the hot spots were analysed in detail during the stays of V.Petržílka (C5, C7-C9) and F.Žáček (C5, C8, C9). Analysis of the hot spots and of the magnetic field connections show that fast particles that are generated in a thin layer in front of the LH grill mouth can travel several times around the torus and that they are likely to cause the observed hot spots.

Retarding field analyser measurements in the JET plasma boundary

I.Ďuran

In collaboration with:

R.A.Pitts, J.Horáček, Association Euratom/Confédération Suisse, Switzerland,
S.K.Erents, G.F.Matthews, Euratom/UKAEA Fusion Association, U.K.

Introduction

Ion temperatures, T_i, and velocity distributions, f(v), in the plasma edge of fusion devices are notoriously difficult to measure and thus rarely available but yet are important plasma boundary quantities. Though requiring the insertion of a material probe into the scrape-off layer (SOL), the Retarding Field Analyser (RFA) is one experimental approach that can access the plasma ion or electron velocity distribution directly. By designing a 'bi-directional' probe, i.e. one which can intercept particles on both sides of a plane oriented perpendicular to the total field line direction at a particular location in the SOL, the device may also be used to simultaneously characterise any net flow that may be present there. In fact, according to recent theoretical work [1], it turns out that the presence of an external flow should have a strong influence on the parallel ion velocity distributions (and hence on the derived ion temperatures) at the upstream and downstream locations of any surfaces inserted into the flowing plasma. The first experimental evidence for this effect was obtained in recent measurements with an RFA in the JET plasma boundary [2].

RFA principle and the JET RFA

Figure 1 (upper panel) illustrates the well known [3, 4] basic principle of RFA operation. Charged particles are transmitted through a small aperture (width ~ λ_D, the Debye Length) and are analysed by retardation in the electric field established through bias potentials applied to a number of grids. Since the electron velocity distribution (and hence the electron temperature, T_e) can to some extent be measured by the simple single Langmuir probe, the primary focus of RFA application is often the ion velocity distribution. An appropriate electrode bias configuration for ion analysis is included in Fig. 1 (upper panel), illustrating how the slit plate is normally negatively biased to repel all but the

Fig. 1. *Illustrating the RFA principle and bias potential arrangement for ion analysis (upper panel) and showing the engineering and assembly of the JET RFA probe head (lower panel).*

highest energy electrons. A positive voltage sweep, V_1, is applied to Grid 1 and a constant negative bias on Grid 2 at a value lower than that applied to the slit eliminates any remaining electrons. The collector at zero volts suppresses any ion induced secondary electrons. In tokamaks, the current-voltage characteristic thus obtained is often experimentally found to be closely consistent with that which would arise if the parallel ion velocity distribution were a Maxwellian shifted in velocity space by an amount equal to that gained by acceleration in the
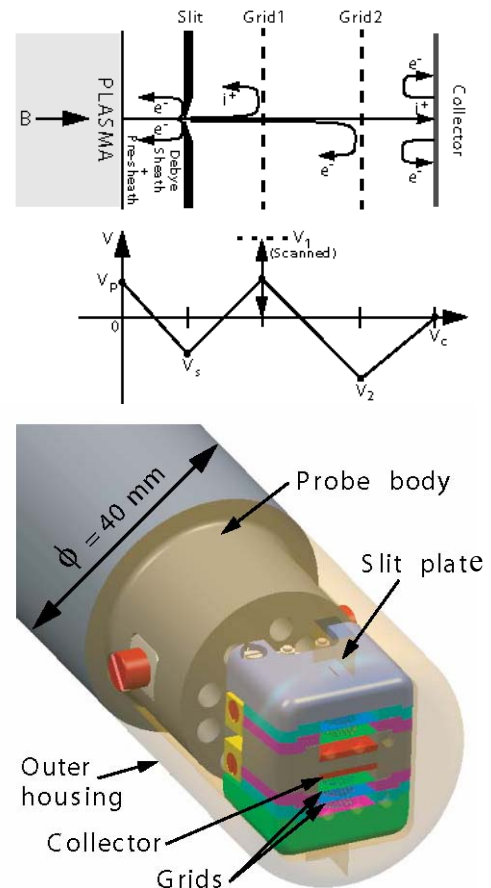
sheath and pre-sheath electric fields [3, 4]. In this case, for values of V_1 exceeding the voltage required to back-off this energy shift, the I-V characteristic can be written in the form: $I_c = I_i \exp(-Z_i V_1/T_i)$ where $I_i = A Z_i T_i e^2/m_i$, Z_i is the ion charge and T_i (in eV) is the ion temperature of the distribution.

A new RFA has recently been designed and successfully operated at JET using the fast reciprocating drive systems to insert the probe head several times into the edge plasma, whilst simultaneously employing a second probe to measure radial profiles of particle flux and T_e for comparison with data from the RFA. The new probe head is illustrated in the form of a false colour solid model illustration in Figure 1 (lower panel). An extensive report on the technical design, construction and performance has recently been completed [5].

Results

An example of the kind of data produced by the diagnostic is given in Fig. 2, from the ohmic phase of a low density, single null lower diverted equilibrium with I_p = 2.0 MA and B_T = 2.4 T, both in the forward, or clockwise direction. The probe is inserted at a point on the upper, low-field-side of the poloidal cross-section and is designed such that the aperture slits (40 µm wide, 3.0 mm long) are aligned closely perpendicular to the total magnetic field direction at this point. For forward I_p, B_T, the slit facing the ion drift direction (the ion, or i-side) intersects field lines spiralling upwards from the outer divertor whilst the electron, or e-side, slit faces the inner divertor. Figure 2 demonstrates that under certain conditions the RFA ion characteristics are clearly consistent with a shifted Maxwellian velocity distribution, though the magnitude of the shift in this case is not that of the true sheath potential fall since bias potentials and currents are measured with respect to the torus potential and not the local slit floating potential, V_f. The shift, V_{shift}, can be appropriately corrected by floating the RFA slits and directly measuring V_f, but at the price of losing the simultaneous measurement of j_{sat}, the ion saturation current density to the plates (by applying a large negative bias, typically -150 V).

It is already clear in Fig. 2 that the i-side/e-side j_{sat} ratio considerably exceeds unity and thus that the RFA is immersed in a flowing SOL plasma. Such strong flow is regularly observed on JET for forward B_T [6] and is usually estimated by
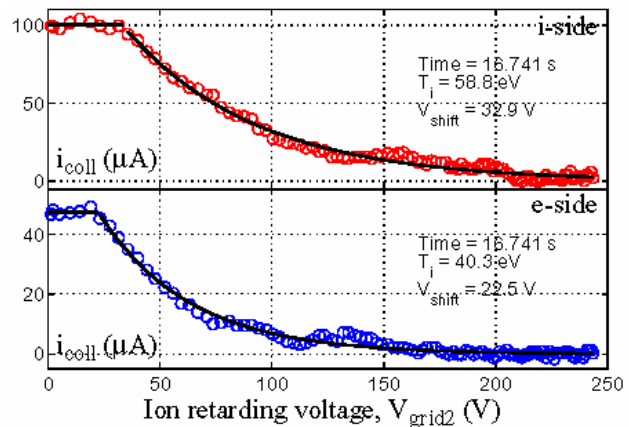

Fig. 2. *Example of RFA IV characteristics and their fits in a single time. Red – RFA ion side, blue – RFA electron side.*
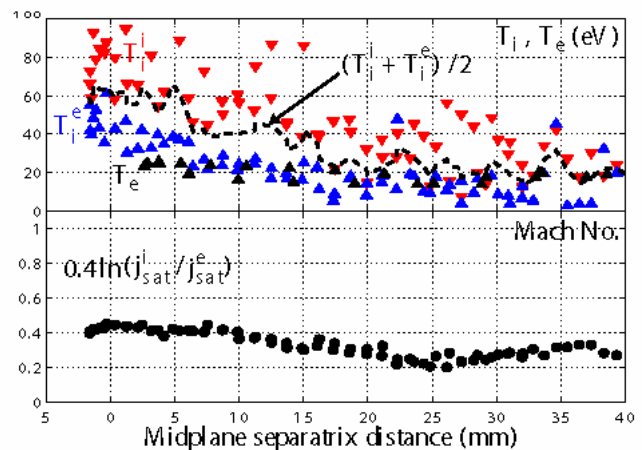

Fig. 3. *Upper panel: radial profiles of T_i^i, T_i^e measured by RFA, and T_e measured by the second reciprocating Langmuir probe. Lower panel: radial profile of Mach number.*

employing fit to the fluid model of Hutchinson [1,7]: $M = 0.4\ln(j_{sat}^{u}/j_{sat}^{d})$ where M is the flow Mach No. (normalised to the isothermal sound speed, $c_s=(e(T_e+Z_iT_i)/m_i)^{1/2}$ (T_i, T_e in eV) and the superscripts u, d denote "upstream" and "downstream" with respect to the flow. The latter is defined as positive if it is directed towards the probe so that the i-side in Fig. 2 is the upstream side and the flow is directed along the total field from outer to inner divertor targets. The example RFA characteristics already show that in addition to the j_{sat} asymmetry, ratio $T_i^{i}/T_i^{e}>1$, where the superscripts i, e, now denote i-side and e-side.

Radial profiles of M, T_i^{i}, T_i^{e} mapped to the mid-plane are plotted in Fig. 3, along with data (black triangles) from a second reciprocating probe head which was inserted at approximately the same time in the discharge at the same poloidal location (but at a different toroidal position) and from which a scanned Langmuir probe provides data for j_{sat}, T_e and V_f on the upstream side only. Although the RFA data are rather scattered, Fig. 3 illustrates that, $T_i^{i} > T_i^{e}$, $(T_i^{i} + T_i^{e})/2 > T_e$ and M > 0 throughout most of the profile (the smoothed, mean ion/electron-side T_i is plotted as the dashed line in Fig. 3 (upper panel)). Error bars have been omitted for clarity, but are generally of order 5% when RFA collector currents are high, becoming more significant at lower currents (and hence further out in the SOL). Concerning the general observation that $T_i > T_e$, this is qualitatively expected in the low density SOL in which these measurements have been obtained. The SOL collisionality parameter, $\nu^*_{SOL} = L_c/\lambda_{ii} \approx 10^{-16} n_eL_c/T_i^2 \sim 1$ (L_c is the probe to target connection length of $\sim$ 40 m) on a flux surface at the point of closest approach to the separatrix in Fig. 3 and so the temperature equilibration time is very much longer than the effective SOL energy confinement time.

Regarding the strong i-side, e-side T_i asymmetry, the data would appear to be the first qualitative experimental demonstration of the recent theoretical assertion [1] that such an effect should be observed by an RFA immersed in a strong plasma flow. This is due to the perturbing effect of the probe itself which depletes ions preferentially on the downstream side, generating strong electric fields and modifying the ion velocity distribution. According to this theory, the real T_i in the plasma cannot be measured by a single-sided RFA in a flowing plasma, but is given rather accurately by the mean value of i side to e-side values provided the drift is not too strong.

References
[1] F. Valsaque, G. Manfredi, J. P. Gunn and E. Gauthier, Phys. Plasmas **9** (2002) 1806.
[2] R.A. Pitts et al, Retarding field analyser measurements in the JET plasma boundary, proceedings of the 30th EPS conference on Plasma Physics and Controlled Fusion, St Petersburg, July 2003.
[3] G. F. Matthews, J. Phys. D: Appl. Phys. **17** (1984) 2243.
[4] R. A. Pitts, Phys. Fluids **B3**, (1991) 2873.
[5] R. A. Pitts et al., submitted to Rev. Sci. Instrum. (June 2003).
[6] S. K. Erents et al., Plasma Phys. Control. Fusion **42** (2000) 905.
[7] K-S. Chung and I. H. Hutchinson, Phys. Rev. A **38** (1988) 4721.

Reciprocating probe system KY3
M.Hron

In collaboration with:
C.Hidalgo, M.A.Pedrosa, Association Euratom / CIEMAT, Spain,
C.Silva, B.Gonçalves, Association Euratom / IST, Portugal,
K.Erents, G.Matthews, M.Stamp, Association Euratom / UKAEA, U.K.
G.Granucci, Association Euratom / ENEA sulla Fusione, Italy

The reciprocating systems on JET are placed in Octants 1 and 5 on the top of the torus. The retarding field analyser RFA and the turbulent transport probe TTP were installed on the reciprocating manipulators during recent campaignes. In frame of his secondement on the JET, M.Hron was trained for manipulation of the reciprocating probe systems. Concerning the physics progamme the TTP is of our interest here first.

Turbulent Transport Probe (TTP)

The TTP, is a probe head that is used on one of the reciprocating probe systems on the JET device. The TTP has nine Langmuir probe tips and its design was optimised in order to measure simultaneously the electrostatic turbulent transport and the parallel Mach number. Therefore, the construction of the probe head allows measurements from two separated radial positions, i.e. radial profile. Three of the tips on one side of the probe, marked 7-9, and one tip, numbered 10, on the other side allow to measure the upstream and downstream quantities (namely the ion saturation current) and denote the parallel Mach number. Further, a suitable connection of the five tips that are radially deeper, on the top of the probe, i.e. number 2-6, allows to measure the ExB induced particle flux and the electron temperature. The particle flux is calculated from the floating potential (U_{fl}) and ion saturation current (I_{sat}) signals, the electron temperature is fitted to an exponential function, that denotes the T_e using one additional measured point, the signal from a tip biased on U=20 V.

Fig. 1. *The probe head of the TTP and numbering of the tips.*

Coupling between turbulent transport and parallel flows in the plasma boundary

The measured radial profiles of the poloidal velocity of fluctuations and parallel flows have been investigated. Our main contribution in the data processing was the correlation analysis and calculation of the probability distribution function (PDF) of parallel flows and transport. The width of autocorrelation functions at their half maximum is in a range of 10-30 μs inside the separatrix (depending on the orientation of the probe versus the magnetic field) while in the SOL is in the range of 50-200 μs and shows much higher scatter. The observed PDFs of transport are clearly non-gaussian while PDFs of parallel flows are rather gaussian.

Further, it was shown in these studies that the radial velocity of fluctuations is in the order of 20 m/s for transport events associated with small deviations from the most probable gradient while it increases up to 500 m/s for local gradients which are large compared to the most probable.

References

[1] C Hidalgo, B Gonçalves, M A Pedrosa, J Castellano, K Erents, A L Fraguas, M Hron, J A Jiménez, G F Matthews, B van Milligen, C Silva: *Empirical similarity in the probability density function of turbulent transport in the edge plasma region in fusion plasmas*, Plasma Phys. Contr. Fusion, 44, 2002, 1557-1564

[2] C. Hidalgo, B. Gonçalves, C. Silva, M. A. Pedrosa, K. Erents, M. Hron, and G. F. Matthews: Experimental Investigation of Dynamical Coupling between Turbulent Transport and Parallel Flows in the JET Plasma-Boundary Region, Phys. Rev. Lett. 91, 065001 (2003)

[3] G. Granucci, A. Ekedahl, J. Mailloux, K. Erents, M. Hron, E. Joffrin, P.J. Lomas, M. Mantsinen, J.-M. Noterdaeme, V. Pericoli-Ridolfini, V. Petrzilka, K. Rantamäki, R. Sartori, C. Silva, A.A. Tuccillo, D. McDonald and JET EFDA contributors: Recent Results of LHCD Coupling Experiments with Near Gas Injection in JET, 30th EPS conference on Plasma Physics and Controlled Fusion, St Petersburg, July 2003,l. 27A

[4] C. Hidalgo, B. Gonçalves, C. Silva, M.A. Pedrosa, K. Erents, M. Hron, G. F. Matthews, R. Pitts: Experimental investigation of dynamical coupling between turbulent transport and parallel flows in the JET plasma boundary region, 30th EPS conference on Plasma Physics and Controlled Fusion, St Petersburg, July 2003,l. 27A

Production of Energetic Particles in Front of the JET LH Grill and Resulting Hot Spots with Potentially High Thermal Loads
V.Petržílka

In collaboration with:
M.Goniche, Association Euratom/CEA, France,
K.Rantamäki, Association Euratom/VTT, Finland

Our association IPP.CR participated in JET parasitic experiments, suggested together by our association (V. Petrzilka) and CEA Cadarache (M. Goniche), and independently by the Finnish association (K. Rantamaki), concerning fast particle production in front of LH grills and ensuing hot spots [1-3].

Hot spots probably caused by the energetic particles generated just in front of the LH grill mouth were observed in C7 in two shots (57091 and 93). Analysis of the observed hot spots and of the magnetic field connections shows that the fast particles produced in a thin layer in front of the grill mouth can travel several times around the torus, and that for observing the hot spots by the CCD camera used for the JET shot videos, we do not need very low q_{95} values from about 3.1 to about 3.5. In frame of our preparations for measurements in C8 and C9 campaigns, hot spots and corresponding magnetic field connections in shots 55761, 3 and 4 were also analysed, please cf. Fig.1 and 2 for the shot 55764. The analysis shows that it is possible to use values q_{95} near to 4.6 for observing the hot spots in the view field of the CCD camera. In other words, magnetic fields 3.4 T and plasma currents near to 2.5 MA can be used, as in Optimized Shear (OS) scenarios.

The observed angular velocity of the hot spot trains agrees well with q variations at the q ramp down. The length of the rotating hot spot trains agrees with mapping of the LH grill poloidal height to the toroidal length of the hot spot trains on the inner apron. The hot spots in the recent shots 57091 and 93 are not bright, the hot spots have diffuse character. They can be seen only by certain video players.

Fig. 1. *Irma screen of the CCD camera view for the JET shot 55764.*

Fig. 2. *Irma brightness in the yellow circle z_1 located in the path of the hot spots train in Fig. 1. JET time=Irma time+39.5 s*

The Infra Red Movie Analyser, IRMA software was also used to analyse the CCD videos of the pulses 58666 to 58668 that showed hot spots on the divertor apron in C8. Unfortunately, the software has not been calibrated at JET to measure the temperature. Consequently, only the brightness can be obtained. Two or three measuring points have been

used on the inner divertor apron and one on the wall for the background brightness. Figures 3 and 4 show the measuring point z3 and the result of the Irma analysis for the JET pulse 58668. The analysis shows clear increases in the brightness of the measuring points in the second phase of the shots. Shots 58666 to 58668 show clearly three peaks in the brightness on the inner apron. The peaks are around t=50 s (starting at about t=49.5 s) from about t=51.1 to 51.9 s and about t=52.3 to 52.5 when the LH power ends. There is a clear correlation with the termination of the brightness of the hot spots and the end of LH power. In these shots, three q_{95} windows with spots are seen. In each of the three shots, these windows are roughly at the same values. The first window is $q_{95} = 5.1$ to 4.5, the second one at $q_{95}= 4.1$ to 3.8 and the last one around $q_{95}=3.8$ just before the end of LH power. The other sets also show clear peaks at the times of the spots seen in the CCD camera. They show spots also around $q_{95}= 3.4$ and $q_{95}= 3.13$.
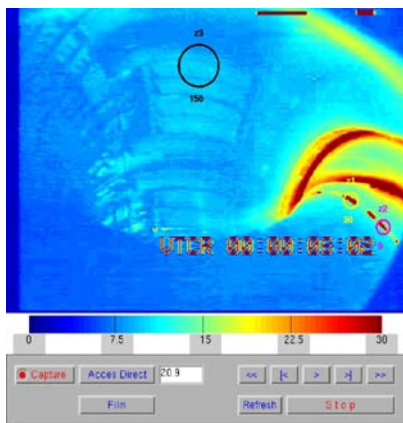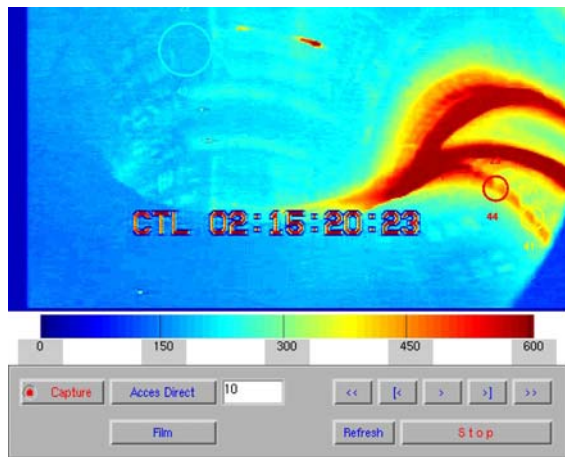

Fig. 3. *Irma screen of the CCD camera view for the JET shot 58668.*

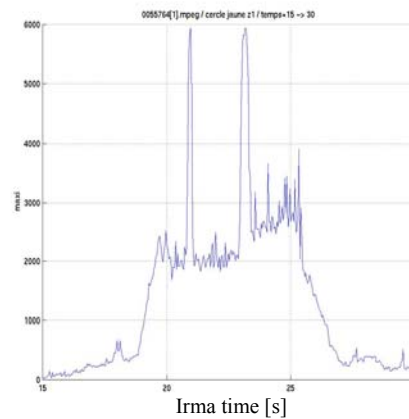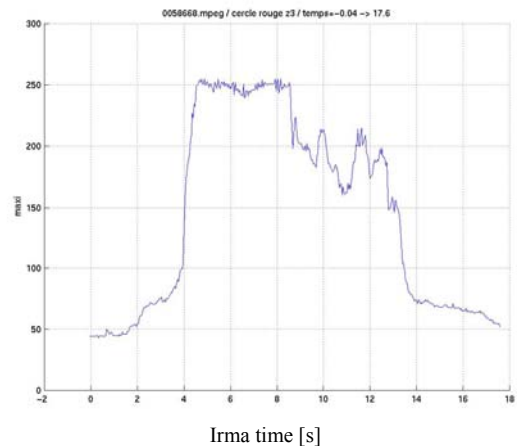**Fig. 4.** *Irma brightness in the red circle z3 located in the path of the hot spots train in Fig. 3.*
JET time=Irma time+39.5 s

The analysis of the observed hot spots and of the magnetic field connections demonstrates that the fast particles produced in a thin layer in front of the grill mouth can travel several times around the torus, similarly as in Tore Supra. According to the analysis versus various parameters, Fig. 5, the main effect is due to the plasma − wall distance, i.e. the distance between the last closed flux surface and the poloidal limiter. The brightness of the spots clearly decreases with increasing distance.
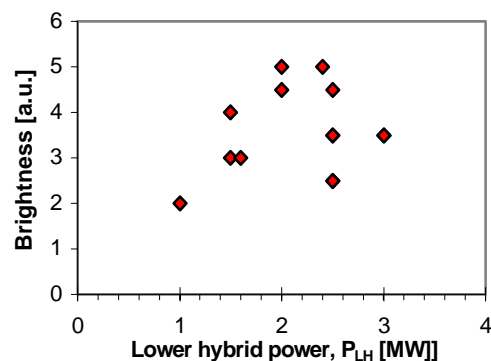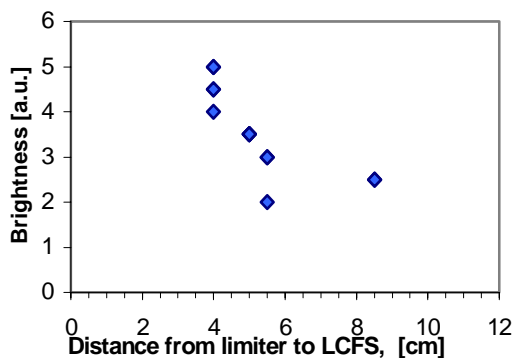
Fig. 5. *Brightness of the hot spots obtained on the CCD camera versus the distance from the limiter to the last closed flux surface (LCFS) and the LH power. The points may represent more than one shot.*

A lower density in front of the grill is not likely to be the reason, since the coupling is very good in most cases due to the gas puffing. Since the coupling well above the cut-off density is a very weak function of the density, this should be investigated in more detail in further work. The preliminary study did not show a clear dependency on the reflection coefficient. However, the propagation of the particle beam further away from the grill could be affected by non-linear effects due to the lower density there. Moreover, the interaction point is changed and further out on the apron the beam hits less recycling surfaces and the brightness is lower for the same heat flux.

References

[1] K.M. Rantamäki, V. Petržílka, A. Ekedahl, K. Erents, V. Fuchs, M. Goniche, G. Granucci, S.J. Karttunen, J. Mailloux, M.-L. Mayoral, F. Žáček and contributors to the EFDA – JET work programme, EPS03 St. Petersburg.

[2] Ekedahl, G. Granucci, J. Mailloux, V. Petrzilka, K. Rantamäki, Y. Baranov, K. Erents, M. Goniche, E. Joffrin, P.J. Lomas, M. Mantsinen, D. McDonald, J.-M. Noterdaeme, V. Pericoli, R. Sartori, C. Silva, M. Stamp, A.A. Tuccillo, F. Zacek and EFDA-JET Contributors, *invited paper*, 15th RF Topical Conference, Moran, USA, May 2003.

[3] G. Granucci, A. Ekedahl, J. Mailloux, K. Erents, M. Hron, E. Joffrin, P.J. Lomas, M. Mantsinen, J.-M. Noterdaeme, V. Pericoli-Ridolfini, V. Petrzilka, K. Rantamäki, R. Sartori, C. Silva, A.A. Tuccillo, D. McDonald and JET EFDA contributors, EPS03 St. Petersburg.

III TECHNOLOGY

1 Technology tasks

The most of the technology tasks within Association EURATOM/IPP.CR deal with study of tritium breeding and properties of various diagnostic and structural elements of future thermonuclear reactor, before and under neutron irradiation. For this purpose two irradiation sites are utilized: light water experimental fission reactor LVR-15 (operated by NRI plc), and the isochronous cyclotron U-120M with the maximum proton energy of 37 MeV (operated by NPI ASCR). Both devices are located in Řež about 20 km from Prague and they are integrated within the Association EURATOM/IPP.CR.

The structure of the technology research of the Association EURATOM/IPP.CR is following:

Contracts under Article 5.1a:
- **Tritium Breeding and Materials**
  - ❖ **Breeding Blanket** (1 task, 1 deliverable)
  - ❖ **Materials Development** (4 tasks, 8 deliverables)
  - ❖ **Materials Development – IFMIF** (3 tasks, 6 deliverables)
- **Physics Integration**
  - ❖ **TPDC Diagnostics – Ceramics** (1 task, 1 deliverable)
- **Vessel/In Vessel**
  - ❖ **Blanket** (1 tasks, 1 deliverable)

Contracts under Article 5.1b:
- **Vessel/In Vessel**
  - ❖ **Blanket** (2 tasks, 2 deliverables)

In August 2002, the NRI and NPI sites in Řež were severely struck by floods that occurred over the territory of the Czech Republic. The technical basement of the cyclotron U-120M has been flooded and all the power supplies for the magnetic and RF systems were destroyed. The operation of the LVR-15 reactor was also substantially hampered by this natural disaster. The recovery lasted approximately till the mid of 2003 and as a result, progress in many technology tasks was slowed down significantly.

1. Tritium Breeding and Materials: Breeding Blanket

Task TW2-TTBC-004a - Helium Cooled Lithium Lead: Processes and Components
(coordinated by NRI Řež; staff: M.Zmítko, P.Hájek, K.Šplíchal, P.Vachtfeidl, V.Richter)

Deliverable 4: Pb-17Li Auxiliary and purification systems. - delivered

> 4a: Design of the Auxiliary PbLi loop
>
> 4b: Design of the Purification system of PbLi (e.g. from Bi) and evaluation of impact on Po production

Achievements:
- Design study of the Pb-Li auxiliary loop including system characteristics, design description, main components characteristics, disposition, operational and design parameters and regimes, instrumentation and control, manufacturing and assembly requirements, testing and maintenance requirements was completed [1].
- Literature review on possible Pb-Li purification techniques, behaviour of bismuth, polonium and mercury including assessment of possible ways of polonium production in Pb-17Li ancillary system was done [2]. Experiments were performed in order to find the best method of removal of corrosion products as bismuth, and other heavy metals, from the eutectic mixture Pb-17Li. Three types of purification devices were tested: i) mechanical filter, ii) cold traps, and iii) magnetic traps. It can be concluded from the experimental observations that *the diffusion type cold trap with a solid phase* shows the best Pb-17Li purification performance for corrosion products and impurities as bismuth and polonium. The cold traps use the fact that many compounds including bismuth has lower solubility in Pb-Li at lower temperature. It is also shown that further investigation of thallium and mercury behaviour in the Pb-17Li eutectic mixture regarding blanket operation conditions is needed.

2. Tritium Breeding and Materials: Materials Development

Task TW2-TTMS-003a - RAFM Steels: Compatibility with Hydrogen and Liquids
(coordinated by NRI Řež; staff: M.Zmítko, K.Šplíchal, V.Masařík, V.Švarc, P.Chvátal)

Deliverable 7: Water corrosion effect inside Eurofer tube under PWR conditions. - delivered

Achievements:
- The test in water loop facility RVS-3 was realized under specified PWR-like thermal-hydraulic (320°C) and water chemistry conditions (maintaining and monitoring of water chemistry parameters: boron, lithium, dissolved hydrogen, oxygen, pH value). Six Eurofer 97 tube specimens were exposed for total of 2000 hours.
- Non-destructive examination of the Eurofer specimens was performed by weighing after 545, 1100 and 2000 hours of exposure to determine the weight losses.
- Destructive examination of the Eurofer specimens surface layers by SEM and EDX was performed. Formation of a protective film was detected. No evidence of pitting or traces of other local attack was found [3].

Deliverable 12: Water corrosion test under PWR conditions on Eurofer tube/tube and tube/plate weldments. - delivered

Achievements:
- The test in water loop facility RVS-3 was realized under specified PWR-like thermal-hydraulic (320°C) and water chemistry conditions (maintaining and monitoring of water chemistry parameters: boron, lithium, dissolved hydrogen, oxygen, pH value).

Four Eurofer 97 ½ CT (Compact Tension) specimens with wedge made from base metal and four made from weld metal were exposed for total of 2,000 hours.

- Destructive examination of the CT specimens was performed. No stress corrosion cracking at the load of the stress intensity factor in the range of 22-34 Mpa.m$^{1/2}$ was identified. No defects such as cracks, pores or cavities have been found neither in the base metal nor in the weld metal or heat affected zone [4].

Deliverable 15: Testing of Eurofer tube under flowing PbLi. - delivered

Achievements:
- The EUROFER 97 tube specimens were exposed in flowing (10 mm/s) Pb-Li at 500°C for total of 2500 hours.
- Non-destructive examination of the specimens after exposure in Pb-Li (weighing to determine metal loss) was done.
- Destructive examinations of the specimens after exposure in Pb-Li by means of light microscopy, SEM, EDX line-scan, and point analysis were employed to study surface morphology, chemical composition and concentration profiles near the steel surface [5].
- Pb-Li interaction with tube specimens resulted in their dissolution that is demonstrated by surface morphology and weight changes. Corrosion attack becomes apparent after a certain incubation period. No considerable decrease of Cr and Fe (elements highly soluble in Pb-Li) was observed under the experimental conditions.

Task TW2-TTMS-001b - RAFM Steels: Irradiation Performance
(coordinated by NRI Řež; staff: P.Novosad, K.Šplíchal, W.Soukupová)
Deliverable 3: Static and dynamic toughness testing at the transition temperature. Neutron irradiation of plates and weldments after up to 2.5 dpa at 200-250°C and post irradiation examination. – in progress
Achievements:
- Chouca–EFDA irradiation rig was constructed and tested. EUROFER base metal plate was delivered from FZ Karlsruhe. Two separate EUROFER plates were welded in CEA Saclay. Small Charpy K.L.S.T specimens (3 x 4 x 27 mm^3) for fracture toughness tests were manufactured, notch prepared, and fatigue pre-crack cycled.
- The irradiation experiment started in September 2003. Irradiation parameters: temperature 235°C, fast (>1 MeV) neutron flux 4.4×10^{13} cm^{-2} s^{-1}, He atmosphere.
- Total irradiation time from beginning of experiment till the end of 2003 is 1560 hours, that is approximately 0.35 dpa and neutron fluence (>1 MeV) 2.4×10^{20} cm^{-2}.

Task TW2-TTMS-003b - RAFM Steels: Compatibility with Hydrogen and Liquids
(coordinated by NRI Řež; staff: M.Zmítko, K.Šplíchal, V.Masařík, P.Hájek, J.Berka, J.Zmítková)

Deliverable 1: Crack growth kinetic and fracture toughness on EUROFER 97 in presence of hydrogen (up to 10 wppm) at RT, 250° C - in progress
Achievements:
- Experimental program covers the hydrogen charging method evaluation and hydrogen induced embrittlement testing. Fracture toughness measurement should be performed by 3-point bend method (ASTM E 399) with K.L.S.T specimens. Crack growth rate should be determined by Slow Strain Rate Test (SSRT) method with tensile specimens.
- Both gaseous hydrogen charging and cathodic hydrogen charging methods have been evaluated. Hydrogen content of charged specimens ranged from 0.8 to 1.7 wppm and it

was lower than required content of 10 wppm. The cathodic hydrogen charging is therefore used at present time.

- The experimental evaluation of cathodic hydrogen charging parameters was continued. Obtained results lead to conclusion that the same charging parameters did not lead to the same level of hydrogen content. The optimal hydrogen charging parameters are verified to achieve controlled hydrogen contents of test specimens which were charged under the same charging parameters.
- SSRT experiments were started with tensile specimens which were cathodically charged on lower hydrogen contents.

Deliverable 4: In-pile PbLi corrosion testing of TBM´s weldments (stiffeners and bottom plate relevant), up to 2 dpa. - in progress
Achievements:
- Pb-Li in-pile rig for irradiation in LVR-15 test reactor was designed with temperature range of 500-550°C in hot part of the rig and 300-350°C in the cold part, and the natural circulation of Pb-Li with flow rate of 0.3 kg/sec.
- The mock-up test in the LVR-15 was done and evaluated. Unfortunately the specified parameters (temperatures) were not achieved – rig was overheated, in the range of specimens up to 800°C was achieved at reactor power 3 MW, Pb-Li natural circulation was observed.
- The thermal performance of the rig at the mock-up experiment has been modelled by a finite elements code COSMOSFloWorks. Completely new Pb-Li in-pile rig design was developed taking into account results of thermal calculations. New design considers smaller amount of Pb-Li in the experimental capsule and wider range of regulation possibilities. Calculation results indicate achievement of the target temperatures in the hot and cold parts of the new rig at the operation reactor power 9 MW.
- Tritium production in the irradiation rig during the test has been performed and possible measures for reduction of tritium production has been assessed (e.g. to use enriched Li-6 isotope in Pb-Li eutectic alloy, employing of special getters etc.)

Task TW3-TTMN-002 - Experiments for the validation of cross-sections up to 55 MeV in an IFMIF-like neutron spectrum. (coordinated by NPI Řež, P.Bém)
Deliverable 5a: Activation experiment on EUROFER. - delivered
Achievements:
- An IFMIF-like white neutron field extending up to 32 MeV was produced at the NPI cyclotron U-120M by bombarding a flowing heavy water target with a 37 MeV proton beam. The irradiation of Eurofer-97 steel samples was performed at two different locations with distances to the source of 1.7 mm and 47 mm and mean neutron flux densities up to 10^{11} cm^{-2}s^{-1} and 10^{10} cm^{-2}s^{-1}, respectively. The induced gamma radioactivity was determined by gamma ray spectrometry at different cooling time intervals using calibrated HPGe detectors. Specific activities of the sample were determined for 21 different product radio-nuclides.
- Activation calculations are under way at FZ Karlsruhe with the ALARA inventory code using the activations cross-sections from the Intermediate Energy Activation File IEAF-2001. The comparison of preliminary calculated and measured induced activities has revealed reasonable agreement for half of the detected radio-nuclides and large discrepancies for the other ones, indicating the need for updating the relevant cross sections in the IEAF-2001 data library.

Deliverable 5b: Neutron transport benchmark on iron. -delivered

- Employing the shadow-bare arrangement of the experiment, it was proven that the room background was effectively suppressed in previous experiments by the detector-shielding assembly. However, only the Monte Carlo computational analysis utilizing the detailed three-dimensional geometry model accurately representing the experimental hall, the iron slab and the shadow-bar arrangement of experiment, carried out at FZ Karlsruhe, is expected to lead to the final conclusions concerning the observed discrepancies with IEAF-2001 data library.

Relevant reports: [6-10].

3. Tritium Breeding and Materials: Materials Development - IFMIF

Task TW0-TTMI–003 - IFMIF – Test facilities. (coordinated by NPI Řež, P.Bém)

Deliverable 8: Experimental tests of activation foils and sub-miniature fission chambers. – delivered

Achievements:

- The high-power neutron source for a simulation of IFMIF spectrum has been build utilizing the $D_2O(p,xn)$ reaction initiated by a 37 MeV proton beam on heavy-water flowing target. The variation of the neutron source intensity during a regular operation of the proton accelerator does not exceed 20%. Collimator-free beam guide to the target station assures low contribution of fast neutron background (below about 0.1%) in the vicinity (up to about 10 cm) of the target. The flux density of about 5×10^{11} cm^{-2}s^{-1} and the mean neutron energy of 12.6 MeV is achieved for 20 μA proton beam current, which is the maximum value available in the negative-ion mode of NPI cyclotron operation. This set-up provides suitable tool for a wide class of integral benchmark experiments relevant to the IFMIF dosimetry - and neutronic calculations tests as well.
- Activation foil irradiations (Co, Au, Ti, Ni, Y, Rh, Nb, Lu, Fe and Bi) have been carried out and the related gamma-ray activity measurements have been performed at NPI by giving the measured data from a set of 6 reactions as input to the neutron spectrum deconvolution code SNL-SAND-II. The neutron spectrum produced in the p(37 MeV)+D_2O source reaction on the cyclotron target has been determined in the energy region 6-20 MeV.
- Prototype miniature fission chambers (^{238}U, ^{237}Np with no fissile deposit) for application as fast neutron monitors in IFMIF built by CEA-Cadarache were tested in the neutron field with IFMIF-like spectrum at the NPI cyclotron-based fast neutron facility. The results of the irradiation experiment have demonstrated that both current and pulse operation of the 8 mm diameter ^{238}U miniature fission chambers for measuring the fast neutron flux in an IFMIF-like environment is possible and, therefore, the use of the planned sub-miniature fission chambers (1.5 mm diameter) should be feasible in IFMIF.

Relevant reports: [11-12].

Deliverable 13: D-Li reaction source term. Experimental verification of the neutron yield based on thick and thin Li-targets. – delivered

Achievements:

- The neutron spectral distributions (spectral yield) from thick lithium target (the thickness of which is greater then energy range of incident particles) were measured at five neutron emission angles (0, 30, 60, 75 and 120 degree with respect to the direction of incident deuteron beam) for 17 MeV and at zero degree for 16.32 MeV deuteron energy by the scintillator pulse-height unfolding technique and the open-

geometry arrangement of experiment. Measured data were found in good agreement with Time-Of-Flight technique data obtained at similar incident energies by other authors.

- Using the difference of zero-degree thick-target yield data measured at deuteron energies of 17 and 16.32 MeV (which is equivalent to the thin-target yield observable), the spectral distribution of double-differential yield (i.e. the cross section) for the Li+d reaction was estimated for the first time.

Relevant reports: [13-17].

Deliverable 14: Neutron data above 20 MeV. Neutron transport benchmark tests. – delivered

Achievements:

- The energy-angular differential yields from a thick heavy water target bombarded by 40 MeV ^{3}He ions were experimentally investigated for the first time to simulate the neutron spectrum of d-Li source of the IFMIF at the NPI cyclotron-based Fast Neutron Facility. The comparison of ^{3}He+D_2O and D+Li neutron source spectra has demonstrated very similar energy-angular distributions.

- A benchmark experiment on iron, the main constituent of the IFMIF high-flux test module, has been performed using the ^{3}He+D_2O source reaction for detectors situated at angles of 0 and 20° with respect to the direction of incident ^{3}He particles. Spectra of neutrons transmitted through a 20 cm thick iron slab were measured with a NE-213 scintillation detector in the energy range 3.5 to 35 MeV by the pulse height technique. The computational analysis was performed at FZ Karlsruhe (FZK) by means of Monte Carlo calculations with the MCNP code using a detailed three-dimensional geometry model to accurately represent the iron slab, the detector shield and the experimental hall. The neutron source distribution was modeled on the basis of the measured double-differential angle-energy neutron yields obtained for the bare heavy water target.

- For the 20° yield spectrum, good agreement is observed for the INPE/FZK evaluation and LANL-150 iron data in the energy range below 15 MeV. In the higher energy domain 15 to 35 MeV the FZK/INPE evaluation satisfactorily represents the experimental results, whereas the LANL-150 data overestimates them by up to 50%. A trend for overestimating the transmission spectra with both iron data evaluations is observed for the 0° yield spectra above approximately 5 MeV of neutron energy.

Relevant reports: [7],[8],[10],[16].

Task TW2-TTMI–003 - IFMIF – Test facilities neutronics. (coordinated by NPI Řež, P.Bém)

Deliverable 13d: Thin target yield from Li(d,xn) reaction at 17 MeV, angular distribution. - delivered

Achievements:

- The upgraded target chamber and the shielded beam dump were installed on the cyclotron beam line to perform thin-target measurements. A special detector shielding with double-conical collimator was designed to suppress the neutron background originating mainly from the scattering of primary neutrons on surrounding objects and room walls. The double-differential yield data of the ^{7}Li(d,xn) reaction were measured at eight different angles in the range from 15 to 120 degree at incident deuteron energy of 17.1 MeV on an ^{7}Li (enriched) self-supporting foil (of 1.4 MeV thickness). Resulting experimental data were compared with prediction of different Monte-Carlo codes developed at FZ Karlsruhe for the d-Li source term description: the M^{C}DeLi code based on a built-in semi-empirical d-Li reaction model, the

M^{C}DeLicious code developed on the basis of evaluated d+^{6,7}Li cross-section data and also the MCNPX code using the built-in ISABEL intra-nuclear cascade model.

- The M^{C}DeLicious calculations predicts fairly well the experimental thick-target yield spectra at zero degree neutron emission while both the M^{C}DeLi and MCNPX calculations are in substantial disagreement with experiment. Similar conclusions hold also for the angle-dependent neutron yield observables. However, some overestimation of M^{C}DeLicious prediction over experiment is observed for the yield and also for the cross-section data. It indicates that further revision of the d+ ^{6,7}Li cross-section database is needed. All models fail to reproduce the structure of higher energy tail of spectra as follows from a comparison of calculated and for the first-time measured double-differential cross-section data of d+^{7}Li reaction. So as high energy neutrons contribute significantly to the damage (large helium production cross-section and larger energy of primary-knock-on atoms), this part of spectra should be described with better accuracy. Therefore, some updating of theoretical approaches seems to be needed.

Report: [13].

Deliverable 14d: Neutron transport benchmark, collimated neutron flux. - delivered
Achievements:

- The experimental set-up of the experiment performed under TW0-TTMI–003 Deliverable 13 has been upgraded in order to account for the inelastic-scattering neutrons from iron into the benchmark analysis. Upgraded scintillator-detector hardware has been utilized to extend registered neutron energy range down to a 700 keV. Double-conical neutron collimator assembly was used to minimize the room-background effect. The iron sample of lower dimensions (disk of 40 cm in diam. and 20 cm thick) was designed to reach optimal arrangement of the experiment. Neutrons escaping the iron disk at zero degree were reliably determined in the energy range from 0.68 to 35 MeV. Resulting spectrum at high energy part indicates a better agreement with MCNP predictions. Final benchmark calculations are in progress at FZ Karlsruhe.

Report: [7].

Task TW3-TTMI–003: IFMIF - Test facility neutronics. (coordinated by NPI Řež, P.Bém)
Deliverable: D6: Measurement of the D-Li source term neutron spectrum between 15 and 120 degree. - delivered
Achievements:

- Recent analysis has indicated that the M^{C}DeLicious code overestimates the production of neutrons with energies less than 2 MeV as due to use the experimental Lone et al. data in evaluating the d+^{6,7}Li cross-section. The Lone data show a rather large neutron production in the low energy range below 2 MeV as compared to most recent thick target data obtained by the Japanese groups. Consequently, an update of the d+^{6,7}Li data evaluation at these neutron energies seems to be needed.
- The double-differential cross-section of the ^{7}Li(d,xn) reaction was measured for the first time at eight different angles in the range from 15 to 120 degree for incident deuteron energy of 17.1 MeV and for neutron energies down to about 1 MeV. Measurements were performed employing the cyclotron-based Fast Neutron Facility (FNF) of the Nuclear Physics Institute (NPI) Řež.
- Resulting experimental data were compared with theoretical prediction of the M^{C}DeLicious code developed at FZ Karlsruhe for the IFMIF De-Li source term on

the basis of evaluated d+^{6,7}Li cross-section data. The M^{C}DeLicious calculations predict fairly well the experimental data for the forward-directed neutron emission at low and medium neutron energies including the lowest energy region below 2 MeV. This finding does not validate previous conclusions derived from integral yield (thick target) experiments. Therefore, the deuteron break-up and compound nucleus excitation processes at low deuteron energies are described quite well by the M^{C}DeLicious code.

- Similar conclusion comes from the comparison of calculated cross section with experimental spectrum at zero-degree neutron emission obtained at NPI by the difference of thick-target yield data measured at 17 and 16.32 MeV deuteron energies.
- It was found that the theoretical predictions based on M^{C}DeLicious code and d-Li evaluated cross sections data fail to reproduce the structure of higher energy tail of neutron spectra corresponding the excitation of ground-, first- and higher states of the *Be nucleus. Some overestimation of M^{C}DeLicious predictions over experiment is evident as well for data at medium and backward angles. It indicates that further revision of the d+ ^{6,7}Li cross-section database is needed. Present data being added to new thin-target experiment data obtained at higher energies by Japanese groups can be used to complete this database.

Report: [18].

4. Physics Integration - TPDC Diagnostics - Ceramics

Task TW3-TPDC-IRRCER: Irradiation effects in ceramics for heating, current drive, and diagnostic systems. (coordinated by IPP Prague, I.Ďuran)
Deliverable 9: Irradiation effects on candidate Hall probes. - delivered
Achievements:
- A fully automated PC based system for periodic in-situ calibration of the Hall sensors during their irradiation in the LVR-15 fission reactor was developed.
- A set of 8 candidate Hall sensors of various types and manufactures was irradiated in research reactor LVR-15 in NRI Rez by fast neutron (E>1 MeV) fluence of 2.5×10^{17} cm^{-2}. This value is the total neutron ITER life time fluence expected at the location of steady state magnetic sensors in ITER (outside the vessel).
- All Hall sensors except one remained operational during the whole irradiation campaign. Some sensors survived the total neutron fluence as high as 1.3×10^{18} cm^{-2}. The sensitivity of the most stable sensor decreased by 6% after irradiation by a reference fast neutron (E>1 MeV) fluence of 2.5×10^{17} cm^{-2}. This deterioration of performance can be handled by proper application of in-situ recalibration techniques to ensure the required precision of the system.

Report: [19].

5a. Vessel/In Vessel - Blanket– Article 5.a

Task TW3-TVB-INPILE: In-pile experiment on PFW Mock-ups.
(coordinated by NRI Řež; staff: M.Zmítko, J.Bohatá, T.Klabik, P.Hájek) - in progress
Deliverable D3: Perform in-pile testing of Be protected PFW mock-ups under heat flux.
Achievements:
- The in-pile rig thermal calculations were performed taking into account heat flux course on the PFW surface.
- The PFW mock-up and support structure stress analysis was done [20].
- The specifications for the heating wires (Thermocoax company products), electrical

sources and control system (Honeywell company product) were prepared and these components were delivered.
- The test rig for Thermocoax heating wires qualification was designed and manufactured.
- Design of the in-pile rig started.
- PFW mock-up was delivered from EFDA for the qualification test.

5b. Vessel/In Vessel - Blanket – Article 5.b

Task TW3-TVM-CFCQ1: Assessment of the Si content of Si impregnated Carbon-Carbon fibre composite. (coordinated by NPI Řež, V.Hnatowicz) - in progress, delayed
Status:
- Task is significantly delayed, because the samples to be analyzed were delivered to the principle investigator only in January 2004.

Task TW3-TVV-EVADIST: Evaluation of VV welding distortions. (coordinated by IAM Brno, L. Junek) – in progress, just started
Status:
- The contract was signed on November 7, 2003. Necessary modifications of the software tools are underway.

2 Underlying Technologies

Activity of Association EURATOM/IPP.CR in this area, complementary to the EFDA Technology work programme, was concentrated on the three tasks.

1. RAFM Steels: Compatibility with Hydrogen and Liquids (coordinated by NRI Řež, M. Zmítko)

Main achievements:

- Special device for out-of-pile testing of liquid metal Pb-17Li behaviour and its interaction with inserted specimens under elevated temperatures (300-500°C) was designed, manufactured, and successfully operated for 3,000 hours. Suitable instrumentation techniques and technological approaches (measurement of temperature and Pb-Li level, flow rate measurement, pressure measurement, use of argon as a cover gas, temperature control, specimens loading and re-loading, …) were verified.

- Tritium and polonium production and accumulation in a special designed irradiation rig Pb-17Li IN-PILE under neutron irradiation was assessed. Polonium is produced in the rig from bismuth, which is present in Pb-17Li as an impurity. Safety relevant measures to be applied during the in-pile rig operation were developed.

2. Plasma spraying of tungsten (coordinated by IPP Prague, staff: J. Matějíček, K. Neufuss, V. Weinzettl (IPP); G. Pintsuk, Y. Koza (FZJ))

Main achievements:

- Tungsten is a candidate material for plasma facing components for ITER and other fusion devices. Plasma spraying is among prospective fabrication technologies, thanks to its ability to coat large areas and the possibility to repair damaged parts. Specimens of plasma-sprayed tungsten (plasma facing layer) and tungsten-copper composite (interlayer for stress reduction) were produced using water stabilized plasma spraying. The specimens properties (shapes of the individual deposited particles, structure and porosity, Young's modulus, and oxide content) were investigated for various compositions of the feedstock powders. The plasma sprayed tungsten layers were tested under high heat fluxes at the electron beam facility JUDITH at Forschungszentrum Julich, to simulate disruption conditions. The coatings were able to absorb about 0.5 GW/m^2 (2.5 MJ/m^2) in thermal shock loading without significant damage.

Report: [21].

3. Calibrated Fast Neutron Source for Activation Benchmark Tests (coordinated by NPI Řež, P. Bém)

Main achievements:

- The objective of the CuCrZr activation experiment is to provide integral experimental data for benchmarking the nuclear data base of EASY (i.e. essentially the EAF cross section file) in the energy range relevant for ITER. The CuCrZr-alloy sample was activated in an intense white neutron field provided by the d+D_2O/Be neutron source at NPI cyclotron at about 10^{11} n/s/cm^2 for 12, 80 and 5500 minutes. Absolute fluence of neutron flux was monitored by Al foils. The time profile of the neutron source strength during the irradiation was monitored by the proton beam current on the source target, recorded by a calibrated current-to frequency converter and PC. Activated samples were investigated by two calibrated HpGe detectors after 10 different cooling times, 10

minutes to 150 days (December 2003). In summary, the 9 activation products were determined from irradiation of CuCrZr sample in the d+Be neutron field. Results of C/E (Calculation/Experimental results) analysis carried out by the Fispact code (with EAF 2003 data library) indicate the need for further investigation of discrepancies in the activation cross-section data.

Relevant reports: [22-24].

LIST OF PUBLICATIONS (TECHNOLOGY)

[1] Final report: P.Hájek, V.Richter, M.Zmítko: *Pb-17Li auxiliary and purification systems: Design of the auxiliary Pb-Li loop for HCLL TBM*, NRI Rez report No.12xxx, July 2004.

[2] Final report: P.Vachtfeidl, K.Splíchal: *Pb-17Li auxiliary and purification systems: Design of the purification system of Pb-17Li and evaluation of impact of Po production*, NRI Rez report No.12067, July 2004.

[3] Final report: K.Splíchal, V.Masarík, V.Svarc, M.Zmítko: *Corrosion behaviour of EUROFER 97 tube in primary water conditions*, NRI Rez report No.12038, March 2004.

[4] Final report: K.Splíchal, P.Chvátal, M.Zmítko: *Corrosion behaviour of base and weld metals of EUROFER 97 in primary water PWR conditions*, NRI Rez report No.12058, April 2004.

[5] Final report: M.Zmítko, K.Splíchal, V.Masarík: *Corrosion and surface conditions of EUROFER 97 steel in Pb-17Li at 500°C*, NRI Rez report No.12016, January 2004.

[6] P. Bém, V. Burjan, M. Götz, M. Honusek, U. Fischer, V. Kroha, U. v. Möllendorff, J. Novák, S. Simakov and E. Šimečková: *Experiments for the validation of cross-sections up to 55 MeV in an IFMIF-like neutron spectrum. Activation experiment on Eurofer & neutron transport benchmark on iron.* Report NPI ASCR Řež, EXP(EFDA)-04/2004.

[7] P. Bém V. Burjan, M. Götz, U. Fischer, J. Novák, U. von Möllendorff, V. Kroha, S. P. Simakov, E. Šimečková and J. Vincour: *Neutron data above 20 MeV: neutron transport benchmark tests, IFMIF-KEP*, JAERI-Tech 2003-005, March 2003, p. 395-400 and Report NPI ASCR Řež, EXP(EFDA)-02/2004.

[8] U. Fischer, S.P.Simakov, U. von Mollendorff, P. Pereslavtsev, P. Bém, A. Konobeev and P.P.H. Wilson: *Validated computational Tools and Data for IFMIF Neutronic Calculations*, AccApp '03 Meeting "Accelerator Applications in a Nuclear Renaissance", Santa Fe, Nov.2003.

[9] S.P. Simakov, U. Fischer, U. von Mollendorf, P. Bém, P. Wilson: *Validation of nuclear data for the IFMIF neutron source*, International Workshop „Fast Neutron Physics", Dresden, Germany, ed. By K. Seidel, H. Freisleben and M. Greschner, Dresden, December 2002, Electronic document.

[10] P. Bém, U. Fischer, S. Simakov, U. v. Möllendorff: *Neutron transport benchmark on iron using a white high-energy neutron field*, Fusion Eng. & Des. **69** (2003) 479.

[11] B. Esposito, M. Angelone, A. Pensa, P. Bém, V. Burjan, M. Götz, M. Honusek, J. Novák, V. Kroha, E. Šimečková, J. Štursa, F. Veselý, C. Blandin and J.P. Hudelot: *Construction and testing of prototype miniature fission chambers for IFMIF* Final report on the EFDA task TW0-TTMN-003, D9 ENEA report, FUS TN MA-R-005, December 2003.

[12] P. Bém, V. Burjan, M. Götz, M. Honusek, V. Kroha, J. Novák, J.Štursa and E. Šimečková, B. Esposito, M. Angelone and A. Pensa C. Blandin and J.P. Hudelot: *Activation foils and subminiature fission chambers: experimental tests* Final report on the EFDA task TWO-TTMN-003, D8 Report NPI ASCR Řež: EXP(EFDA)-01/2004.

[13] P. Bém, V. Burjan, M. Götz, U. Fischer, V. Kroha, U. v. Möllendorff, J. Novák, S. Simakov [+] and E. Šimečková: *D-Li reaction source term: Experimental verification of neutron yield based on a thick and thin Li-targets*, Report NPI ASCR Řež EXP(EFDA)-05/2004.

[14] P. Bém et al., Proc 9th International Seminar on Interaction of Neutrons with Nuclei:"Neutron Spectroscopy, Nuclear Structure, Related Topics", 23-26 May 2001, JINR Dubna, p. 465.

[15] P. Bém V. Burjan, M. Götz, U. Fischer, J. Novák, U. von Möllendorff, V. Kroha ,S. P. Simakov, E. Šimečková and J. Vincour: *D-Li reaction source term – Experimental verification of neutron yield*, IFMIF-KEP, JAERI-Tech 2003-005, March 2003, p. 375.

[16] S.P. Simakov, U. Fischer et al., Journal of Nuclear Materials, **307-311**(2002), 1710-1714.

[17] U. Fischer, S.P.Simakov, U. von Mollendorff, P. Pereslavtsev, P. Bém, A. Konobeev, P.P.H. Wilson: *Validated computational Tools and Data for IFMIF Neutronic Calculations*, Sixth International Meeting on Nuclear Application of Accelerator Technology (AccApp '03), San Diego, June 2003, p.1000.

[18] P. Bém, V. Burjan, M. Götz, U. Fischer, V. Kroha, U. v. Möllendorff, J. Novák, S. Simakov and E. Šimečková: *IFMIF test facility neutronics:Measurement of the D-Li source term neutron spectrum between 15 and 120 degree*, Report NPI ASCR Řež EXP(EFDA)-06/2004.

[19] I. Ďuran, L. Viererbl, R. Všolak, V. Červa, M. Hron, J. Stockel, I. Bolshakova, R. Holyaka, G. Vayakis: *Irradiation effects on candidate Hall probes*, final report on EFDA Task TW3-TPDC-IRRCER Del. 9, June 2004.

[20] V.Hörzenberger, P.Hájek: *Numerical simulation of thermo-elastic loading of PFW rig*, NRI report, June 2004.

[21] Pintsuk, G. - Döring, J.-E. - Hohenauer, W. - Linke, J. - Matejicek, J. - Smid, I. - Tietz, F.: Microstructural and mechanical properties of plasma sprayed W/Cu-graded composites for extreme

thermal conditions; Proc. 2003 World Congress on Powder Metallurgy & Particulate Materials (PM2TEC; Las Vegas, Nevada; June 8-12, 2003), Metal Powder Industries Federation, Princeton, NJ, USA, pp. 6.107 - 6.118.

[22] P. Bém, V. Burjan, M. Götz, M. Honusek, V. Kroha, J. Novák, E. Šimečková: *Activation of dosimetry foils in the NPI Řež p-D2O neutron field of the IFMIF-like spectrum: a comment to data accuracy of gamma-ray intensities*, NEMEA workshop „Neutron measurements and evalutions for applications", 5.-8.11.2003, Budapešť, 4p.

[23] P. Bém, V. Burjan, M. Götz, M. Honusek, V. Kroha, J. Novák, E. Šimečková: *The NPI cyclotron-based fast neutron source: test of flux density by the foil activation method.* Ibis.

[24] P. Bém, V. Burjan, M. Götz, J. Hep, M. Honusek, U. Fischer, V. Kroha, U.v. Möllendorff, J. Novák, S. Simakov and E. Šimečková: *Experiment to validate EAF activation data: Activation on CuCrZr in NPI d-Be neutron field* Workshop on Activation Data EAF 2005, Prague, June 2004.

IV Keep-in-Touch Activities on Inertial Confinement

The main topics of the keep-in touch activities on inertial confinement undertaken in the Association EURATOM/IPP.CR within the reporting period are summarized in the following list.

- Improvement of the homogeneity of target illumination by reduction of laser beam imperfections carried out on the Prague Asterix Laser System (PALS).
- Theoretical study of electron and ion acceleration in laser plasmas.

Main results are listed here:

- The experimental work undertaken in the Prague Asterix Laser System (PALS), in the keep-in-touch activity context, was aimed at smoothing of inhomogeneities induced by imperfections of the laser beam incident on the surface of directly illuminated targets. A multi-frame interferometer system, designed for PALS at IPPLM Warsaw was used for preliminary time-resolved measurements of electron density distributions in the laser-produced plasmas. Efficient energy transfer and smoothing effects in laser-irradiated foam targets have been observed [1].

- The influence or random processes on electron and ion acceleration in laser plasmas was studied theoretically. Enhanced particle acceleration has been found in laser plasmas interacting with an additional phase-randomized laser beam [2], [3].

References:

[1] M. Kalal, J. Limpouch, E. Krousky, K. Masek, K. Rohlena, P. Straka, J. Ullschmied, A. Kasperczuk, T. Pisarczyk, S.Yu. Guskov, A.I. Gromov, V.B. Rozanov, V.N. Kondrashov, *Thermal Smoothing by Laser-Produced Plasma of Porous Matter*, Fus. Sci. & Tech., Vol. **43**, No. 3 (2003) 275-281.

[2] V. Petrzilka, L. Krlin, J.A. Tataronis, *Plasma Flows, Density Perturbations and Charge Separation Fields Resulting from Electron Acceleration in Two Crossed Laser Beams*, 30th EPS conference on Plasma Physics and Controlled Fusion, St Petersburg, July 2003, ECA, **27**A (2003) P4.150.

[3] J.A. Tataronis, V. Petrzilka, L.Krlin: *Controlled Ion Acceleration in Two Crossed Laser Beams Propagating in Plasmas*, 45th APS Annual Meeting of the Division of the Plasma Physics, October 27-31, 2003, Albuquerque, New Mexico, USA, paper KP1.078.

Ablation processes in complex planar laser targets

J.Ullschmied, K.Jungwirth, B.Králiková, E.Krouský,
K.Mašek, M.Pfeifer, K.Rohlena, J.Skála, M.Kálal, J.Limpouch

In collaboration with:

T.Pisarczyk, S.Borodziuk, A.Kasperczuk, P.Pisarczyk, Institute of Plasma Physics and Laser Microfusion, Warsaw, Poland,
S.Gus'kov, I.Ya.Doskach, V.Rozanov, A.I.Gromov, P.N. Lebedev Institute of Physics, Moscow, Russia
V.N.Kondrashov,Troitsk Institute for Innovation and Fusion Research, Troitsk, Russia

Experiments on laser interaction with planar targets of various types represent a starting point for analysis of numerous physical phenomena accompanying implosion of complex spherical targets, on which the idea of laser fusion is based. The experiments utilizing ablatively accelerated planar targets can model large pellet shells in their early implosion phase. Instead of imploding a pellet, a disk target can be accelerated and treated as a section of a sphere (until convergence effects dominate). In planar configuration it is possible to access also the cold back of the target, which is difficult to access in the experiments with real pellets.

The experiments performed at the PALS laboratory within the keep-in-touch activity context in the period 2002-2003 were aimed at investigation of energy transfer and shock wave generation in planar targets driven both by direct laser illumination and by laser-driven macroparticles. In another series of experiments the crater creation in massive targets and smoothing of inhomogeneities induced by imperfections of the laser beam by foam layers were studied. Theoretical part of the work consisted e.g. in elucidating the role of heat transport in the smoothing mechanism inside the dense plasma regions at the double pulse interaction, and in studies of fast electrons and ions production by laser beams.

Laser pulses were delivered by the upgraded PALS facility. Its new auxiliary and diagnostic beam lines and new main beam delivery options made it possible to illuminate and diagnose laser targets by sequences of laser pulses of various colours – at the basic wavelength 1315 nm, and at its red (668 nm) and blue (438 nm) harmonics. Output energy in the main laser beam (pulse duration 0.4 ns) was varied between 100 J and 500 J. Depending on the focusing conditions the focused power density at the target could be adjusted to values from $10^{14}\,W/cm^2$ up to $10^{16}\,W/cm^2$.
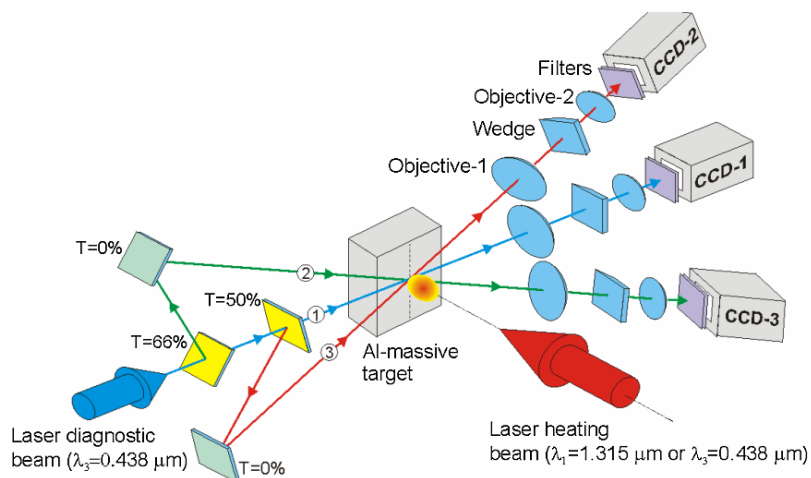

Fig. 1. *Simplified scheme of the 3-frame interferometric system*

The work was carried out in close co-operation with physicists from the Polish Institute IPPLM in Warsaw, from the Russian Institutes PIAS in Moscow and TRINITI in Troitsk, and from the Czech Technical University in Prague. Time-resolved interferometry and shadowgraphy of the targets was applied as one of the main diagnostic tools. Density of the laser-produced plasma was measured by means of a 3-frame polari–interferometric system with automated image processing, developed for PALS by T. Pisarczyk and his colleagues from IPPLM Warsaw. A simplified scheme of the interferometer is depicted in Fig. 1.

The above diagnostic system exploits a probing beam at the third harmonics derived from an auxiliary laser beam. A delay time between the successive channels is set to 3 ns, while the probing time of the first channel is varied for individual shots. Each of three recording channels is equipped with a CCD camera of the Pulnix TM-565 type, with a matrix of 768 x 512 pixels.
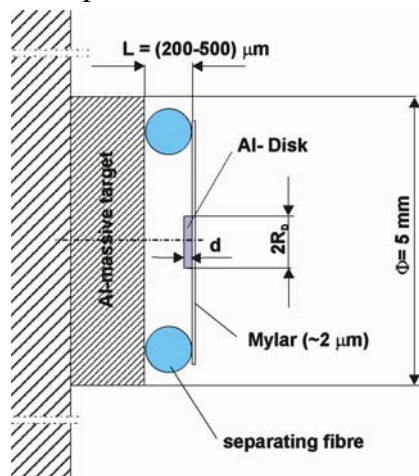

Fig. 2. *The target holder used in the double-target experiments*

For the space behind the target to be accessible for interferometry, a special target holder has been developed and used. The target arrangement depicted in Fig. 2 made it possible to investigate ablative acceleration and crater formation in various types of double targets, the front part of which consists either of a single foil with attached disk, or of more complex structures covered e.g. by low-density foams. Craters in the massive part of the target were created by a direct laser irradiation, or by impact of the foil fragments and ablatively accelerated disks. The shapes and volumes of the craters were determined by employing wax replica technology and microscopy.

Interferograms of undercritical plasma regions in the corona and at the target rear can be used for reconstructing the plasma density, while denser plasma regions and opaque parts of targets are seen in shadowgraphic parts of the pictures. Processing of the recorded
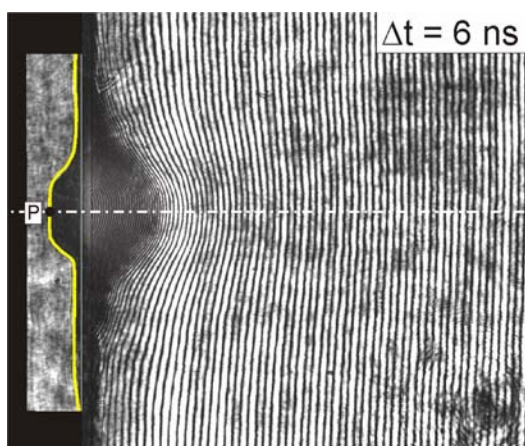

Fig. 3a. *Interferogram/shadowgram of a laser-exploded foil*
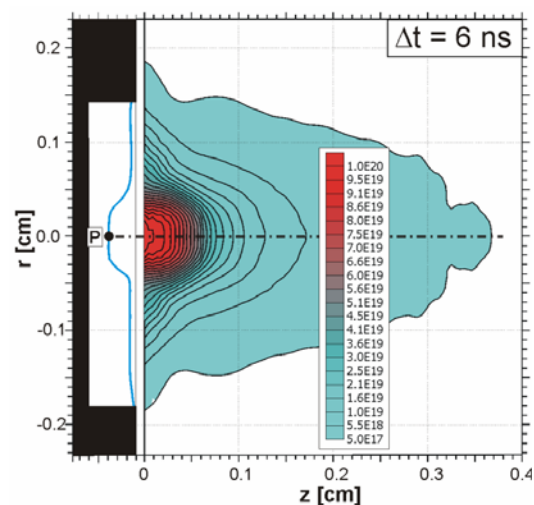

Fig. 3b. *Processed densitogram of an exploding-foil plasma*

interferograms included parasitic noise filtering, comparison of object and reference interferograms, and a subsequent reconstruction of radial electron density distributions. An illustrating sample taken from a sequence of interferograms and resulting densitograms of the plasma generated on a foil target is shown in Fig. 3.

Based on the interferometric and crater volume data, detailed information on the plasma contour and its expansion, on the spatial distribution of electron density, total electron number and velocity of accelerated macroparticles has been obtained for various parameters (energy, wavelength) of the irradiating laser beam. In addition, the values of laser energy absorption coefficient, ablation loading efficiency and efficiency of energy transfer were determined both in the case of a direct laser beam action and at a laser-driven impact of macroparticles [1-3].

The experimental results were analysed and interpreted by using a recently developed two-dimensional theoretical model [4] and numerical simulations by means of the two-dimensional Lagrangian hydrodynamic code ATLANT-HE [5], which includes all the physical phenomena important in the above experiments, such as electron and ion heat conductivity, laser radiation absorption, fast electron generation and transport. The change of the focal spot radius at different laser shots made it possible to test the role of the two-dimensional plasma expansion effect on the shock wave characteristics. For smaller beam radii (<100 µm) the plasma torch expansion has a clearly two-dimensional character. On the contrary, at larger beam radii (>300 µm) it can be reasonably regarded as one-dimensional.

In experiments with laser-irradiated polystyrene foam targets efficient energy transfer and smoothing effect have been observed [6]. The recorded interferograms show a good symmetry, smooth fringes and absence of any local plasma perturbations at the target rear. For interpretation of the experimental data a novel theory of formation of laser light absorption region and of ablation pressure generation in porous matter has been developed [7]. In particular, two stages of homogenisation of porous matter, important for comprehension of the anomalously high absorption of laser radiation in supercritical foams, have been identified: the first, a fast stage of partial homogenisation is followed by a much slower second stage, leading to a uniform medium.

References

[1] S. Borodziuk, A. Kasperczuk, T. Pisarczyk, K. Rohlena, J. Ullschmied, M. Kalal, J. Limpouch, P. Pisarczyk:, Application of the Laser Application of laser simulation method for the analysis of crater formation experiment on PALS laser, Czech. Jour. Phys. 53 (2003), No.9, 799-810.

[2] T. Pisarczyk, S. Borodziuk, A. Kasperczuk, S. Gus'kov, I.Ya. Doskach, V. Rozanov, J. Ullschmied, K. Jungwirth, B. Kralikova, E. Krousky, K. Masek, M. Pfeifer, K. Rohlena, J. Skala, M. Kalal, J. Limpouch, P. Pisarczyk: Experimental and Theoretical Investigations of Craters Formation in Solids in PALS Experiments, Symp. Plasma 2003, 9 – 12.9. 2003, Warsaw, Poland, P 4-6, Proceedings on CD.

[3] T. Pisarczyk, S. Borodziuk, A. Kasperczuk, K. Jungwirth, B. Kralikova, E. Krousky, K. Masek, M. Pfeifer, K. Rohlena, J. Skala, J. Ullschmied, M. Kalal, J. Limpouch, P. Pisarczyk: Application of the Laser Simulation Method of Crater Creation in the Laser-Al Solid Target Experiment on the PALS Facility, Journal of High Temperature Material Processes 7 (3), 319-326, 2003.

[4] I. Ya. Doskach, T. Pisarczyk, S. Gus'kov, K. Jungwirth, M. Kalal, A. Kasperczuk, B. Kralikova, E. Krousky, J. Limpouch, K. Masek, M. Pfeifer, K. Rohlena, V. Rozanov, J. Skala, J. Ullschmied: Laser-produced post-pulse crater formation in solids observed in

PALS facility interaction experiment, Proc. ECLIM 2002, SPIE 5228 (2003), pp. 121-130.

[5]   A. B. Isakov, N. N. Demchenko, I. G. Lebo , V. B. Rozanov, V. F. Tishkin: 2D Lagrangian code "ATLANT-HE" for simulation of plasma interaction with allowance for hot electron generation and transport, ECLIM 2002, Proc. SPIE 5228, 143-150.

[6]   J. Limpouch, S. Guskov, A. I. Gromov, M. Kalal, A. Kasperczuk, V. N. Kondrashov, E. Krousky, B. Kralikova, K. Masek , T. Pisarczyk, M. Pfeifer, K. Rohlena, V. Rozanov, J. Skala, J. Ullschmied: Thin foil acceleration by the pressure of laser-produced plasma of porous matter, Proc. ECLIM-2002, SPIE 5228 (2003), pp. 111-120.

[7]   M. Kalal, J. Limpouch, E. Krousky, K. Masek, K. Rohlena, P. Straka, J. Ullschmied, A. Kasperczuk, T. Pisarczyk, S.Yu. Guskov, A.I. Gromov, V.B. Rozanov, V.N. Kondrashov:, Thermal Smoothing by Laser-Produced Plasma of Porous Matter, Fus. Sci. & Tech., Vol. 43, No. 3 (2003) 275-281.

Novel electron and ion accelerator configurations
V.Petržílka, L.Krlín

In collaboration with:
J.A. Tataronis, University of Madison, Wisconsin, USA

One of the topics of our theoretical modeling is a study of novel electron and ion accelerator configurations. The principle idea is to explore acceleration enhancement by an additional randomized phase laser beam. We found a significant acceleration enhancement in configurations like PBWA (Plasma Beat Wave Accelerator) and LFWA (Laser Wake Field Accelerator). Perhaps the most interesting appears to be our last study of electron acceleration in a single main electron beam, provided that another additional randomized perpendicularly propagating laser beam is present. One of the important features of this novel configuration is that there is no threshold on the lower value of the injection velocity of electrons to be accelerated.

Through numerical modeling of the relativistic test particle motion of an ensemble of electrons in a plane laser beam, we show in the present contribution that a significant electron acceleration arises if an additional perpendicularly propagating transverse plane laser beam with a randomized phase is present. The acceleration mechanism is analogous to the electron acceleration due to de-phasing of the electron motion in a plane transverse laser beam by random kicks. The „random kicks" are now provided by the additional randomized laser beam, which propagates perpendicularly to the direction of propagation of the main laser beam, and which is polarized along the direction of the main laser beam propagation. The power flux intensity of the additional beam can be typically much lower than the power flux intensity of the main laser beam. As the acceleration rate can be to a certain degree controlled by the power flux intensity of the additional beam, we present the dependence of the maximum and average energy of the accelerated electrons on the electric field intensity of the additional beam. We assume that the additional transverse laser beam can be spontaneously randomized either by plasma turbulence, or artificially by random phase plates. The
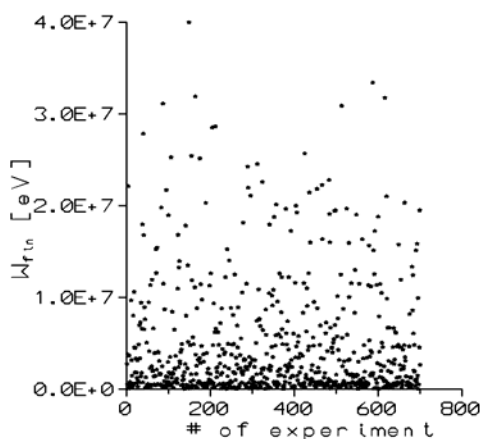

Fig. 1. *Final energy of accelerated electrons for electric field intensity 300 MV/cm of the additional laser beam.*
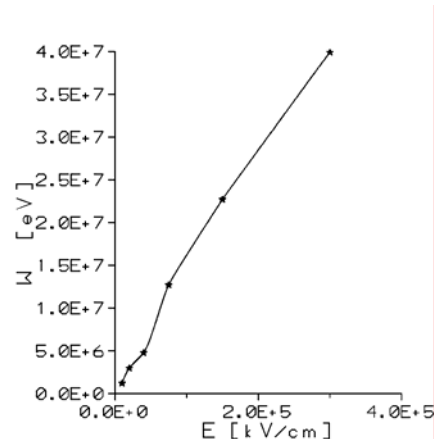

Fig. 2. *Maximum electron energy in the ensemble, in dependence on the intensity of the additional laser* beam.

relativistic equation of electron motion is for a single set of initial conditions always solved in 700 numerical experiments for various realizations of the random phase of the additional laser beam. The laser frequency and laser beam electric field intensities chosen for the test particle computations match the parameters available at the Prague Asterix Laser System (PALS). Then, even thermal plasma electrons having energies of several eV may be accelerated to energies of several MeV.

We also performed a 3-d two-fluid analysis of perturbations in plasmas that result from the generation of fast electrons in two crossing laser beams. Electrons are accelerated in a single plane laser beam that is in the presence of an additional (secondary) perpendicularly propagating plane laser beam with a randomized phase. For the modeling of the ion flow, we developed an advanced version of our 3-d two-fluid numerical code originally developed for the analysis of the local generation of fast electrons in large tokamaks. We found that rather significant plasma density perturbations and plasma flows can arise as a consequence of the primary electron acceleration and the ensuing Coulomb separation potential, as Figs. 3 and 4 show.
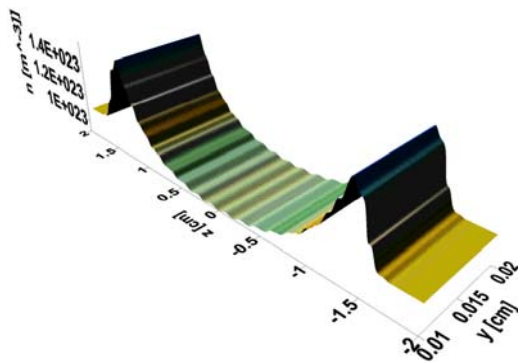

Fig. 3. *Plasma density profile just after the end of the laser pulse.*
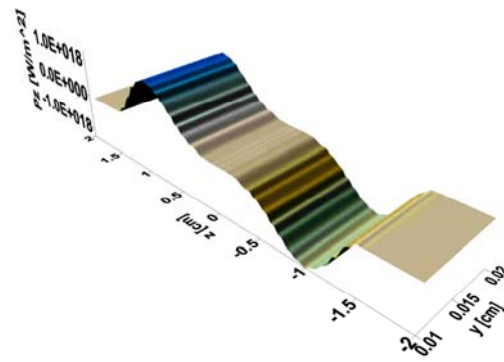
Fig. 4. *Power flux density profile just after the end of the laser pulse.*

It is possible to control the resulting power flux carried by the plasma flow by varying the electric field intensity of the additional randomized laser beam.

References
[1] V. Petrzilka, L. Krlin, J. Tataronis: Electron Acceleration in a Plane Laser Beam Arising from Randomizing the Electron Motion by an Additional Laser Beam, in Proc. Of the 29th EPS Conference on Plasma Physics and Controlled Fusion (CD), paper P1.201, 17-21 June 2002, Montreux, Switzerland.
[2] V. Petrzilka, L. Krlin, J.A. Tataronis, Plasma Flows, Density Perturbations and Charge Separation Fields Resulting from Electron Acceleration in Two Crossed Laser Beams 30th EPS 2003 St. Petersburg Conference (CD), paper 4.150.
[3] J.A. Tataronis, V. Petrzilka, L.Krlin, Controlled Ion Acceleration in Two Crossed Laser Beams Propagating in Plasmas, 45th APS Annual Meeting of the Division of the Plasma Physics, October 27-31, 2003, Albuquerque, New Mexico, USA, paper KP1.078.

V Outreach and Public Information Activities

V.Weinzettl, M.Řípa, J.Mlynář

As a consequence of enhancement of the international collaboration between the Czech Republic and EU in the field of thermonuclear fusion research, the Association EURATOM IPP.CR has been established at the end of 1999. However, a popularization of physical research and its results could be done only due to a personal activity of enthusiastic employees till 2002. In spring 2003 Vladimir Weinzettl, Milan Ripa and Jan Mlynar (all from IPP Prague) applied for an internal grant of IPP. It was accepted as a standard project, which confirms a need to build up a positive image of a fusion reasearch also in Czech Republic, and a will to finance it that more extensive popularization projects could be started. In April Vladimir Weinzettl has been officially appointed to be a contact person for PI of Czech Association, so direct access to PIG EFDA ftp server and to EFDA-JET Website was acquired.

The first fruit of a public information effort became the presentation of the Association EURATOM IPP.CR for the well-known European Fusion Expo exhibition. Nearly two minutes long video introduces the two big contributors to a physical programme of Czech Association – the Institute of Plasma Physics and the Nuclear Research Institute Rez plc. Also big posters show an importance of a research in the associated institutes and understandably explain its main goals.

However, the basic focus is driven to a PI work for a public in the Czech Republic. The biggest effort was split into two main fields – direct excursions to the CASTOR tokamak, and thermonuclear fusion presentations in public media. A lot of students from basic to high schools were invited to visit the Institute of Plasma Physics, especially the tokamak department. However, not only students are interested by a fusion science. More than two hundreds enthusiasts and common man came to see CASTOR during first half of this year. New presentation materials for excursions both were made in Czech and English languages.

The interest of the media in ITER construction helps the PI men to publish more articles on fusion, to address the public via Czech TV or radio. On the other hand, most people think the plasma physics is something very far from their everyday lives, and it is very hard to draw attention of general public.

In general, the public information (PI) activities can be divided into two groups: autonomous and correlated.

Issuing posters and brochures, making video spots and web pages, organising popular lectures, excursions and open days are all examples of autonomous activities. In these activities, the form and contents of information are fully in charge of the author(s). Articles and/or interviews for media are typical examples of the correlated PI. Their informative contents are limited by constraints set by objective needs and personal views of media professionals. These constraints vary from relatively open collaboration to completely narrow-minded rejection of communication. In the latter case, the common argumentation is that the subject is too complex to be covered. We always attempt to overcome such prejudices. The more influential the media are, the more challenging the work is. Huge efforts must be spent in order to pass a brief information to a daily newspaper or to TV broadcast. However, the impact of such an information on public is substantial compared to the „more friendly" media. Personal contacts with media professionals are vital in this respect and any opportunity to develop them must be seized (conferences, Open days, printed materials…). Any possibility to exchange experience in fusion PI on international level is quite significant too.

The following list includes both activity dedicated exclusively to the Association and activity where the Association is only a part of the whole.

LIST OF ACTIVITIES
Papers

[1] M.Řípa: **Setkání generací (Generation rendezvous),** VTM, Vol LVI, 2002, No 3, p. 23

[2] M.Řípa: **Symposium o fyzice a technice plazmatu po dvacáté (The 20th Symposium on Plasma Physics and Technology),** Akademický bulletin, 2002, No 7/8, p.25

[3] M.Řípa: **Plazma se dosud krotí jen velmi obtížně (Still difficult to restrain a plasma)**, Hospodářské noviny, June 13, 2002, p.3

[4] M.Řípa (editor): **Institute of Plasma Physics**, The Academy of Sciences – For economy and society, Technologické centrum AV ČR, 2002 (Czech and English mutation)

[5] M.Řípa: **Moře energie obklopuje Greifswald (Energy sea enclosed Greifswald),** VTM, **Vol LV,** 2001, No 12, p. 15

[6] J.Tuček: **Jak spoutat energii vodíkové bomby (How to harness H-bomb energy)**, MFD, December 14, 2002 (consultants: F.Žáček, M.Řípa)

[7] M.Řípa: **Věřím, že termojaderné elektrárny mají budoucnost (I believe in fusion power plants' future – Interview with Jan Mlynar)**, Mladá Fronta Dnes, March 1, 2003, p. C11

[8] J.Tuček: **Spoutávání vodíkové bomby (Harnessing of H-bomb)**, Hospodářské noviny, part Věda a lidé p. 7, March 6, 2003 (consultant: M.Řípa)

[9] M.Řípa**: Termojaderná elektrárna – naše energetická naděje? (Fusion power plant – our energy chance?),** Technický týdeník, No12, March 26, 2003

[10] M.Řípa: **Jak vařit z vody (How to boil from water),** Respekt, **Vol XIV**, No 20, May 12-18, 2003, p.20

[11] M.Řípa: **Jan Mlynář komunikuje s veřejností na JET v Culhamu (Jan Mlynar communicates with public on JET at Culham)**, Akademický bulletin, No 5, 2003, p. 10

[12] M.Řípa: **Termojaderná elektrárna se stává skutečností (Fusion Power Plant becomes truth),** Mladá Fronta Dnes, June 21, 2003, p. C10

Posters

[1] V.Weinzettl, M.Řípa: **Association EURATOM IPP.CR** (Czech and English mutation), spring 2003

[2] V.Weinzettl, M.Řípa, TiKAV ČR: **Akademie na prahu Evropské unie (Academy on the sill of the European Union)**, May 2003

Television and broadcast (video / audio)

[1] K.Blažková: **Plasma – čtvrté skupenství hmoty (Plasma – four states of matter***: Television interview with Jan Stöckel)* Česká televize, Dobré jitro, June 12,2002, 6:20 hours

[2] K.Pospíšilová: **Co je to vlastně plazma a proč poutá takový zájem…? (What the plasma is and why it is so interesting…? –** *Broadcast interview with Pavel Šunka and Jan Píchal***),** Český rozhlas, Velké malé zprávy, June 13, 2002, 9:40 hours

[3] V.Kunz, Popularis: **Slunce na zemi (The Son on the Earth – television story),** Česká televize, January 9, 2003, 17:30 hours (co-ordinator: Institute of Plasma Physics)

[4] K.Pospíšilová: **Mlynář PR na JET (Jan Mlynar – PR on JET***: Broadcast interview with Jan Mlynar***),** Radiožurnál– May 13, 2003, 17:40 hours

[5] K.Pospíšilová, V.Weinzettl: **Jak se Vám žije (***Broadcast interview with Vladimír Weinzettl***)**, Radiožurnál– May 11, 2003, 11:10 hours

[6] V.Weinzettl, M.Řípa, Mediaware Prostějov: **Videospot Association EURATOM IPP CR for FusionExpo**, posted to Dr. Hughes Desmendt on May 21,2003

Lectures

[1] V.Svoboda: **Termojaderná fúze (Thermonuclear fusion)** Physical Week on Faculty of Nuclear Science and Physical Engineering, Czech Technical University, June 2002; followed by CASTOR tokamak excursion

[2] P.Chráska, **moderátor semináře Energie z jádra (Workshop Energy from Nucleus Moderator)**, GAČR, Praha, June 24, 2002

[3] V.Svoboda: **Fyzikální základ jaderné fúze a cesta k její realizaci (Physical base of nuclear fusion and the way to its implementation),** seminář Energie z jádra (Workshop Energy from Nucleus), GAČR, Praha, June 24, 2002

[4] V.Svoboda: **Tudy cesta nevede (This direction is not right)** „Student union" by Faculty of Nuclear Science and Physical Engeeniring, Czech Technical University; followed by CASTOR tokamak excursion, August 2002

[5] J.Stöckel: **Energetika na bázi termojaderného slučování (Energy on the thermonuclear fusion base)**, Konference českých a slovenských fyziků (Czech and Slovak Physics Conference), Plzeň, September 10, 2002

[6] M.Řípa: **Termojaderná energie včera, dnes a zítra (Thermonuclear energy yesterday, today and tomorrow),** High school Čáslav, May 5, 2003

[7] V.Svoboda: **Termojaderná fúze (Thermonuclear fusion),** High School Prague, March 2003

[8] V.Svoboda: **Termojaderná fúze (Thermonuclear fusion)** Physical Week on Faculty of Nuclear Science and Physical Engineering, Czech Technical University, June 2003; followed by CASTOR tokamak excursion

[9] L.Nocera, Z.Sedláček: **Světlušky ve větru: nerozřešené záhady fyziky mezihvězdného prostoru (Firefliers in the wind: Unsolved mystery of the interstellar space physics)**

Others

- V.Weinzettl: **guider of the CASTOR tokamak excursions, materials for excursions** (Czech and English mutation)
- V.Weinzettl: **mail and post correspondence with fusion enthusiasts**
- J.Mlynar, employee of Institute of Plasma Physics, is a responsible for public relations **at the EFDA JET Close Support Unit**, Culham, U.K. since March 2003.

VI

Training and Education Activities

The Summer Training Course 2003 on the CASTOR Tokamak

V.Weinzettl, J.Stockel, S.Zoletnik

Operation of the next step fusion devices, such as ITER, will require a new generation of physicists who are familiar with all aspects of experimental work on tokamaks. Their practical education can be accelerated substantially by getting them in direct touch with experimental reality. For that purpose, small-scale experiments would offer the optimal solution. One of those available in Europe is the small but very flexible CASTOR (Czech Academy of Sciences TORus) tokamak routinely operating in the Institute of Plasma Physics in Prague, Czech Republic. The tokamak is equipped with basic diagnostics, a good data acquisition system and a reasonable software package for data processing. Daily, about 50-60 reproducible discharges with the interpulse rate comparable to 10 minutes can be easily achieved. The permanent staff is experienced in education and training of Czech as well as foreign students. The Czech and Hungarian Euratom Associations (IPP.CR and HAS) decided to exploit all these benefits and jointly organize **the Summer Training Course (SUMTRAIC) on the CASTOR Tokamak**. The first run has been successfully performed on June 2-6, 2003, with participation of ten Hungarian students (graduate and post-graduate) and three Hungarian supervisors. Only those students were accepted for participation who passed an exam on a one-semester introductory course on fusion, this way they were already familiar with concepts and theory of fusion.

Intensive preparatory works began several weeks before the training course. The students were divided into three experimental groups; each of them was supervised by one Czech and one Hungarian senior physicist. Comprehensible manuals describing particular diagnostics and data processing have been prepared beforehand by the supervisors, this way the students became familiar with the SUMTRAIC activities well in advance. The Hungarian side had also organized a teaching seminary of the IDL software in Budapest. The students brought to Prague portable computers already equipped with the software suitable to access the CASTOR database and to process the basic data.

The first day of the training course was devoted to an introduction of key elements of the CASTOR (vacuum, power supplies, diagnostics etc). Several standard shots were done employing students as operators and basic experimental data were processed. The following days, the experimental groups have performed topical measurements (focused this time on Langmuir probes, spectroscopy and plasma fluctuations measurements) according to a tentative shot plan. One student of each group was selected to operate the tokamak, another one took care on the particular diagnostics and the remaining students checked and processed data. The last day was dedicated to the discussion of results and the preparation of presentations. The training course was completed on Friday afternoon by a joint workshop, where students presented the main experimental achievements.

It was concluded that the first SUMTRAIC fulfilled its main goal, to demonstrate the basic activities related to a real fusion experiment in practice - measurements, data processing, discussion of results and their presentation, including experimental failures (unexpected crash of the main turbo-molecular pump of CASTOR). The next training course

is envisaged to be organized next June in a similar way. It is agreed to extend it (~10 days) to leave more time for discussions and possibly for writing short reports at the end of the course. Participation from all over Europe is welcome. A web-based fusion education course will be available for interested students well in advance at the homepage of the Hungarian Association.

SUMTRAIC participants in the tokamak's garden